Aus dem Charité Comprehensive Cancer Center
der Medizinischen Fakultät Charité – Universitätsmedizin Berlin

DISSERTATION

Targeted guanylyl cyclase C for optimization of circulating colorectal cancer cells enrichment and isolation

zur Erlangung des akademischen Grades
Doctor medicinae (Dr. med.)

vorgelegt der Medizinischen Fakultät
Charité – Universitätsmedizin Berlin

von

Yong Liu

aus Zhejiang, China

Datum der Promotion: 08.12.2017

Table of Contents

Abstract 6

List of abbreviations 9

Introduction 12

1 Colorectal cancer and classification 12

2 Liquid biopsy and genomic detection approach 13

3 CTC enrichment and biomarkers 14

4 GCC and its ligands 16

Methods 18

List of reagents 18

List of buffers and kits 19

List of devices and materials 19

List of antibodies and isotype controls 20

Characters of CRC cell lines used for GCC antibody staining 21

Overview of conjugated antibodies and ICs used for CTC staining 22

1 IHC staining of GCC in rectal cancer and adjacent normal mucosal tissues 23

2 GCCmRNA detection from peripheral blood of CRC patients 23

2.1 Sample collection from CRC patients 23

2.2 Extraction and detection of RNA 23

2.3 PCR amplification 24

2.4 GCCmRNA detection 24

3 Optimization of CD45+ cell depletion experiments (from healthy donors) 24

3.1 Blood sample collection from healthy donors 24

3.2 Tumor cell counting 24

3.3 Removal of erythrocyte 24

3.4 Removal of CD45+ cells by CD45 depletion 25

3.5 Additional depletion of CD45+ depleted cells 25

4 Staining of GCC antibody in SW620 cell and T84 cell 25

5 Optimization of method stained by GCC antibody 26

5.1 Optimization of GCC antibody staining in T84 cell line 26

5.2 Staining of GCC antibody in colon cancer cell lines 26

6 Detection of tumor cells by flow cytometry 27

6.1 Method and principle of flow cytometry detection 27

6.2 Sample analysis by flow cytometry 27

7 Collection and assessment of data 27

7.1 Collection of patients' clinical data 27

7.2 Scoring and assessment of IHC staining 27

7.3 Statistical assessment of circulating GCCmRNA 28

Results 29

1 IHC staining of GCC in samples of tumor tissues and normal mucosal tissues of the rectum (data from patients treated in the Surgical Department of Colorectal Cancer in Zhejiang Cancer Hospital, Hangzhou, China) 29

1.1 Clinico-pathologic characteristics of rectal cancer patients 29

1.2 GCC expression in tumor tissues and normal mucosal tissues of the rectum 29

1.3 Comparison of GCC staining in tumor tissues and normal mucosal tissues of the rectum 31

2 GCCmRNA detection in peripheral blood of CRC patients (data on patients treated in the Surgical Department of Colorectal Cancer in Zhejiang Cancer Hospital, Hangzhou, China) 32

2.1 Clinico-pathologic characteristics of patients 32

2.2 Correlation of patients' characteristics with DFS and OS in the overall population 33

2.3 Kaplan Meier survival curve analysis of DFS and OS 34

2.4 Kaplan Meier survival curve analysis of GCCmRNA levels by stage stratification 35

2.5 Multivariate Cox regression analysis of DFS and OS (with or without stage stratification) 36

2.6 Assessment of GCCmRNA in multivariate Cox regression model 37

3 Optimization of negative enrichment approach of CTCs 38

3.1 Negative enrichment of CTCs (blood samples from healthy volunteers) 39

3.2 Optimization of negative enrichment approach 39
4 GCC expression in different colon cancer cell lines 42
5 Staining of GCC antibody in T84 cell line by indirect method 44
5.1 Antibody titration 44
5.2 Antibody staining in T84 cell line 45
6 Staining of Alexa488-conjugated GCC antibody in T84 cell line 45
6.1 Synthesis and titration of Alexa488-conjugated GCC antibodies 45
6.2 Staining of Alexa488-conjugated GCC antibodies in T84 cell line 46
7 Staining of FITC-conjugated GCC antibody in T84 cell line 47
7.1 Antibody titration 47
7.2 Optimization of GCC antibody staining in T84 cell line 48
8 Unspecific staining of GCC antibody in leukocytes 49
8.1 Multi-stained of tumor cells by GCC, CK and EpCAM 49
8.2 Multi-stained of tumor cells with Alexa488-conjugated GCC, CK and EpCAM 51
8.3 Comparison of leukocytes single-stained with GCC, CK and EpCAM 52
8.4 Unspecific staining of GCC antibodies and secondary antibody in leukocytes 53
8.5 Summary of leukocytes stained with unconjugated and conjugated GCC antibodies 55
9 Intracellular and surface staining of leukocytes by FITC conjugated GCC antibodies 55
10 Summary of T84 cells and leukocytes stained by three GCC antibodies 57
Discussion 59
1 Optimization of CD45+ cell depletion in CTC enrichment protocol 59
2 GCC expression in tumor and normal adjacent mucosal tissues of the rectum 61
3 GCC expression in colon cancer cells and T84 cells 62
4 GCC mRNA detection in peripheral blood of metastatic CRC patients 62
5 Nonspecific staining of conjugated GCC antibodies in leukocytes 64
6 Conclusions and future direction 67
Bibliography 68
Affidavit 76

Curriculum vitae 77

Acknowledgement 79

List of figures and tables

List of figures

Figure 1A: Expression of GCC protein (negative) in cancer tissues and normal mucosal tissues of the rectum with magnification ×20, ×100 and ×400 30

Figure 1B: Expression of GCC protein (weak) in cancer tissues and normal mucosal tissues of the rectum with magnification ×20, ×100 and ×400 30

Figure 1C: Expression of GCC protein (moderate) in cancer tissues and normal mucosal tissues of rectum with magnification ×20, ×100 and ×400 31

Figure 1D: Expression of GCC protein (strong) in cancer tissues of rectum (no strong staining is found in normal mucosal tissues of rectum) with magnification ×20, ×100 and ×400 31

Figure 2: Intensity of GCC expression in paired tumor and normal mucosal tissues of rectum 31

Figure 3: Comparison of GCC intensity between paired tumor and normal mucosal tissues of rectum 32

Figure 4: Kaplan Meier survival analysis of DFS and OS 35

Figure 5: Kaplan Meier survival analysis of GCCmRNA levels with DFS and OS by stage stratification 36

Figure 6: Illustration of tumor cells losing during CD45 cell depletion step 40

Figure 7: Illustration of improving recovery rate by additional depletion of depleted CD45+ cells 40

Figure 8: Increasing recovery rate by additional depletion(total 150 SW620 cells added in and recovered) 41

Figure 9: GCC antibody staining in six colon cancer cell lines 43

Figure 10: GCC antibody staining in six colon cancer cell lines during their first passage after thawing from frozen tubes 44

Figure 11: Summary of antibody staining in T84 colon cancer cell line 45

Figure 12: Illustration of antibody staining by direct and indirect staining methods 46

Figure 13: Optimization of Alexa488-conjugated GCC antibody with different volume and incubating time 47

Figure 14: Fluoroscopic detection of GCC antibody staining in T84 cells 47

Figure 15: Optimization of FITC-conjugated GCC antibody staining in T84 cells 48

Figure 16: Surface and intracellular staining of FITC-conjugated GCC antibody in T84 cells 49

Figure 17: T84 cells and leukocytes multi-stained by GCC, CK and EpCAM 50

Figure 18: T84 cells and leukocytes stained by negative control, IC and GCC antibody 50

Figure 19: T84 cell recycled by Alexa488-conjugated GCC antibody by direct staining method 51

Figure 20: T84 cells and leukocytes stained with negative control, IC and Alexa488-conjugated GCC antibody 52

Figure 21: Comparison of leukocytes single-stained by GCC, CK and EpCAM 53

Figure 22: Leukocytes stained by GCC antibodies and secondary antibody 54
Figure 23: Illustration of leukocytes stained by antibodies in fluoroscopic detection 54
Figure 24: Leukocytes surface stained by FITC-conjugated GCC antibody 56
Figure 25: Leukocytes intracellular stained by FITC-conjugated GCC antibody 57

List of tables

Table 1: Comparison of GCC expression in tumor tissues and normal mucosal tissues of rectum 32
Table 2: Association of circulating GCCmRNA level and clinical characteristics 33
Table 3: Multivariate Cox regression model analysis of DFS 38
Table 4: Multivariate Cox regression model analysis of OS 38
Table 5: Effect of GCCmRNA level in multivariate Cox regression model 38
Table 6: Recovery rate of SW620 cell double stained by CK and EpCAM 39
Table 7: Recovery rate of SW620 cells by normal and additional CD45 cell depletion 41
Table 8: Summary of GCC staining in different colon cancer cell lines 44
Table 9: Summary of leukocytes stained by GCC based on indirect and direct staining methods 55
Table 10: Summary of T84 cells and leukocytes stained by three GCC antibodies 58

Title: Targeted guanylyl cyclase C for optimization of circulating colorectal cancer cells enrichment and isolation

Abstract (383 words)

Introduction: CTC (Circulating tumor cell) can provide molecular characterization of metastatic tumor cells and dynamically monitor therapy strategy, but CTC may lose epithelial biomarker expression during metastasis. The aim of our research is to increase the CTC detection rate by optimizing CTC staining and recovery and specifically evaluate GCC (guanylyl cyclase C) as a marker for circulating colorectal cancer cells.

Methods: GCC protein was detected and compared in paired rectal cancer tissues and normal mucosal tissues from 80 cases by immunohistochemistry (data from China). Circulating GCCmRNA was detected from 160 stage I-III colorectal cancer patients by qRT-PCR, and analyzed with long -term survival (data from China). Several negative CTC enrichment-based protocols were used and optimized to increase the recovery rate of colorectal cancer cells. Several GCC antibodies were evaluated for staining of colorectal cancer cell lines and leukocytes by flow cytometry.

Results: GCC protein was significantly over-expressed in rectal cancer tissues compared to paired normal mucosal tissues. High GCCmRNA level in peripheral blood was significantly associated with tumor emboli in vessels, lymph node metastases, mesenteric root lymph node metastases and poor survival. Together with tumor embolus in vessel and mesenteric root lymph node metastasis, GCCmRNA was a hazard factor for predicting poor patients' survival by multivariate COX regression analysis. For optimizing CTC enrichment, the recovery of spiked CTC could be improved by an average of 16.23% by introducing a second round of depletion of the already negatively depleted CD45+ fraction. High GCC staining in T84, moderate in LS174T and low in other colon cancer cell lines were observed. Additionally, all the colon cancer cell lines showed a high percentage of cells expressing GCC (it ranged from 53.12% to 97.01%) at their first passage from frozen tube. Unfortunately, however, non-specific surface and intracellular binding of two conjugated GCC antibodies was observed (average rate 50.29% and 53.67%) when compared to isotype controls (average rate 10.74%), which restricts further application of GCC antibodies for CTC detection from patients.

Conclusions: Additional depletion of CD45+ depleted fraction can increase the recovery rate of CTCs. Nonspecific binding of three GCC antibodies in leukocytes restricts their application in clinical practice. GCC antibodies without nonspecific binding site should be designed for CTC detection of colorectal cancer in the future.

Key words: colorectal neoplasm, circulating tumor cell, guanylyl cyclase C, flow cytometry

Titel: Guanylylcyclase C als Marker zur Optimierung der Anreicherung und Isolation von zirkulierenden kolorektalen Krebszellen

Zusammenfassung (357 Wörter)

Einleitung: Die Analyse CTC (zirkulierender Tumorzellen) wird entwickelt, um metastatische Tumoren molekular zu charakterisieren und Therapiestrategien dynamisch zu überwachen. Eine wesentliche Limitation ist aber die instabile Expression epithelialer Marker auf CTC. Das Ziel unserer Forschung ist es, die Wiederfindungsrate von CTC durch die Verwendung neuer gewebespezifischer Merker zu optimieren.

Methoden: Das GCC-Protein (konjugierte Guanylylcyclase C) wurde als interessanter Marker definiert. Zunächst wurde die Expression von GCC beim Rektumkarzinom an gepaarten Proben von Tumorgewebe und normaler Schleimhaut an 80 Fällen durch Immunhistochemie verglichen (Daten aus China). Blutproben von 160 Patienten im Stadium I-III-Darmkrebs in China wurden durch qRT-PCR auf GCCmRNA untersucht und die Daten mit der Überlebenszeit verglichen. Mehrere Protokolle zur CTC-Anreicherung wurden entwickelt um die Wiederfindungsrate von Darmkrebszellen zu optimieren. GCC-Antikörper wurden hierfür mit Farbmarkern konjugiert bzw. konjugierte käuflich erworben und auf ihre Eignung zur Isolation von kolorektalen Tumorzellen in der Durchflusszytometrie getestet.

Ergebnisse: GCC-Protein war in Rektumkarzinom im Vergleich zur normalen Schleimhaut stark überexprimiert. Hohe GCCmRNA-Spiegel im peripheren Blut waren signifikant mit Tumor-Embolien in Gefässen, Lymphknotenmetastasen, Lymphknotenmetastasen in der Mesenterialwurzel und schlechterem Überleben assoziiert. In der multivariaten Analyse waren Tumor Emboli, und Lymphknotenmetastasen in der Mesenterialwurzel und GCCmRNA

unabhängige Risikofaktoren für das Überleben, mit oder ohne TNM-Schichtung. Als Optimierungsschritt für die CTC-Anreicherung wurde zusätzlich durch Recycling der CD45-positiven, CTC-abgereicherten Fraktion nochmals durchschnittlich 16% der eingesetzten Tumorzellen wiedergewonnen. Die GCC-Färbung war in T84 Zellen hoch, moderat in LS174T und niedrig in anderen Darmkrebszellen. Allerdings zeigten alle Colon-Krebszelllinien einen hohen Prozentsatz an GCC (von 53,12% bis 97,01%) in ihrer ersten Kulturpassage, die bei weiterer Kultivierung abnahm. Problematisch war eine nicht-spezifische Färbung von Leukozyten bei Oberflächen- und intrazellulärer Färbung mit den beiden selbst konjugierten GCC-Antikörpern (mittlere Rate 50,29% und 53,67%) und auch mit dem nachträglich kommerziell erworbenen direkt konjugiertem Antikörper, was die Anwendung von GCC-Antikörpern für die CTC-Detektion bei Patienten beschränkt.

Schlussfolgerungen: Nach der CD45-Depletion kann die Wiederfindungsrate von CTCs durch zusätzliches Recycling von CTC aus der CD45+ Fraktion erhöht werden. Aufgrund der unspezifischen Färbung von Leukozyten können die GCC-Antikörper für die CTC-Erkennung trotz der guten Färbeeigenschaften bei Darmkrebszelllinien nicht verwendet werden, spezifische konjugierte GCC-Antikörper ohne Kreuzreaktion mit Leukozyten wären notwendig.

Schlüsselworte: Kolorektales Karzinom, zirkulierende Tumorzellen, Guanylylcyclase C, Durchflusszytometrie.

List of abbreviations

Abbreviations	Full name
Ab	Antibody
ACTH	Adrenocorticotropic hormone
APC	Allophycocyanin
ATCC (company)	American Type Culture Collection
BEAMing	Technique based on beads, emulsion, amplification and magnetics
CA199	Carbohydrate antigen 199
CD	Cluster of Differentiation
CEA	Carcinoembryonic antigen
cfDNA	Cell free DNA
cGMP	Cyclic guanosine monophosphate
CI	Confidence Interval
CIMP	CpG island methylator phenotype
CIN	Chromosomal instability
CK	Cytokeratin
cold-PCR	Co-amplification at lower denaturation temperature PCR
CRC	Colorectal cancer
CTC	Circulating tumor cell
ctDNA	Circulating tumor DNA
DAB	Diaminobenzidine
DEPC	Diethylpyrocarbonate
DFF	Dean flow fractionation
DFS	Disease-free survival
DNA	Deoxyribonucleic acid
ECM	Extracellular matrix
EDTA	Ethylene diamine tetraacetic acid
EGFR	Epidermal growth factor receptor
EMEM	Eagle's Minimum Essential Medium
EMT	Epithelial-mesenchymal transition
Em (nm)	Emission wavelength in nanometers
EpCAM	Epithelial cell adhesion molecule
EPISPOT	Epithelial ImmunoSPOT

Ex (nm)	Excitation wavelength in nanometers
Fab	Fragment, antigen-binding
FACS	Fluorescence activated cell sorting
FAP	Familial adenomatous polyposis
FAST	Fiber-optic array-scanning technology
FBS	Fetal bovine serum
Fc	Fragments, crystallisable
FcR	Fc receptor
FcγR	Fc-gamma receptor
FCS	Fetal calf serum
FDA	US Food and Drug Administration
Fig	Figure
FITC	Fluorescein isothiocyanate
GCC	Guanylyl cyclase C
GTP	Guanosine triphosphate
HNPCC	Hereditary nonpolyposis colorectal cancer
HRP	Horseradish peroxidase
H_2O_2	Hydrogen peroxide
H_2O	Water
HR	Hazard Ratio
IC	Isotype control
Ig	Immunoglobulin
IHC	Immunohistochemistry
IL-10	Interleukin 10
ISET	Isolation by size of epithelial tumor cells
MAP	MUTYH-associated polyposis
MAP	MIDI-Activated Pyrophosphorolysis
MET	Mesenchymal-epithelial transition
min	Minute
mRNA	messenger RNA
miRNA	MicroRNA
MLH1	MutL homolog 1
MSI	Microsatellite instability

MSH2	MutS protein homolog 2
NGS	Next generation sequencing
OS	Overall survival
PBS	Phosphate buffered saline
PE	R-Phycoerythrin
PerCP	Peridinin Chlorophyll
PFS	Progression-free survival
PH	Power of hydrogen
PKG	cGMP-dependent protein kinase or Protein Kinase G
qPCR	Real-time polymerase chain reaction
qRT-PCR	RT-PCR / qPCR combined technique
RBC	Red blood cell
RNA	Ribonucleic acid
rpm	Resolutions per minute
RT-PCR	Reverse transcription polymerase chain reaction
Sig	Significance
ST	Heat-stable enterotoxin
SPSS	Statistical Package for the Social Sciences
SSA	Selective size amplification
TERT	Telomerase reverse transcriptase
TGF	Transforming growth factor
UICC	Union for International Cancer Control
USA	United States of America
WGS	Whole-genome sequencing

Introduction

1. Colorectal cancer and classification

CRC (colorectal cancer) is the third most common cancer worldwide, accounting for nearly 700,000 reported deaths every year [1, 2]. It is reported that nearly half of the cases (54%) occurred in more developed regions, especially in the area of eastern Asia, Europe and America [1, 2]. Even though detailed screening and multidisciplinary treatments, including radical surgery, chemotherapy, radiotherapy and immunotherapy are applied for early, advanced and metastatic CRC patients, the reported deaths due to metastatic progression are one third of the overall CRC cases[2].

CRC is defined as malignant neoplasms of the colon, rectum and appendix. Nearly 20-30% of these are hereditary CRCs, which comprise the Lynch syndrome (also called hereditary nonpolyposis colorectal cancer, HNPCC), FAP (familial adenomatous polyposis), attenuated FAP and MAP (MUTYH-associated polyposis)[3], in parallel with the major population (70-80%) of sporadic CRC. Sporadic CRCs are commonly formed through the accumulation of somatic genetic and epigenetic events, which include loss-of-function defects among selected tumor suppressor genes and gain-of-function defects in selected oncogenes [4-6].

CRC is not a homogeneous disease, according to the molecular mechanistic variations during its invasion and diversion. Among these CIN (chromosomal instability), MSI (microsatellite instability), and CIMP (the CpG island methylator phenotype) are distinct molecular pathways that have been involved in CRC carcinogenesis and its metastasis [7]. CIN is characterized by imbalances in the chromosome number and a loss of heterozygosity[8], while MSI is associated with inherited CRC cases stemming from mutations in DNA mismatch repair genes, such as MLH1, MSH2 and MSH6. CIMP is commonly found in sporadic CRC and characterized by the aberrant methylation of tumor suppressor genes, which leads to their inactivation [7, 9].

Colorectal cancers are histopathologically classified on the basis of tumor invasion depth (T stage), lymph node involvement (N stage) and distant organ metastases (M stage) [10, 11]. These three stages are combined into an overall stage definition, which provides a clinical therapeutic guide for decision-making. Although classification based on TNM and UICC (Union for International Cancer Control) stage provides significant prognostic information and guides therapy strategies, the response and outcome of individual CRC patients to therapy are still under investigation [10, 12]. It is well established to recommend adjuvant chemotherapy for UICC stage III patients and those stage II patients with additional risk factors, however, not all subsets of these patients seem

to benefit from chemotherapy[13]. The same phenomenon is also seen in those stage IV patients who are treated a combination of chemotherapy, radiotherapy and tumor targeted therapy. Most of the studies and multiple central clinical trials suggest that apart from histopathological stage, additional tumor biomarkers may be a better monitoring tool for therapy guidance and outcome prediction of CRC patients. Thus, searching for specific and sensitive tumor biomarker is urgently needed for identifying individual patients at high risk of relapse who might benefit from adjuvant therapy and targeted therapy.

2. Liquid biopsy and genomic detection approach

Undoubtedly, tissue biopsy is always the gold standard for solid tumor diagnosis and having the genomic sources for further molecular detection and analysis, but liquid biopsy might be a suitable platform for the purpose of real-time tracking circulating micro-metastases, monitoring treatment strategy and detecting tumor recurrence after clinical treatment. Liquid biopsy is commonly described as the analysis of circulating tumor-related DNA, RNA and CTC (circulating tumor cells) in the blood of humans and has considerable potential for detection, diagnosis and monitoring of metastases [14]. While protein-based tumor biomarkers have been used in routine pathologic detection for many years, the ability to detect mutations in circulating DNA, RNA and CTC is still a challenge, as pointed out in clinical practice [15, 16]. Furthermore, by using circulating biomarkers, including cfDNA (cell-free DNA), ctDNA (circulating tumor DNA), mRNA (messenger RNA), miRNA (microRNA) and CTCs, supporting circulating metastasis detection and therapeutic strategies, liquid biopsy has the potential of dynamically providing molecular information about carcinomas without invasive tissue biopsy.

As a genomic tumor burden in circulation, ctDNA levels can be used for guiding therapy strategy and efficacy assessment by detecting mutations and alterations of gene methylation, and indicating spread of circulating malignancy [17, 18]. Furthermore, as a proof of principle, it has been shown that high levels of mutant alleles in the plasma are a clear indicator of response to treatment in metastatic colorectal cancer setting [19]. mRNA is a large family of RNA molecules that convey genetic information from DNA to the ribosome, where they specify the amino acid sequence of the protein products by gene expression. The biomarkers that have been analyzed from peripheral blood CTCs or serum/plasma include CEA (carcinoembryonic antigen), CK20 (cytokeratin 20), GCC (guanylyl cyclase C), Survivin, TERT (telomerase reverse transcriptase) and EGFR (epidermal growth factor receptor) [20, 21]. These biomarkers have been detected with variable frequencies and have been shown to possess diagnostic potential and prognostic value[22]. MiRNAs are endogenous 19–22 nucleotides, long non-coding RNA molecules that mediate

post-transcriptional gene silencing by miRNA degradation or the inhibition of translation initiation [23]. Even though several individual miRNAs and miRNA signatures are strongly associated with diagnosis, metastasis and survival, their ability to predict prognosis or response to therapy is still uncertain [23-25]. CTCs are tumor cells present in the peripheral blood of patients with an advanced or metastatic stage that can carry a host of information from primary tumors. Increasing CTC numbers can provide valuable information of tumor relapse or treatment failure, but non-standard isolation approaches with low selective numbers of CTCs from circulation limit their clinical application in early-stage malignancies [26]. In the past few decades, flow cytometry was one of the best techniques for tumor cell detection and enrichment. However, advances in single-cell genomics offer attractive alternatives for capturing information that clarifies cellular identity and function[27]. Together with cytometry technology and single-cell analysis, genetic approaches based on mutation detection and genetic sequencing are now used on CTCs enriched, which will contribute to clinical diagnosis and antitumor treatment.

Recent studies have shown that plasma is a better source of circulating DNA, and highly sensitive quantitative PCR assays might increase the sensitivity of detecting circulating tumor-associated genetic aberrations of mutated alleles [28, 29]. Techniques used for the detection of tumor-associated genetic aberrations include BEAMing (technique based on beads, emulsion, amplification and magnetics) [30], NGS (next-generation sequencing) or WGS (whole-genome sequencing) [31, 32], digital PCR[33, 34], cold-PCR (co-amplification at lower denaturation temperature PCR)[35], MAP(MIDI-activated pyrophosphorolysis) [36] and mass spectrometry genotyping assay-mutant-enriched PCR[37]. All of these techniques of liquid biopsy are based mainly on gene profiling and molecular analysis of DNA or RNA. Additionally, their clinical applicability depends on the costs of detection, high-quality DNA and extensive data analysis with a dedicated tumor bio-information bank [31, 33, 38]. It is important to consider that deep-sequencing of somatic mutations for clinical use is still not routinely performed[39], and it is also urgently necessary to establish suitable personalized panels based on the available sequencing results from tumor cells of individuals undergoing clinical treatment[33, 40, 41].

In summary, unlike tissue biopsies, liquid biopsies can dynamically represent tumor-associated genetic aberrations derived from all cancerous lesions in patients. Based on improved detection platforms and techniques, oncogenes and tumor cell-based liquid biopsies are expected to be widely used in clinical practice[42].

3. CTC enrichment and biomarkers

Unlike other markers of liquid biopsy, CTC can carry and provide more bio-information on living tumor cells in the circulation. The molecular characterization of CTCs is considered as real-time liquid biopsy for patients with cancer metastases[42]. The roles of CTCs in tumor treatment include estimation of the risk for tumor relapse, dynamic monitoring of therapy strategy, identification of targeted biomarkers in therapeutic resistance mechanisms, and illustration of tumor heterogeneity during metastasis processes [42-44]. Because of the extremely low concentration of CTCs in peripheral blood of cancer patients (equal to one tumor cell against the background of millions of leukocytes), the correct enrichment and detection of CTCs in clinical practice remains technically challenging [42, 44]. Approaches to CTC enrichment include a large number of technologies based on the different properties of CTCs that distinguish them from surrounding leukocytes, other are described as physical properties (size, density, electric charges, deformability) and biological properties (expression of cell surface proteins, cellular viability and invasion capacity). The physical-based methods include: DFF (dean flow fractionation)[45], cell density-based enrichment[46], size-based cell enrichment by filtration[47], SSA(selective size amplification)[48], 3D microfiltration[49], ISET (isolation by size of epithelial tumor cells)[50, 51], NanoVelcro CTC Chip[52] and TelomeScan[53] that allows isolation of viable CTCs by their differences in size, density and morphology properties. The advantage of physical properties is based on physical methods to separate CTCs without molecular labeling and cellular binding, but they have the limitation of not removing leukocytes thoroughly and requiring further identification of CTCs separated [54].

It is widely accepted that EpCAM(epithelial cell adhesion molecule), CK(cytokeratin) and CEA are essential biomarkers for CTC enrichment of CRC. Recently, several new biological assays that isolate cells based on the expression of cell surface markers have been developed for improving detection speed and efficiency[43, 55], such as the CellSearch® assay, the Herringbone-CTC chip, and flow cytometry-based approaches which apply EpCAM as positive selection and leukocyte antigen CD45 as negative selection. There are several biological assays for CTC enrichment, including CellSearch® assay[56], CTC-chip[57], Herringbone-chip[58, 59], AdnaTest[60], EPISPOT(Epithelial ImmunoSPOT)[61], MagSweeper [55, 62], Negative depletion CTC enrichment strategy[63], Millennium Sciences IsoFlux[64], Cynvenio Liquid Biopsy platform[43], FACS (Fluorescence activated cell sorting)[65] and FAST (Fiber-optic array-scanning technology) [66]. Among all the biological assays listed, the CellSearch® assay is the only assay approved by FDA (Food and Drug Administration)[67]. The CellSearch® system harvests CTCs by anti-EpCAM-coated magnetic beads, and a subsequent immunocytochemistry process helps to identify CTCs (DAPI+ / CK+ / CD45-) from non-specifically captured leukocytes (DAPI +/ CK- /

CD45+)[67]. The majority of CTC enrichment techniques rely on the expression of EpCAM and CK because of their wide expression in most epithelial malignancies[68]. However, many of these biological selection technologies are criticized for their reliance on cell surface expression of EpCAM to capture CTCs because some tumors down-regulate expression of EpCAM during EMT (epithelial-mesenchymal transition) [69]. During this process, tumor cells lose expression of some specific epithelial markers, including E-cadherin, EpCAM and CK, gain expression of mesenchymal cytoskeletal and adhesion proteins such as vimentin and N-cadherin [70, 71]. The mechanics of EMT also enables epithelial tumor cells to acquire a fibroblast-like morphology during their transition and become aggressive by resisting apoptosis and treatment[72]. Hence, the major limitation of the CTC enrichment approaches based on EpCAM or CK are that they may lose tumor cells lacking expression of epithelial biomarkers, and only enrich CTCs with epithelial expression, which finally obtain CTCs with insufficient molecular information [73]. Unlike EpCAM and CK, CEA is a glycoprotein which is present in human fetal colonic tissues but not in normal adult colon, and increased amounts are associated with adenocarcinoma, especially CRC. Serum CEA level is associated with risk of disease recurrence and tumor progression during treatment or after treatment surveillance [74]. Increasing CEA levels are thought to relate to the increasing risk of higher tumor burden and poorer survival[75]. However, the level of CEA is generated by normal or extra-intestinal cells and less by CRC cells. CEA levels also increase during pregnancy and as a result of smoking. They all limit its use for predicting tumor relapse in CRC patients [74, 76]. Therefore, because of these drawbacks of commonly used biomarkers, more specific and sensitive biomarkers of CRC beyond the influence of EMT processes and other non-neoplastic factors are required for CTC enrichment and isolation.

4. GCC and its ligands

GCC (Guanylyl cyclase C) is a trans-membrane cell surface receptor that functions in the maintenance of intestinal fluid, electrolyte homeostasis and cell proliferation [77]. As an important enzyme in humans, GCC is encoded by the GUCY2C gene, and its expression is restricted to intestinal epithelial cells from duodenum to rectum but not in extra-intestinal tissues [78]. Endogenous ligands such as hormones guanylin and uroguanylin or exogenous ligands like bacterial heat-stable enterotoxin (ST) can bind to the extracellular domain of GCC protein, which facilitates the conversion of cytosolic GTP (guanosine triphosphate) to cGMP (cyclic guanosine monophosphate), then finally activates the cGMP-dependent PKG (protein kinase G) and signaling pathway[20, 79]. In addition to its role in the regulation of fluid and electrolyte balance, GCC also plays a protective role against colorectal tumorigenesis [80], silencing of the GCC

signaling axis by loss of hormone ligands leads to increasing glycolysis, proliferation and leaky intestinal barrier associated with colorectal tumorigenesis [81]. It is noteworthy that although GCC ligands guanylin and uroguanylin are significantly decreased in nearly 90% of all CRCs, expression of GCC receptor persists in CRC [80, 82]. Thus, the extracellular ligand-binding domain of GCC is antigenically unique, indicating a unique set of GCC ligands[77]. Furthermore, the GCC-restricted expression in intestine and its persistence in both primary and metastatic CRCs regardless of location or tumor grade have been confirmed by studies of immunohistochemistry (IHC), in situ ligand binding and RT-PCR [83].

Unlike many targeted antigens, GCC is over-expressed at mRNA and protein levels in >80% of colon and rectal tumors compared to adjacent normal mucosa [83-86]. GCC is also a crucial tumor biomarker for identifying occult metastases in the lymph nodes and peripheral blood associated with the prognosis of CRC due to its highly restricted expression [87]. GCCmRNA was further investigated by multiple previous studies in peripheral blood of CRC patients, extra-intestinal malignancies, non-malignant lesions of the intestine and healthy volunteers by RT-PCR technology. No GCCmRNA was detected in healthy volunteers, non-malignant intestinal lesions or in extra-intestinal malignancies [84, 88, 89]. Comparisons of multiple epithelial cell markers (CK19, CK20, CEA and GCC) have demonstrated that GCC is one of the most sensitive and specific markers of circulating CRC cells [88, 90]. Indeed, GCCmRNA is now thought to be an essential index for searching metastatic CRCs in circulation, predicting tumor relapse and survival of CRC patients [85, 88, 89, 91].

Currently, the major hurdle of liquid biopsy is the absence of sensitive and specific CRC biomarkers for tracking occult tumor cells from blood, lymph node or bone marrow in clinical practice. The limitation of CTC enrichment and isolation approaches based on EpCAM or CK is that only epithelial cell-specific markers are available, which may only catch CTCs with epithelial markers and lose CTCs without epithelial markers[73]. GCC expression was deeply analyzed and reported at mRNA and protein level in all primary and metastatic CRC cells regardless of EMT processes, but not in CTCs. Hence, GCC may fulfill the criteria of a specific and sensitive marker for CTC enrichment from metastatic CRC patients, but further assessment and evaluation of GCC antibody for CTC isolation are required.

Above all, in order to optimize the antibody-based CTC enrichment approach of metastatic CRC patients, we assessed the GCC antibody staining in colon cancer cell lines and leukocytes, combined with previous analyses of GCC detection in tissue samples and peripheral blood, evaluating the possibility of including GCC staining as a CRC-CTC specific biomarker.

Methods

1) List of reagents

Reagent	Company	Catalog Number	Volume
Ethanol (≥99.8%)	ROTH	K928.4	5L
Hydrogen peroxide solution 30 % (w/w) in H_2O	Sigma-Aldrich	H1009-500ML 7722-84-1	500ml
EasySep 10× Red Blood Cell Lysis Buffer	Stem Cell Technologies	#20120	100ml
PBS Dalbecco(w/o Ca^{2+}, Mg^{2+})	Biochrom	L1825	500ml
Fetal Bovine Serum (FBS), heat inactivated	Thermo Fisher Scientific	10500-064	500ml
BD-Vacutainer EDTA Röhrchen (K2EDTA 1.8mg/mL)	BD Bioscience	367525	10ml
BD-Vacutainer Heparin Röhrchen (Li-Heparin 17IU/mL)	BD Bioscience	367526	10ml
EDTA	Sigma-Aldrich	E7889	100ml
37%Formaldehyd	Sigma	F1635	500ml
Hanks salt solution	Biochrom	L2015	500ml
Ultra-pure water	Biochrom	L0020	1000ml
Acetic acid glacial	Sigma-Aldrich	537020	100ml
Trypanblue solution (0.4%)	Sigma	T8154	100ml
Saponin	Biochrom	84510	100g
Hydrazoic acid sodium salt (NaN3)	Merck	8223350250	250g
FcR Blocking Reagent, human	MACS	130-059-901	2ml
Comp Beads Anti mouse IgK	BD Biosciences	51-90-9001229	6ml
Comp Beads Negative Control	BD Biosciences	51-90-9001291	6ml
EasySep® CD45 Depletion Kit (CD45 Cocktail)	Stem Cell Technologies	18259	1ml
EasySep® CD45 Depletion Kit (magnetic nanoparticles)	Stem Cell Technologies	18259	2*1ml
RPMI Medium 1640 (1×)	Thermo Fisher Scientific	21875-034	500ml
DMEM/F12(1:1) (1×)	Thermo Fisher Scientific	11330-032	500ml

Alexa Fluor® 488 Antibody Labeling Kit	Thermo Fisher Scientific	A20181	5 reactions, 100μl each

2) List of buffers and kits

Name	Components
Quantitative PCR kits (Guangzhou Dahui Biotech)	RNA TRIzol, Reaction solution I (350μl/tube) ×1 tube, Reaction solution II (1100μl/tube) ×1 tube, Reverse transcriptase (25μl/tube) ×1 tube, Taq enzyme (12.5μl/tube) ×1 tube, Quantitative standards (50μl / tube) ×4 tube.
Alexa Fluor® 488 antibody labeling kit (Catalog No: A20181)	Alexa Fluor® 488 reactive dye (Component A) 5 vials; Sodium bicarbonate (Component B) ~84 mg; Purification resin, 30,000 MW size–exclusion resin in PBS, pH 7.2, plus 2mM sodium azide (Component C) ~10 mL; Spin columns (Component D) 5 columns; Collection tubes (Component E) 5 tubes.
Pierce Concentrator, PES, 30K MWCO; 0.5ml (Catalog No: 88502)	25 pack for sample volumes of 100-500 μl MWCO:30,000
Acetic acid (2%)	1:50 acetic acid (100%) in PBS
Formaldehyde (1%)	1:37 formaldehyde (37%) in PBS (4°C)
Fresh recommended buffer	PBS + 2% FCS + 2mM EDTA (4°C)
Permeabilization solution 100×	10% Saponin + 5% NaN3 in 5ml Hanks BSS (sterile filtrate)
Permeabilization solution 1×	1:100 permeabilization solution (100×) in Hanks BSS (4°C)
RBC lysis buffer 1×	1:10 RBC lysis buffer (10×) in ultra-pure water (4°C)
PBS+2%FCS 50ml	1ml FCS + 49ml PBS
PBS-3%BSA solution 50ml	48.5ml PBS + 3% Albumin fraction V 1.5ml + NaN3 0.05mg
1ml normal goat serum (1:20 dilution)	50μl normal goat serum + 950μl PBS-3%BSA solution

3) List of devices and materials

Name	Company	Catalog Number
50ml tube	BD Biosciences	352070
15ml tube	BD Biosciences	352096

FACS tube	BD Biosciences	352052
10µl filter tip	Biozym	VT0200
100µl filter tip	Biozym	770100
1250µl filter tip	Biozym	VT0270
Slim piper	Sarstedt Inc	86.1172.001
Cell culture flask, 50ml, 25cm^2	Greiner Bio-one	690175
Cell culture flask, 250ml, 75cm^2	Greiner Bio-one	658175
5ml	Corning Inc	357543
10ml	Corning Inc	357551
25ml	Corning Inc	357525
Reaction vessels 1.6ml blue	Biozym Biotech	710162
Cell Scraper(25cm)	Sarstedt Inc	83.1830
Penicillin-Streptomycin(P/S)	Biochrom	A2213
Pipette reference (0.5-10µl)	Eppendorf	4910 000.018
Pipette reference (10-100µl)	Eppendorf	4910 000.042
Pipette reference (100-1000µl)	Eppendorf	4910 000.069
Pipetus®-akku	Hirschmann Laborgeräte	9907200
EasySep® Magnet	Stem Cell Technologies	18000
Centrifuge 5804 R	Eppendorf	110110364
REAX 2000	Heidolph	541.19
Incubator (400 HY-E)	Bachofer GmbH	B492.1116
Hemocytometer Neubauer improved	Marienfeld Superior	0640030
FACS CANTO II (8 color, blue/red/violet)	BD Biosciences (San Jose, CA 95131)	338962
Kendro Laboratory Products KS9	Kendro	40439758
Kendro Laboratory Products BB6220 0	Kendro	51007494
ABI 7500 Fast Real-Time PCR System	Applied Biosystems	4351104
37°C thermostat(type 1002)	Labortechnik	10611493e
Microscope	Karl Zeiss	471202-9903

4) List of antibodies and isotype controls

Name	Company	Catalog Number	Product format

Mouse anti-human GC-C Antibody (537)	Santa Cruz Biotechnology	sc-100302	100µg IgG2b/1 ml PBS
EnVision Detection Systems Peroxidase/DAB, Rabbit/Mouse	Dako Diagnostics	K406511-2	150 test
Alexa488 fluor® conjugated Goat anti-mouse IgG (H+L)	Jackson Immuno Research Inc	115-545-003	1.5 mg/ml
Alexa fluor® 488 anti-human CD4 mouse IgG2bκ	Biolegend	317420	100 test
GUCY2C(FITC) (2G7)	US Biological	207688-FITC	100µg/100µl
Mouse IgG2bκ Isotype Control FITC	eBioscience	11-4732	0.5 mg/ml
CD45 Cocktail	Stem Cell Technologies	#18259C.1	1ml/50µl
Mouse anti-human EpCAM-PerCPCy5.5	BD Bioscience	347199	20µl /50test
PerCPCy5.5 IgG1 κ (mouse)	BD Bioscience	347221	20µl
Mouse anti-human Cytokeratin-PE (Ck-7 and Ck-8)	BD Bioscience	347204	20µl /50test
PE IgG2aκ (mouse)	BD Bioscience	555574	20µl /100test
Mouse anti-human CD45 Pacific Blue	ExBio	PB-222-T100	100test
Mouse anti-human CD53 Pacific Blue	ExBio	PB-227-T100	100test

5) Characters of CRC cell lines used for GCC antibody staining

Name	**Disease Source**	**Culture Properties**	**Genes Expression**	**Cellular Products**	**Culture Media**
T84 (ATCC® CCL-248™)	CRC, 72 years, male	Adherent	CEA; keratin; GCC	CEA; keratin; GCC	DMEM: F-12 Medium +5% FBS
SW620 (ATCC® CCL-227™)	Dukes' C, 51 years, male	Adherent	CEA	NA	RPMI1640 Medium+10% FBS
SW480 (ATCC® CCL-228™)	Dukes' B, 50 years, male	Adherent	CEA; keratin;	CEA; keratin; TGF beta	RPMI1640 Medium+10% FBS

HCT116 (ATCC® CCL-247™)	CRC, adult, male	adherent	CEA	CEA; keratin	McCoy's 5A Medium+10% FBS
Colo205 (ATCC® CCL-222™)	Dukes' D, CRC, 70 years, male	mixed adherent and suspension	CEA; keratin; IL-10	CEA; keratin IL-10	RPMI1640 Medium+10% FBS
Colo320 (ATCC® CCL-220.1™)	Dukes' C, CRC, 55 years, female	mixed, adherent and suspension	serotonin; norepinephrine ; epinephrine; ACTH; parathyroid hormone	serotonin; norepinephrine ; epinephrine; ACTH; parathyroid hormone	RPMI1640 Medium+10% FBS
LS174T (ATCC® CL-188™)	Dukes' B, CRC, 58 years, female	adherent	CEA, IL-10, IL-6, mucin	CEA, IL-10, IL-6, mucin	EMEM + 10% FBS

6) Overview of conjugated antibodies and ICs used for CTC staining

Staining sorting	Marker	Label	Staining (µl)	IC(µl)	Source	Isotype
Surfaces staining	CD53	Pacific Blue	4	No	mouse	IgG1
	CD45	Pacific Blue	4	No	mouse	IgG1
	EpCAM	PerCPCy5.5	20	1.6	mouse	IgG1κ
	GCC	Alexa 488	2	1	mouse	CD4 IgG2bκ
	GCC	FITC	15	5	mouse	IgG2bκ
	CD4 (IC)	Alexa 488		1	mouse	IgG2bκ
Intracellular staining	CK	PE	15	1.8	mouse	IgG2aκ

1. IHC staining of GCC in rectal cancer and adjacent normal mucosal tissues:

Pairs of rectal cancer tissues and adjacent normal mucosal tissues from the same CRC patients were sliced and incubated in Xylene 2 times for 5 minutes. The slices were incubated with different concentrations of ethanol from 100%, 90%, 80% to 70% for 3 minutes per step, followed by a washing step with distilled water for 3 minutes. As an endogenous peroxidase blocking step, 3% H_2O_2 was added for 5 minutes at room temperature and washed with distilled water 2 times for 3 minutes. As an antigen retrieval step, a water bath was performed in EDTA buffer (PH 9.0) for 20 minutes and slices were cooled at room temperature, washed with distilled water 2 times for 3 minutes, then washed with PBS 2 times for 3 minutes. As an antibody staining step, mouse anti-human GCC monoclonal Antibody (537) (Santa Cruz Bio, Dilution: 1: 200) was added and incubated for 1 hour at room temperature, followed by a washing step with PBS 2 times for 3 minutes. The secondary antibody Goat anti-Mouse Envision Flex (Dako Diagnostics, Glostrup, Denmark, Dilution: 1:100) labeled with HRP was added and incubated at room temperature for 20 minutes, followed by a washing step with PBS 2 times for 3 minutes. Then a coloration step was performed as 5-minute incubation at room temperature with DAB reagent (DAKO Diagnostics, Glostrup, Denmark) followed by a 5-minute washing step with distilled water until cell membrane staining was observed under the microscope. Then slices were counter-stained in hematoxylin for 3 minutes, washed with distilled water for 2 minutes and dehydrated with ethanol gradually from 70% to 80%, 90%, 100% for 2 minutes per step. After adding Xylene, each slice was dried and topped with a coverslip and neutral gum. Finally, specimens were examined and evaluated by two pathologists.

2. GCCmRNA detection from peripheral blood of CRC patients

2.1 Sample collection from CRC patients: Blood samples were drawn simultaneously for the detection of GCCmRNA. Peripheral venous blood was obtained at the time of clinical staging before surgery. The first 2ml blood was discarded in order to minimize the possibility of false-positives by epithelial skin cells and the remaining 5 ml of blood was then collected into EDTA-containing vacutainer tubes. All samples were processed within 2 hours of collection, immediately stored in cryovials, frozen in liquid nitrogen and stored at −80°C until mRNA detection.

2.2 Extraction and detection of RNA: RNA was extracted from peripheral blood with GCCmRNA quantitative PCR kits (Dahui Biotechnology, Guangzhou, China) according to manufacturer's instruction. First, a 5ml blood sample was diluted and 2ml lymphocytes separation medium was added and incubated 5 minutes at 4°C. After centrifuging, the leukocyte layer was carefully drawn off. Then, 0.5ml RNA TRIzol and 0.2ml chloroform were added, after

incubation and centrifuging at 4°C, the upper layer was carefully transferred into sterile centrifuge tubes. After that, an equal volume of isopropanol was added, followed by 10-minutes' incubation and 10-minute centrifugation at 12000rpm, 4°C. The upper supernatant was removed and 75% ethanol was added for washing the RNA precipitate. Then ethanol was carefully drawn out, the precipitate dissolved in DEPC H_2O and the concentration of RNA was determined.

2.3 PCR amplification:

Primer sequences of GCCmRNA:

Up-stream primer 5′ TACGGCTCAATCGCCTTGAC 3′;

Down-stream primer 5′ ATCGTAAGGCTAGCCAGTA 3′;

Taqman probe 5′ -FAM-TCATGCACCGTAACGTAGC-TAMRA- 3′.

Quantitative RT-PCR System was prepared in 0.2-ml sterilized PCR reaction tube as follows: reaction solution II (44.5μl), Taq enzyme (0.5μl), template (PCR product) (5μl), total reaction volume (50μl). A group of positive standards were detected before the experiment. The reaction was performed by a denaturation step of 2 minutes at 93°C followed by 40 cycles from 95°C for 15 seconds to 60°C for 60 seconds.

2.4 GCCmRNA detection: GCCmRNA was detected by an ABI 7500 Fast Real-Time PCR System (Applied Biosystems, Foster City, CA, USA). The concentration of GCCmRNA (unit: gene copy number/μl) was calculated automatically by instrument as follows: A (copy number/μg total RNA) = B (copy number/μl cDNA)/OD260 value of sample RNA×5/6.

3. Optimization of CD45+ cell depletion experiments (from healthy donors)

3.1 Blood sample collection from healthy donors: Peripheral venous blood was obtained before experiments. The first 1 ml of blood was discarded in order to minimize the possibility of false-positives by epithelial skin cells. Then 10ml blood was collected into Heparin vacutainer tubes and stored in an incubator (Bachofer GmbH, Germany, 400 HY-E) at room temperature.

3.2 Tumor cell counting: A certain number of SW620 (colon cancer cell line, ATCC® CCL227™) was spiked in healthy blood for assessing the efficiency of the staining by EpCAM and CK in CD45 depletion approach [92]. T84 cell (colon cancer cell line, ATCC® CCL248™) was used for assessing the staining efficiency of GCC, EpCAM and CK. SW620 and T84 cells were counted by Hemocytometer (Marienfeld Superior, Cat-0640030) and diluted at concentrations of 0, 50, 100, 150, 200 or 300 cells per 1ml PBS.

3.3 Removal of erythrocyte: 20ml 1×RBC lysis buffer (Stem Cell Technology, Cat-20120) was added into a 50-ml tube and kept at room temperature for 15 minutes. 5-ml blood sample was slowly pipetted into RBC lysis buffer, and 0, 50, 100, 150, 200 or 300 tumor cells were pipetted

into each tube. After 15-minute's incubation and 5-minute's centrifuging, supernatant were poured out, tumor cells were re-suspended and washed with 50ml PBS. Then FRB was added and cell suspension was transferred into 5-ml FACS tube (BD falcon, Cat-352052) for cell counting. The total cell number was determined by Hemocytometer, and the required volume of FRB, CD45 beads and cocktails were calculated based on the cell number.

3.4 Removal of CD45+ cells by CD45 depletion: According to the previous protocols [92, 93], FRB was added to obtain a cell concentration of 5×10^7 cells/ml. Human CD45 depletion kits (cocktail, 50µl/ml, EasySep™, StemCell®, Cat-18259 and magnetic beads, 100µl/ml, EasySep™, StemCell®, Cat-18259) were added for leukocyte binding. Tubes with cell suspension were put into magnet (Stem Cell Technology, Cat-18000) to separate CD45+ and CD45- cells. The CD45- supernatant was pipetted into a fresh FACS tube, and supernatants remaining in the tube (labeled with CD45+ leukocytes fraction) were kept as unstained control for the flow cytometry analysis. The CD45- fraction was mixed and divided equally into two FACS tubes as staining sample and IC.

3.5 Additional depletion of CD45+ depleted cells: Here, we supposed that CD45+ leukocytes were combined with magnetic beads and locked on the wall of tubes by magnetic force, which also locked CD45- tumor cells. For the purpose of recovering more tumor cells, additional CD45 depletion of depleted CD45+ solution was performed in our experiments. Hence, after the first cycle of CD45 depletion, additional recycling of tumor cells by washing the wall of the FACS tube with PBS was performed, followed by an additional CD45 depletion.

4. Staining of GCC antibody in SW620 cell and T84 cell:

After CD45 depletion, 10µl FCR blocks were added to block Fc receptor in tumor cells, then surface-staining with antibody and IC was performed as follows: Alexa 488-conjugated Anti GCC antibody (Santa Cruz Biotechnology, Cat sc-100302) 15µl and Alexa fluor®488 anti-CD4 IgG2bκ (Biolegend, Cat-317420) 1µl were used only for staining T84 cells, PerCPCy5.5-conjugated Anti EpCAM antibody (BD, Cat-347199) 20µl, Pacific Blue conjugated CD45 antibody (ExBio, Cat-PB-222-T100) 4µl, Pacific Blue-conjugated CD53 antibody (ExBio, Cat-PB-227-T100) 4µl and PerCPCy5.5 conjugated IgG1κ (BD, Cat-347221) 1.6µl were used for staining SW620 and T84 colon cells. After the surface staining step, 1% formaldehyde and 1×permeabilization solution were added for intracellular staining as follows: PE conjugated CK antibody (BD, Cat-347204) 15 µl and PE conjugated IgG2aκ (BD, Cat-555574) 1.8 µl. Then 250µl PBS were added for flow cytometry analysis, or 1ml 1% formaldehyde was added and samples were kept in dark at 4°C overnight for analysis.

5. Optimization of method stained by GCC antibody:

5.1 Optimization of GCC antibody staining in T84 cell line: We performed experiments for the purpose of optimizing the suitable staining concentration and volume of the primary GCC antibody and the secondary antibody on T84 cells. T84 cells were calculated and diluted at a concentration of 1×10^6 cells/ml PBS. Normal goat serum (1:20 dilution with PBS-3%BSA solution) was added to block Fc receptor in tumor cells. Antibodies and ICs were added as follows: 1) 2µl primary GCC antibody, 2) 5µl primary GCC antibody, 3) 2µl anti-human CD44 APC-conjugated IgG2b (positive control), 4) 2µl CD7-unconjugated IgG2a (positive control), 5) 2µl IL2RA CD25-unconjugated IgG1 (positive control), 6) 2µl PTPRC-unconjugated CD45 (positive control), 7) 2µl PBS (negative control), 8) 5µl FITC-conjugated IgG2a (IC), 9) 5µl FITC-conjugated IgG2b (IC), 10) 5µl Alexa Fluor 488 anti-human CD4 antibody IgG2bκ (IC). All samples were incubated at 4°C in the dark for 1 hour, and 20µl normal goat anti mouse Alexa Fluor 488 was added as secondary staining. Then, all samples were washed with PBS and 200-300µl of PBS was added for analysis.

5.2 Staining of GCC antibody in colon cancer cell lines: Primary GCC antibody with secondary antibody staining in different colon cancer cell lines and two conjugated GCC antibodies (Alexa Fluor 488-conjugated GCC antibody and FITC-conjugated GCC antibody) was performed in the T84 cell line. The colon cell lines T84 (ATCC® CCL248™), SW620 (ATCC® CCL-227™), SW480 (ATCC® CCL-228™), HCT116 (ATCC® CCL-247™), Colo205 (ATCC® CCL-222™), Colo320 (ATCC® CCL-220.1™) and LS174T (ATCC® CL-188™) were diluted to a concentration of 1×10^6 cells/ml, and normal goat serum (1:20 dilution with PBS-3%BSA solution) was added for blocking Fc receptors on tumor cells.

Antibodies were added to six colon cancer cell lines as follows: 1) 2µl primary GCC antibody, 2) 5µl Alexa Fluor 488 anti-human CD4 IgG2bκ (IC), 3) 2µl PBS (negative control), all samples were incubated at 4°C in the dark for 1 hour. Alexa 488-conjugated and FITC-conjugated GCC antibody and IC were used for staining as follows: 1) 1µl primary GCC antibody, 2) 1µl conjugated GCC antibody, 3) 2µl conjugated GCC antibody, 4) 2µl anti-human CD44 APC-conjugated IgG2b (positive control), 5) 2µl CD7 unconjugated IgG2a (negative control), 6) 2µl CD25 unconjugated IgG1 (negative control), 7) 2µl PBS (blank control), 8) 5µl Alexa Fluor 488 anti-human CD4 antibody (IC). All samples were washed with 1ml PBS, normal goat anti mouse Alexa Fluor 488 was added into the tube 1) for secondary staining. Finally, all samples were washed with 1ml PBS and 200-300µl PBS was added for analysis.

6. **Detection of tumor cells by flow cytometry:**

6.1 Method and principle of flow cytometry detection: Flow cytometry is a valuable platform based on cell counting, cell sorting and biomarker detection. By aligning interesting cells in a stream of fluid, flow cytometry can analyze multi-parametric physical and chemical characteristics of samples at a rate of up to thousands of particles per second. Fluorophores are commonly conjugated to specific antibodies that selectively recognize targets on the cell membrane or intracellular structures. Each fluorophore has a characteristic peak excitation and emission wavelength. Therefore, the combination of labels depends on the wavelength of the lasers used to excite the fluorophores and the detectors available[94]. Flow cytometry is widely used in basic research, pathological analysis and clinical practice, especially in fields of transplantation, hematology, tumor and immunology [95-97]. Recently some of the FACS systems were able to deposit single cells in micro-well plates with high purity, enabling researchers to do downstream analyses such as NGS [98].

6.2 Sample analysis by flow cytometry: Before flow cytometry detection, samples were washed with 2ml PBS and centrifuged at 1700rpm, 4°C for 5 minutes; supernatant was poured out and 200-300μl PBS was added. Then samples were analyzed by FACS Canto II. After all the data of interested on samples were recorded, further analyses were performed with software FlowJo7.

7. Collection and assessment of data:

7.1 Collection of patients' clinical data: All patients had undergone surgical treatment in the Surgical Department of Colorectal Cancer of Zhejiang Cancer Hospital, Hangzhou, China. We recruited a total of 80 patients with rectal cancer for IHC analysis of tissue samples and 160 CRC patients for circulating GCCmRNA detection. Peripheral blood samples from five healthy donors were included as negative control. Patients with a known second neoplastic disease or benign intestinal tumors or at stage IV were excluded from the study. Routine pathological examinations were performed for diagnosing of all 240 tumor samples from 240 patients. The clinical follow-up was performed at periodic intervals with CT scan, tumor biomarker detection and colonoscopy, as well as letter, telephone and comprehensive review, in order to ascertain whether the patients were alive or dead, and evaluate whether they had developed local recurrences or distant organ metastases. All study protocols were approved by the Institutional Review Board and informed consent was obtained from all study participants.

7.2 Scoring and assessment of IHC staining: The semi-quantitative score system and assessment were used as generate overall scoring for each tissue sample, only clear staining on

the tumor cell membrane was considered positive reaction, while diffuse cytoplasmic or granular staining was diagnosed as negative. Based on this approach, the overall staining index (score values 0-12) was determined by multiplying scores for staining intensity and the scores for positive percentage per visible area by microscope [83]. Staining intensity was scored as follows: 0, negative; 1, weak; 2, moderate; and 3, strong. And the frequency of positive cells was defined as follows: 0, less than 5%; 1, 6%-25%; 2, 26%-50%; 3, 51%-75% and 4, 75%-100%. Finally, overall scores were then recorded as indexes into four categories as follows: negative (score 0), weak (score 1-4), moderate (score 5-8) and strong (score 9-12). Chi-square tests were performed to examine the relationship of IHC staining scores of GCC antibody with other clinical and pathological characteristics. Further, IHC staining of GCC was compared between rectal cancer and normal mucosal tissues by rank sum test based on overall scores of GCC staining. All statistical tests were two-sided and had a 95% CI (confidence interval), $P<0.05$ was considered statistically significant. All statistical analyses were performed using PASW statistics software version 23.0 (SPSS Inc, Chicago, IL, USA).

7.3 Statistical assessment of circulating GCCmRNA: We selected a cut-off value of 500 copies for GCC mRNA based on (1) the manufacturer's instructions and internationally used cut-off levels, (2) previous results [99]. The GCCmRNA copy numbers were stratified by clinical stage for comparison with DFS and OS. Those clinic-pathologic characteristics that showed significant association with DFS and OS in univariate analysis were added for multivariate Cox regression model analysis equivalent to Backward Stepwise selection (Conditional LR). Multivariate analysis was carried out to estimate the HR (hazard ratio) for survival according to mRNA copy numbers adjusted by other characteristics. Kaplan-Meier curves with Log-rank test were also computed to evaluate OS or DFS for given GCCmRNA levels and clinico-pathologic variables. All statistical tests were two-sided and had a 95% CI, $P<0.05$ was considered statistically significant. All statistical analyses were performed using PASW statistics software version 23.0 (SPSS Inc, Chicago, IL, USA).

Results

1. IHC staining of GCC in samples of tumor tissues and normal mucosal tissues of the rectum (Data from patients treated in the Surgical Department of Colorectal Cancer in Zhejiang Cancer Hospital, Hangzhou, China):

1.1 Clinico-pathologic characteristics of rectal cancer patients: Detailed information on clinic-pathological characteristics of the patients and their relationship with 5 years DFS and OS can been found in supplementary table 1. The mean age was 53.23 years (range from 38 to 76 years) and the study population comprised of 44 (36.9%) males and 36 (63.1%) females. Based on UICC Classification of Colorectal Cancer, 15 patients (19.4%) were classified as stage I, 22 patients (36.3%) as stage II and 43 patients (44.4%) as stage III. Among all those clinical-pathological characteristics, only tumor emboli in vessels showed significant correlation with 5 years OS (HR 0.163, 95 % CI 0.027 to 0.976, P=0.047).

1.2 GCC expression in tumor tissues and normal mucosal tissues of the rectum: The intensity of GCC staining were separated into four degrees (negative, weak, moderate and strong) with three magnifications (×20, ×100, ×400), to better assess and compare the GCC expression in tumor and normal mucosal tissues of the rectum (see Figure 1A, 1B, 1C, 1D, original magnification ×20, ×100, ×400):

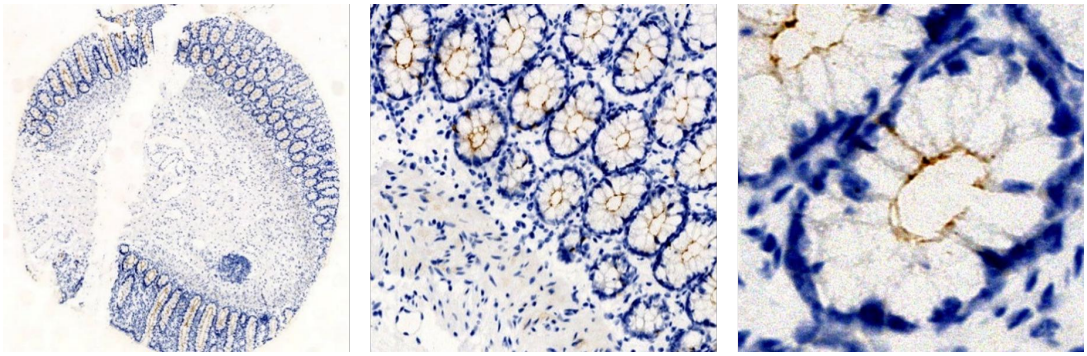

Normal ×20 Normal ×100 Normal ×400

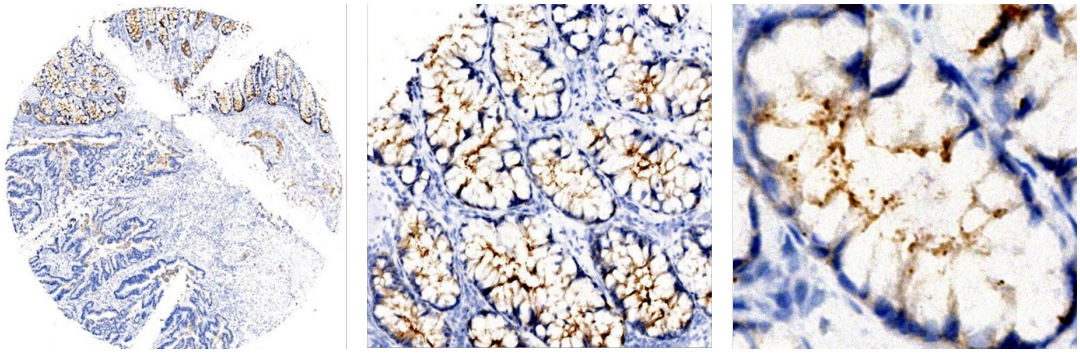

Cancer ×20 Cancer ×100 Cancer×400

Figure 1A Expression of GCC protein (**negative**) in cancer tissues and normal mucosal tissues of the rectum with magnification ×20, ×100 and ×400.

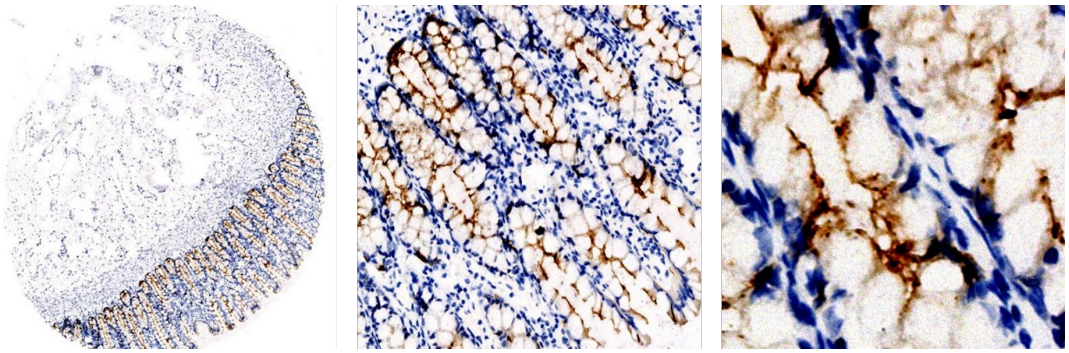

Normal ×20 Normal ×100 Normal ×400

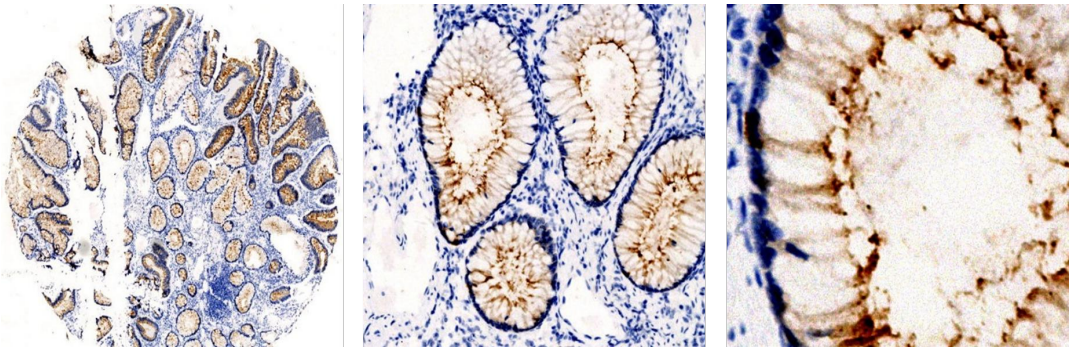

Cancer×20 Cancer×100 Cancer×400

Figure 1B Expression of GCC protein (**weak**) in cancer tissues and normal mucosal tissues of the rectum with magnification ×20, ×100 and ×400.

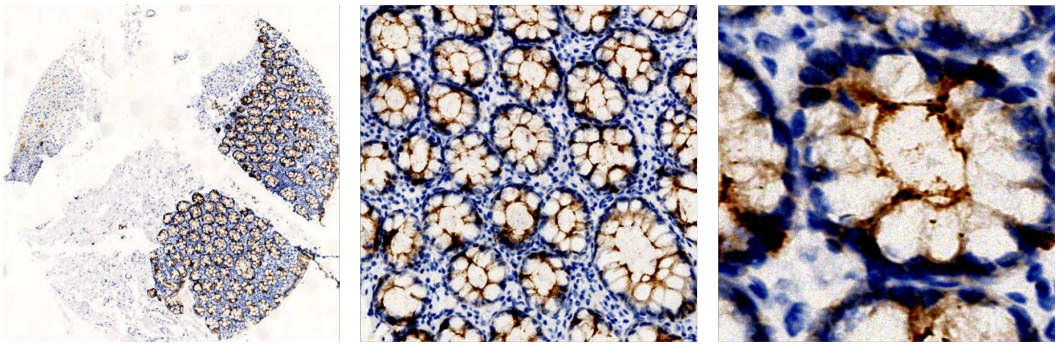

Normal ×20 Normal ×100 Normal ×400

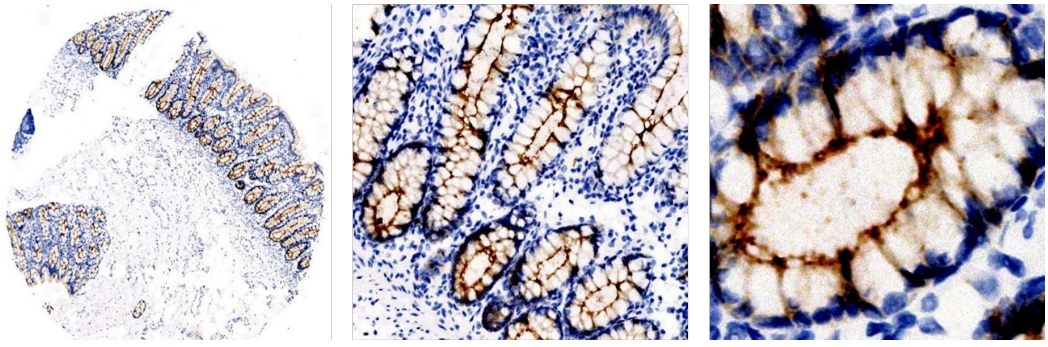

Cancer×20 Cancer×100 Cancer×400

Figure 1C Expression of GCC protein (**moderate**) in cancer tissues and normal mucosal tissues of the rectum with magnification ×20, ×100 and ×400.

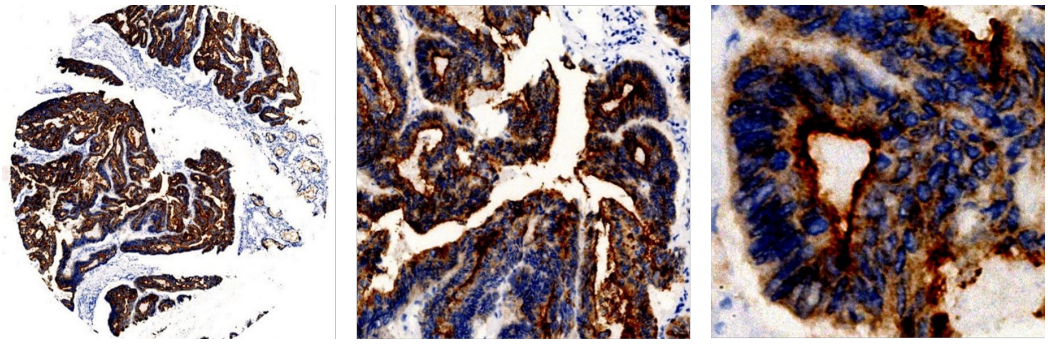

Cancer×20 Cancer×100 Cancer×400

Figure 1D Expression of GCC protein (**strong**) in cancer tissues of the rectum (no strong staining is found in normal mucosal tissues of the rectum) with magnification ×20, ×100 and ×400.

1.3 Comparison of GCC staining in tumor tissues and normal mucosal tissues of the rectum: As illustrated in Figure 2 and Figure 3, higher GCC expression in tumor tissues than in normal mucosal tissues of rectum was observed, and the difference of GCC intensity highlight GCC overexpression in tumor tissues at higher frequencies than those in adjacent normal mucosal tissues of the rectum. Wilcoxon test was used to compare the GCC expression between tumor and adjacent normal mucosal tissues of the rectum (table 1). Based on positive ranks (normal>cancer), Z value of Wilcoxon test showed significant GCC protein overexpression in tumor tissues compared with normal mucosal tissues of the rectum.

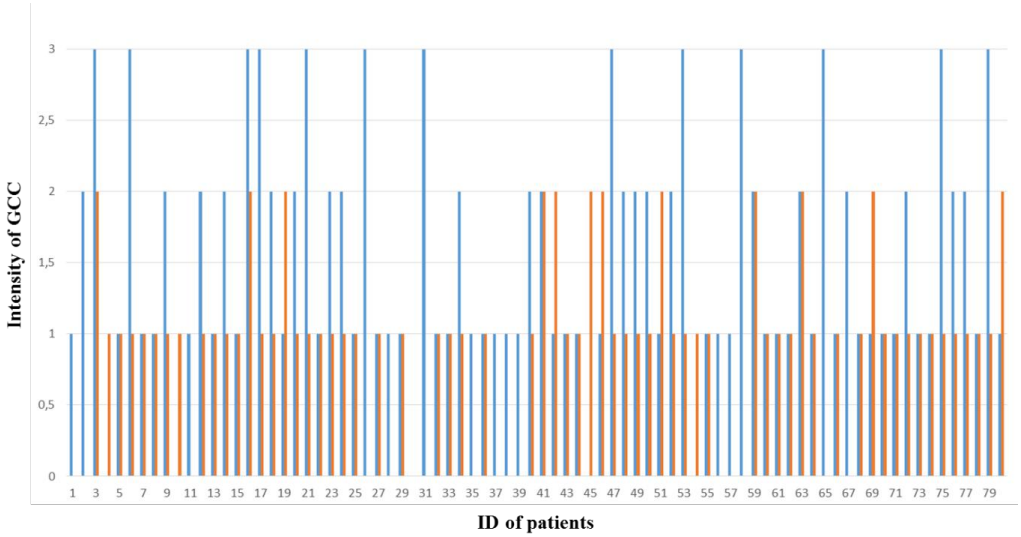

Figure 2 Intensity of GCC expression in paired tumor and normal mucosal tissues of rectum. The blue column indicates intensity of GCC expression in rectal tumor tissues, the orange column indicates intensity of GCC expression in rectal normal mucosal tissues, no column indicates no GCC expression. The number in vertical axis indicates intensity of GCC staining, and each number in lateral axis refers to corresponding patient.

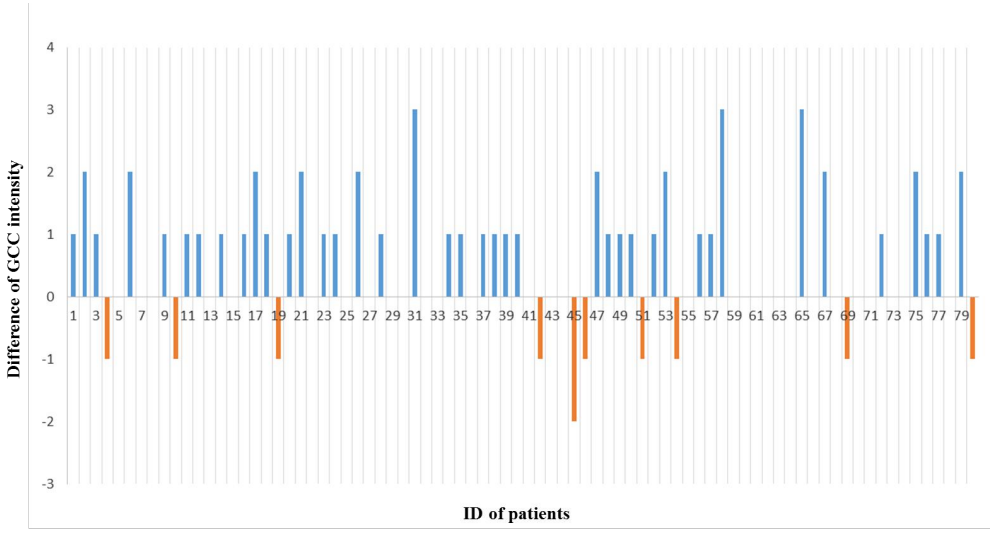

Figure 3 Comparison of GCC intensity between paired tumor and normal mucosal tissues of rectum. The blue column indicates GCC intensity in tumor tissues higher than normal mucosal tissues of the rectum, the orange column indicates GCC intensity in tumor tissues lower than normal mucosal tissues of rectum, no column indicates same intensity of GCC expression in paired rectal tumor and normal mucosal tissue. The number along the vertical axis indicates intensity of GCC staining, and each number along the lateral axis refers to the corresponding patient.

Table 1 Comparison of GCC expression in tumor tissues and normal mucosal tissues of rectum

Intensity of GCC expression	normal < cancer	normal > cancer	normal = cancer	Total
Number of paired samples	40	10	30	80
Wilcoxon test: Z value				-4,352[d]
Asymptotic Significance (2-sided)				<0.001*

d. Based on normal > cancer. *: P<0.05, indicates significant.

2. GCCmRNA detection in peripheral blood of CRC patients (data on patients treated in the Surgical Department of Colorectal Cancer in Zhejiang Cancer Hospital, Hangzhou, China):

2.1 Clinico-pathologic characteristics of patients: The mean age was 56.78 years (range from 29 to 84 years). The study population comprised of 101 (36.9%) males and 59 (63.1%) females, with 60 (37.5%) colon carcinomas and 100 (62.5%) rectal carcinomas. Based on UICC Classification of Colorectal Cancer, 31 patients (19.4%) were classified as stage I, 58 patients (36.3%) as stage II and 71 patients (44.4%) as stage III (see supplementary table 2). Stages II and

III patients at risk for metastasis were treated with standard venous or oral chemotherapy regimens. Altogether, 59 patients (36.9%) received only surgical treatment, while 37 patients (23.1%) also received oral chemotherapy and 64 patients (40.0%) also received venous chemotherapy after surgical treatment. The higher GCCmRNA levels in peripheral blood were significantly associated with tumor emboli in vessels (P<0.001), lymph node metastases (P=0.044), mesenteric root lymph node metastases (P=0.008), poorer DFS (P<0.001) and poorer OS (P<0.001) (table 2).

Table 2 Association of circulating GCCmRNA level and clinical characteristics

Variables	Total n =160(%)	GCC mRNA >500 copies/μl	
Tumor emboli in vessels		n (%)	P value
No	121(75.63%)	30(24.79%)	
Yes	39(24.37%)	27(69.23%)	<0.001*
Lymph node metastases			
No	90(56.25%)	26(28.89%)	
Yes	70(43.75%)	31(44.29%)	0.044*
Mesenteric root lymph node metastases			
No	149(93.13%)	49(32.89%)	
Yes	11(6.87%)	8(72.73%)	0.008*
Survival status			
alive	140(87.50%)	40(28.57%)	
dead	20(12.50%)	17(85.00%)	<0.001*
Disease Free status			
No	124(77.50%)	33(26.61%)	
Yes	36(22.50%)	24(66.67%)	<0.001*

Subjects' demographics and clinical characteristics are represented as n (%). Dispersion of GCC mRNA levels are summarized as n (%) for a given subjects' demographic and clinical characteristic and compared using a non-parametric method, Mann–Whitney U test or Kruskall Wallis test, due to the ordinal data type of GCC mRNA level.
*: P<0.05, indicates significantly associated with subjects' demographics and clinical characteristics.

2.2 Correlation of patients' characteristics with DFS and OS in the overall population: Univariate Cox regression model analysis demonstrated that poor DFS was significantly associated with the presence of GCCmRNA>500 copies/μl in blood, tumor emboli in vessels, lymph node metastases, mesenteric root lymph node metastases, ulcerative pathological type, poor differentiation type, TNM stage III and high CA199 values in peripheral blood (total P value

<0.05). While GCCmRNA>500 copies/μl in blood, CK20mRNA >500 copies/μl in blood, tumor emboli in vessels, lymph node metastases, mesenteric root lymph node metastases, poor differentiation type and tumor size larger than 5 cm were significantly associated with poor OS (total P value <0.05) (see supplementary table 3).

2.3 Kaplan Meier survival curve analysis of DFS and OS: Based on data published in previous articles [17, 24], we selected variables which had a P value <0.05 in our univariate Cox regression model analysis, and analyzed them by using a multivariate Cox regression model method equivalent to Backward Stepwise (conditional LR) analysis. We used Kaplan Meier survival curves to evaluate the relationship of DFS or OS with the following five prognosis-related factors which showed significant differences in univariate and multivariate Cox regression model analysis: 1) GCCmRNA levels (Fig 4A, 4B), 2) emboli in vessels (Fig 4C), 3) mesenteric root lymph node metastases (Fig 4D, 4F), 4) peripheral blood CA199 levels (Fig 4E) and 5) differentiation type (Fig 4G). A log-rank test showed a significant difference in OS and DFS rates with GCCmRNA levels and other relative characteristics (all P<0.05).

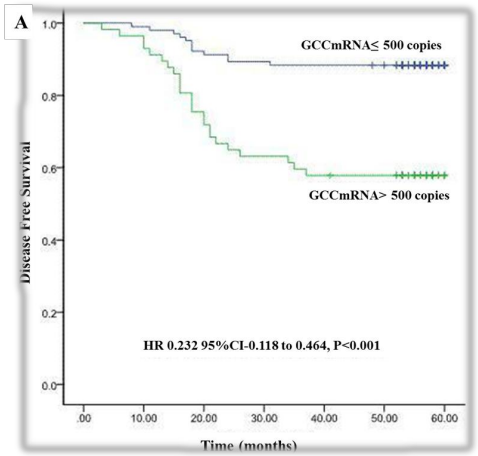

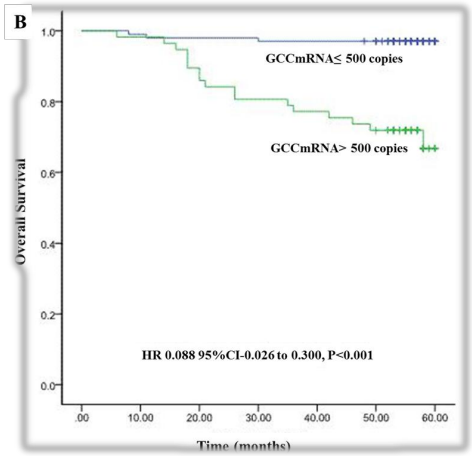

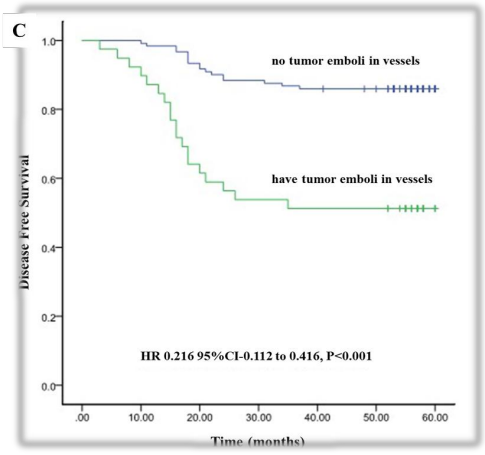

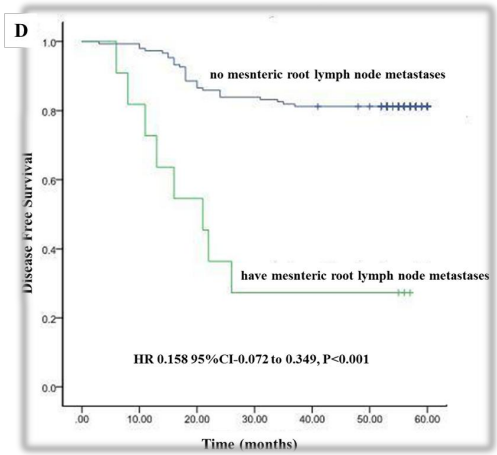

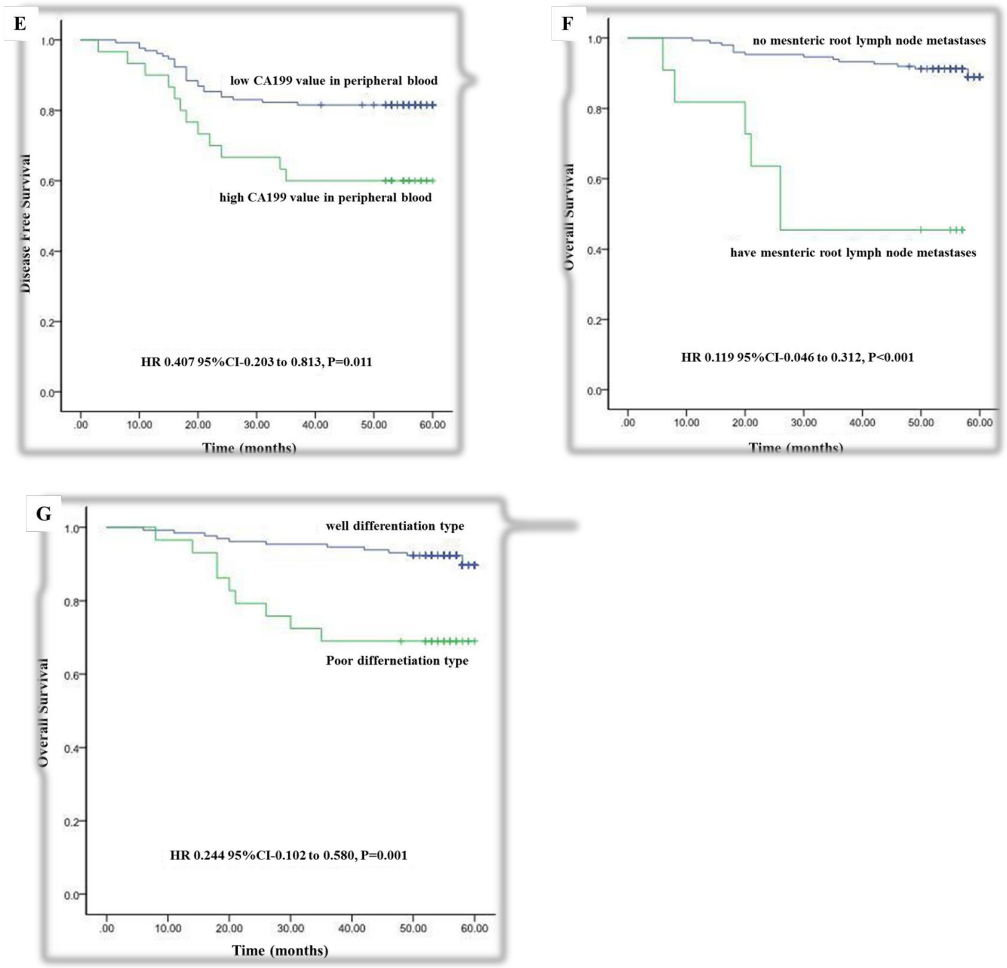

Figure 4 Kaplan Meier survival analysis of DFS and OS. Kaplan Meier survival curves indicate DFS with GCCmRNA (Fig 4A), tumor emboli in vessels (Fig 4C), mesenteric root lymph node metastases (Fig 4D), peripheral blood CA199 levels (Fig 4E) and OS with GCCmRNA (Fig 4B), mesenteric root lymph node metastases (Fig 4F), differentiation type (Fig 4G).

2.4 Kaplan Meier survival curve analysis of GCCmRNA levels by stage stratification: We further selected GCCmRNA for univariate survival analysis based on TNM stratification because of the significant association of GCCmRNA with DFS and OS. According to the stage stratification, Kaplan Meier survival curves showed a significant association between poor DFS and poor OS with high GCCmRNA in stages I, II and III (see Figure 5, total P value<0.001).

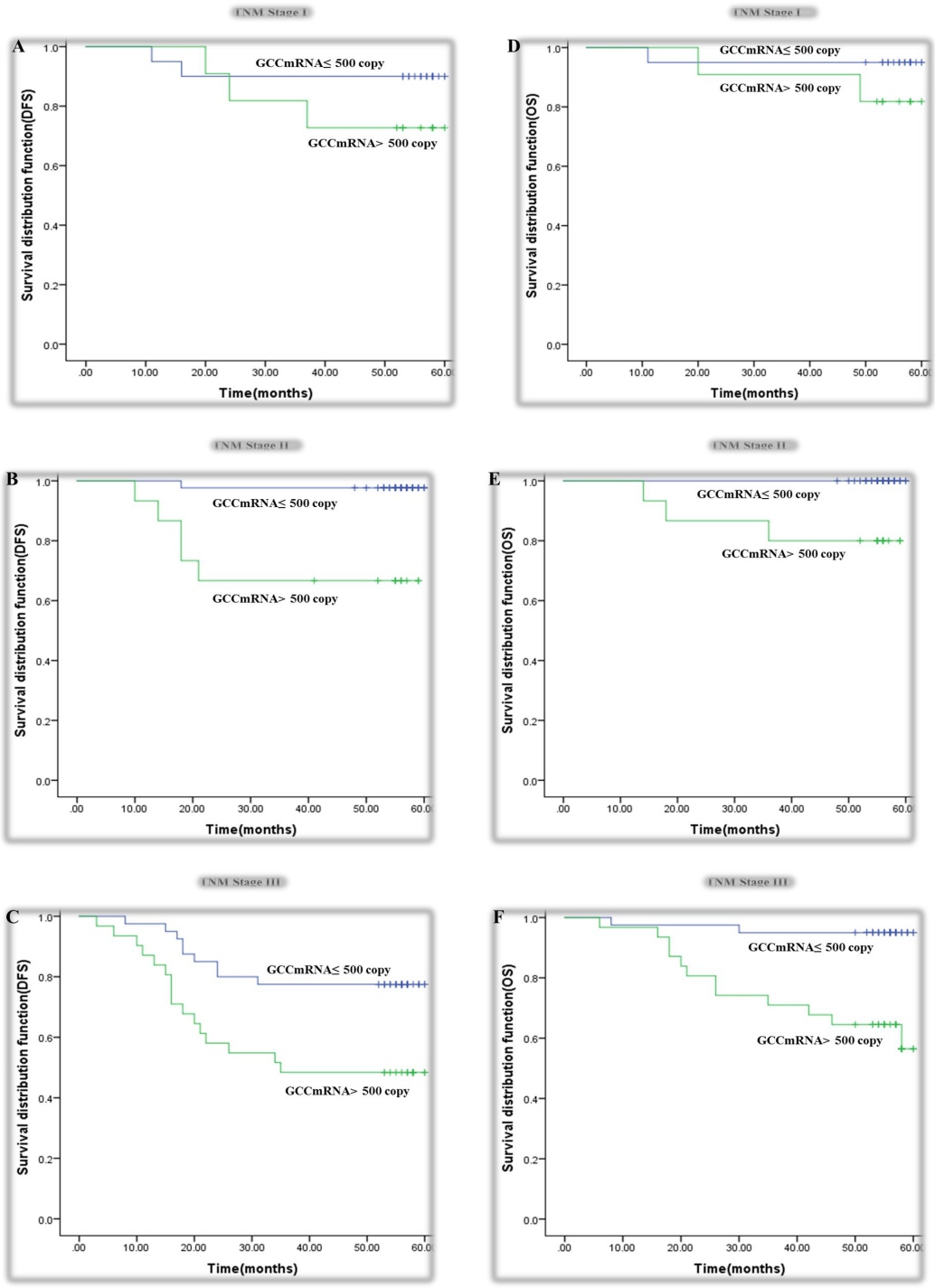

Figure 5 Kaplan Meier survival analysis of GCCmRNA levels with DFS and OS by stage stratification. Kaplan Meier survival curves indicate GCCmRNA levels higher than 500 copies/μl related to poor DFS in A (stage I), B (stage II), C (stage III) and poor OS in D (stage I), E (stage II), F (stage III) (total P value<0.001).

2.5 Multivariate Cox regression analysis of DFS and OS (with or without stage stratification): Multivariate Cox statistical survival analyses showed a significant association between 1) DFS and GCCmRNA level, tumor emboli in vessels, tumor location, mesenteric root

lymph node metastases, CA199 levels and 2) OS and GCCmRNA levels, mesenteric root lymph node metastases and differentiation types (see supplementary table 4 and 5). Stratified with TNM stage, multivariate Cox statistical survival analyses showed a significant association of poor DFS with GCCmRNA>500 copies/μl in peripheral blood, presentation of mesenteric root lymph node metastasis and tumor located in colon. The same significant association of poor OS with GCCmRNA>500 copies/μl in peripheral blood, presentation of mesenteric root lymph node metastasis and poor differentiation type were also observed in statistical analysis. Based on multivariate Cox regression analysis, we get the following equations of multivariate Cox regression model of DFS and OS:

Multivariate Cox regression model equation of DFS:

$$h(t, x)=h0(t, x) \exp(1.218X_1+0.919X_2+0.916X_3+0.868X_4-0.722X_5)$$

Multivariate Cox regression model equation of DFS with stage stratification:

$$h(t, x)=h0(t, x) \exp(1.305X_1+1.096X_3-0.768X_5)$$

Multivariate Cox regression model equation of OS:

$$h(t, x)=h0(t, x) \exp(2.245X_1+1.307X_3+1.312X_6)$$

Multivariate Cox regression model equation of OS with stage stratification:

$$h(t, x)=h0(t, x) \exp(2.173X_1+1.380X_3+1.310X_6)$$

X_1: GCCmRNA in peripheral blood, X_2: tumor embolus in vessel, X_3: Mesenteric root lymph node metastasis, X_4: CA199 value, X_5: tumor location, X_6: differentiation type.

2.6 Assessment of GCCmRNA in multivariate Cox regression model: By data analysis we found that GCCmRNA was the major high-risk factor in multivariate Cox regression analysis of DFS and OS. As an exploratory analysis we took GCCmRNA out of the multivariate Cox regression model in order to assess the strength of GCCmRNA. As results, we found out, regardless of whether GCCmRNA was included in multivariate Cox regression model or not, GCCmRNA always had a greater influence on DFS and OS than other factors in the model. A further likelihood ratio test showed that GCCmRNA was the most important factor ($P<0.001$) which should not be excluded from multivariate Cox regression model of DFS and OS (see tables 3, 4 and 5).

Table 3 Multivariate Cox regression model analysis of DFS

	DFS (exclude GCCmRNA)			DFS (include GCCmRNA)		
	B	Sig.	Exp(B) 95% CI	B	Sig.	Exp(B) 95% CI
GCCmRNA in peripheral blood	exclude	exclude	exclude	1.218	0.001	3.382(1.599, 7.153)
Tumor embolus in vessel	1.246	0.001	3.475(1.658, 7.284)	0.919	0.019	2.507(1.162, 5.409)
Mesenteric root lymph node metastasis	1.033	0.023	2.809(1.154, 6.839)	0.916	0.039	2.500(1.049, 5.959)
CA199 values				0.868	0.016	2.383(1.175, 4.831)
Tumor location				-0.722	0.039	0.486(0.244, 0.966)

Table 4 Multivariate Cox regression model analysis of OS

	OS (exclude GCCmRNA)			OS (include GCCmRNA)		
	B	Sig.	Exp(B) 95% CI	B	Sig.	Exp(B) 95% CI
GCCmRNA in peripheral blood	exclude	exclude	exclude	2.245	<0.001	9.440(2.708, 32.910)
Mesenteric root lymph node metastasis	1.208	0.030	3.345(1.121, 9.980)	1.307	0.012	3.695(1.327, 10.288)
Differentiation type				1.312	0.005	3.714 (1.486, 9.283)
Tumor embolus in vessel	1.328	0.014	3.773(1.306, 10.902)			
CK20mRNA in peripheral blood	0.992	0.038	2.696(1.057, 6.879)			

Table 5 Effect of GCCmRNA level in multivariate Cox regression model

	-2 Log Likelihood		Difference of (1) and (2)	Chi-square	df	Sig.
	Exclude GCC(1)	Include GCC(2)				
DFS	332.965	316.737	16.228	32.456	1	<0.001
OS	171.023	160.503	10.52	21.04	1	<0.001

3. Optimization of negative enrichment approach of CTCs

3.1 Negative enrichment of CTCs (blood samples from healthy volunteers): Defined amounts of SW620 colon cancer cells (0 cells, 25 cells, 50 cells, and 100 cells) were spiked in blood from healthy volunteers. SW620 cells were characterized as EpCAM+/CK+/CD45- human colon tumor cells and imitated as CTCs of CRC patients; protocol efficiency was assessed by the recovery rate of EpCAM and CK labeled SW620 cells after CD45 depletion. In our results, the recovery rate of SW620 cells ranged from 46% to 66% (average rate 54%) by EpCAM and CK double positive staining, while for only CK positive staining the average recovery rate was 188.50%, and 89.25% for only EpCAM positive staining (see table 6 and supplementary table 6).

Table 6 Recovery rate of SW620 cell double stained by CK and EpCAM

Total cells added Number	EpCAM- CK+ Number (percentage %)	EpCAM+ CK- Number (percentage %)	EpCAM+ CK+ Number (percentage %)	Only CK+ Number (percentage %)	Only EpCAM+ Number (percentage %)
25	17 (68%)	7(28%)	12(48%)	29(116%)	19 (76%)
50	70(140%)	19(38%)	25(50%)	95(190%)	44 (88%)
50	56(112%)	28(56%)	23(46%)	79(158%)	51(102%)
50	116(232%)	27(54%)	24(48%)	140(280%)	51(102%)
50	78(156%)	8(16%)	33(66%)	111(222%)	41 (82%)
50	44 (88%)	3 (6%)	33(66%)	77(154%)	36 (72%)
100	172(172%)	62(62%)	52(52%)	224(224%)	114(114%)
100	108(108%)	22(22%)	56(56%)	164(164%)	78 (78%)
Average rate	134.50%	35.25%	54%	188.50%	89.25%

3.2 Optimization of negative enrichment approach: In order to optimize the recovery rate of SW620 cells by negative enrichment, SW620 colon cancer cells were divided into two subgroups with a normal amount of CD45 cocktail (50µl/ml) +magnetic beads (100µl/ml) and high amount of CD45 cocktail (62.5µl/ml) +magnetic beads (125µl/ml). Furthermore, we postulated that in magnetic force, some of CD45- tumor cells were locked or fixed on the wall of the FACS tube by CD45+ leukocytes clumps (see Figure 6), and potentially removed together with CD45+ leukocytes after the CD45 depletion step. To increase the recovery rate of tumor cells, an additional depletion step was performed for the depleted CD45+ cells fraction, followed by CK and EpCAM double staining, to investigate and detect those SW620 cells that

were caged by CD45+ leukocytes clumps (see Figure 7). Different groups of SW620 cells (50, 75, and 150 cells) were recovered and detected to confirm the reliability of the results.

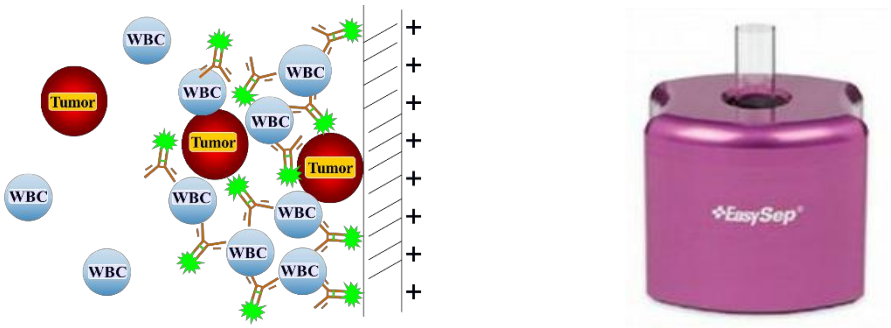

Figure 6 Illustration of tumor cells losing during CD45 cell depletion step. Tumor cells(red) are locked on the wall of FACS tube by leukocytes(blue) clumps in magnet.

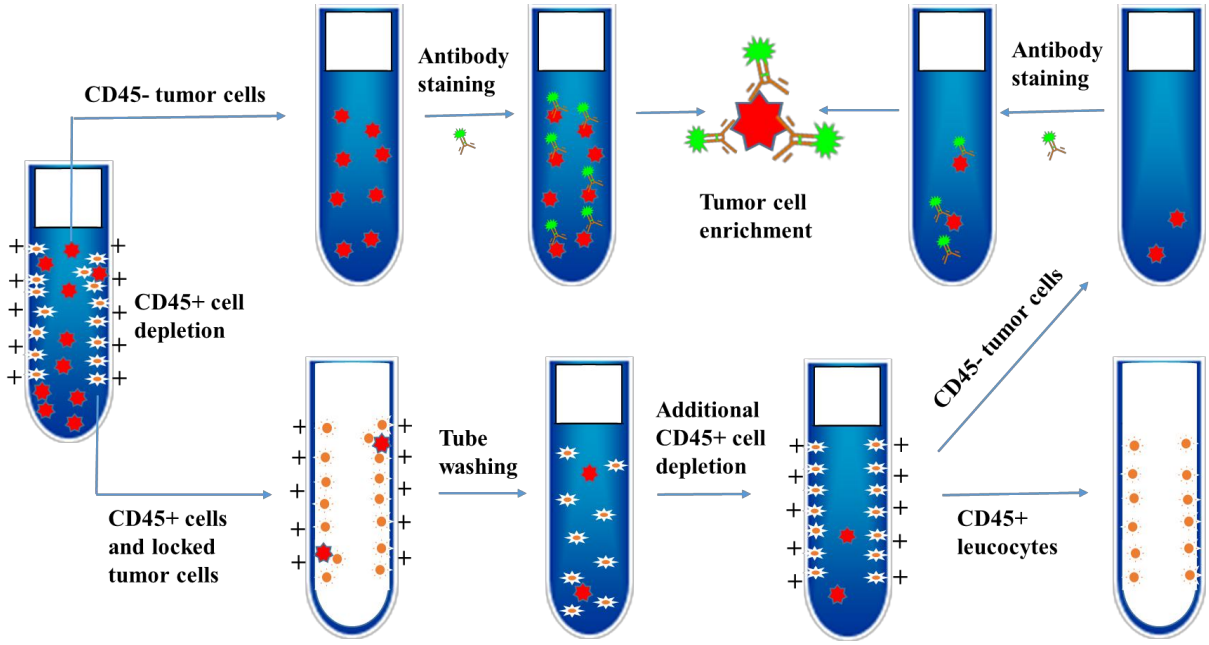

Figure 7. Illustration of improving recovery rate by additional depletion of depleted CD45+ cells. The locked tumor cells(red) are recovered by additional depletion of depleted CD45+ cell clumps(white) in the FACS tube and antibody(green) staining.

Our results showed that nearly 60.85% of SW620 cells (range from 52%~70%) were recovered by one CD45 depletion, while an average of 16.23% SW620 cells (range from 2.67%~28%) were recovered by an additional depletion step, which increased the total recovery rate to 77.00% (range from 59%~94%). The tumor cell recovery rate by normal dosage of CD45 cocktail and magnetic beads was higher than high dosage. Furthermore, all samples showed a increasing recovery rate with an average of 16.23% by additional depletion from the depleted CD45+ cell

fraction (see table 7 and supplementary table 7). As shown in Figure 8, the recovery rate of SW620 colon cell is 60.67% (91/150) by normal depletion and 23.33% (35/150) recovery rate by an additional depletion, which increased the total recovery rate up to 84% (126/150).

Table 7 Recovery rate of SW620 cells by normal and additional CD45 cell depletion

Group	A1	B1	A2	B2	A3	B3	Average recovery rate
SW620 cells in blood samples	150	150	75	75	50	50	
Recovery rate by one round CD45 depletion	91/150 (61.09%)	78/150 (52.00%)	48/75 (64.00%)	39/75 (52.00%)	35/50 (70%)	33/50 (66%)	60.85%
Recovery rate by CD45 depletion from CD45+ solution	35/150 (23.33%)	34/150 (22.67%)	2/75 (2.67%)	5/75 (6.7%)	7/50 (14%)	14/50 (28%)	16.23%
Total recovery rate	126/150 (84.00%)	112/150 (74.67%)	50/75 (66.67%)	44/75 (58.67%)	42/50 (84%)	47/50 (94%)	77.00%

Group A added normal usage of cocktail and beads, group B added high dosage of cocktail and beads,

1, 2, 3 indicate subgroups of 150, 75 and 50 SW620 colon cancer cells added in and recovered.

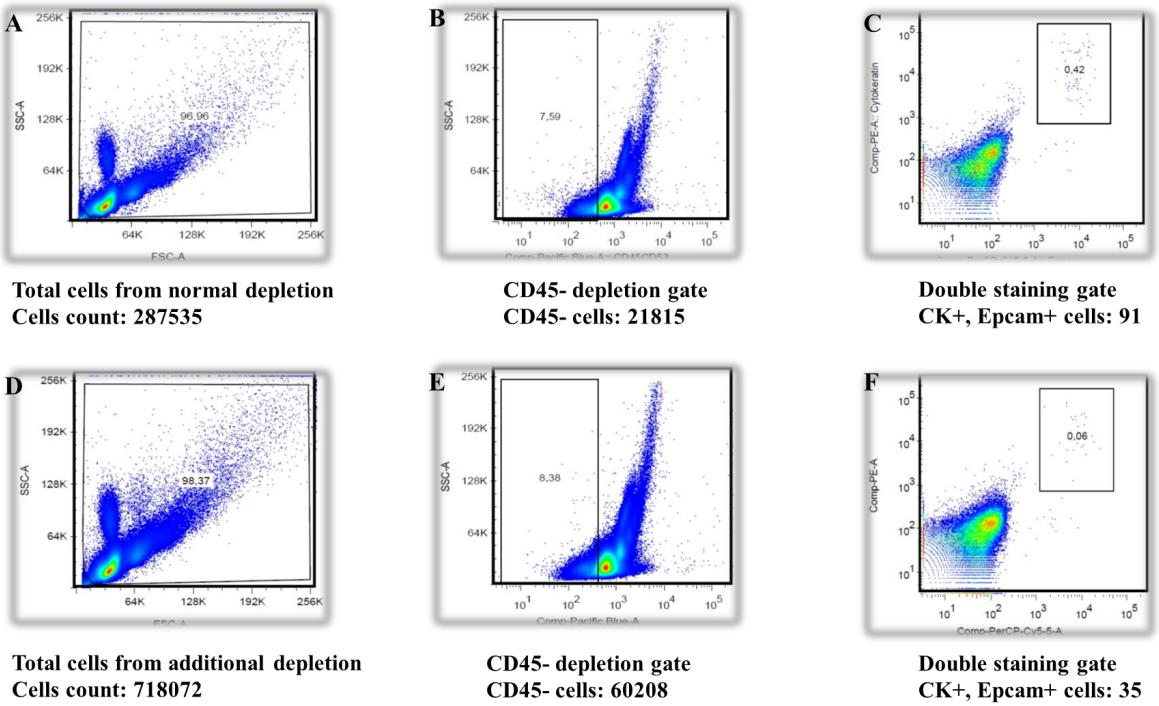

Figure 8 Increased recovery rate by additional depletion (total 150 SW620 cells added in and recovered). A, B, C show 60.67% (91/150) SW620 cells recovered by CK and EpCAM double staining from normal depletion. D, E, F show additional 23.33% (35/150) SW620 cells recovered by additional depletion of depleted CD45+ cells fraction and CK and EpCAM double staining.

4. GCC expression in different colon cancer cell lines We tested GCC expression in different colon cancer cell lines by antibody staining. The results showed a low positive rate of GCC expression in SW480 (8.26%), SW620 (8.88%), HCT116 (2.94%), Colo205 (7.30%) and Colo320 (6.17%) colon cancer cell lines, and moderate positive rate in LS174T colon cells (43.41%) (See Fig 9 and table 8). Interestingly, an unexpected high GCC positive rate was observed (ranged from 53.12% to 97.01%) in almost all colon cancer cell lines at their first passage after thawing from frozen tubes in nitrogen (See Figure 10 and table 8).

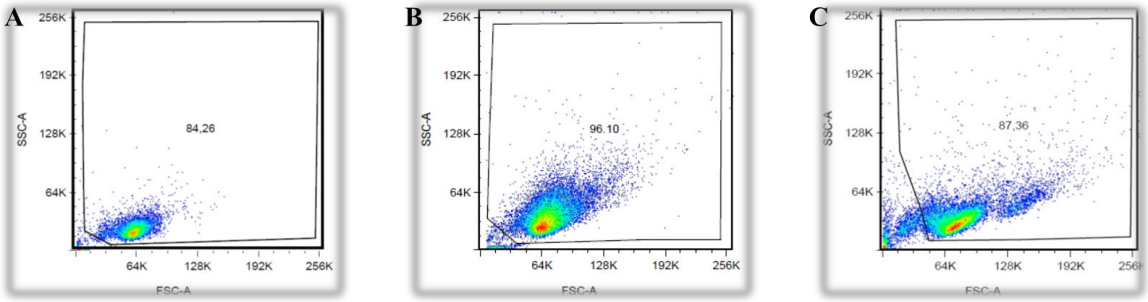

SW620 cell line
Total cells: 8426

SW480 cell line
Total cells: 19221

HCT116 cell line
Total cells: 17471

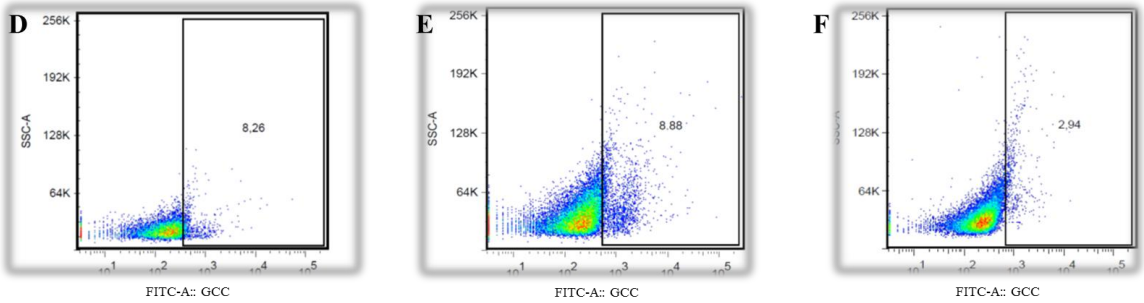

SW620 cell line
GCC+ cells: 723

SW480 cell line
GCC+ cells: 1707

HCT116 cell line
GCC+ cells: 513

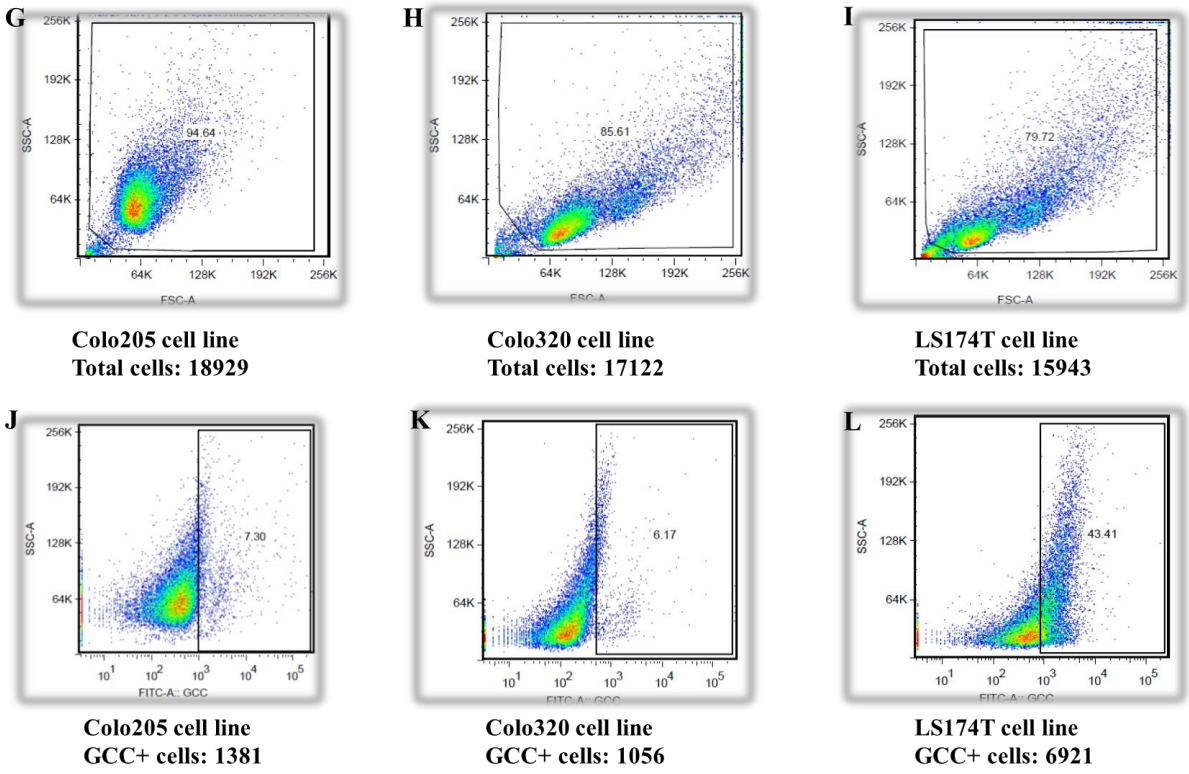

Figure 9 GCC antibody staining in six colon cancer cell lines. A, B, C, G, H and I show SW620, SW480, HCT116, Colo205, Colo320 and LS174T colon cancer cell lines for staining in scatter plot; D, E, F, J, K and L show GCC+ gate of six colon cancer cell lines.

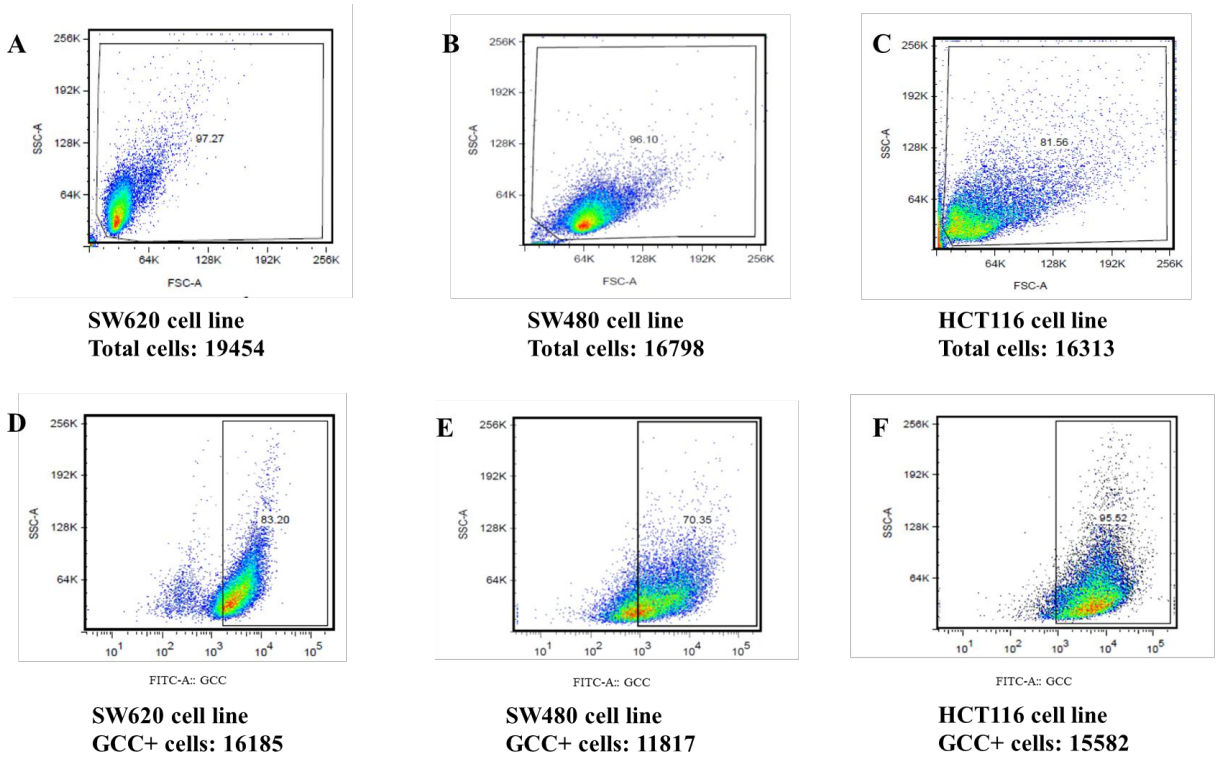

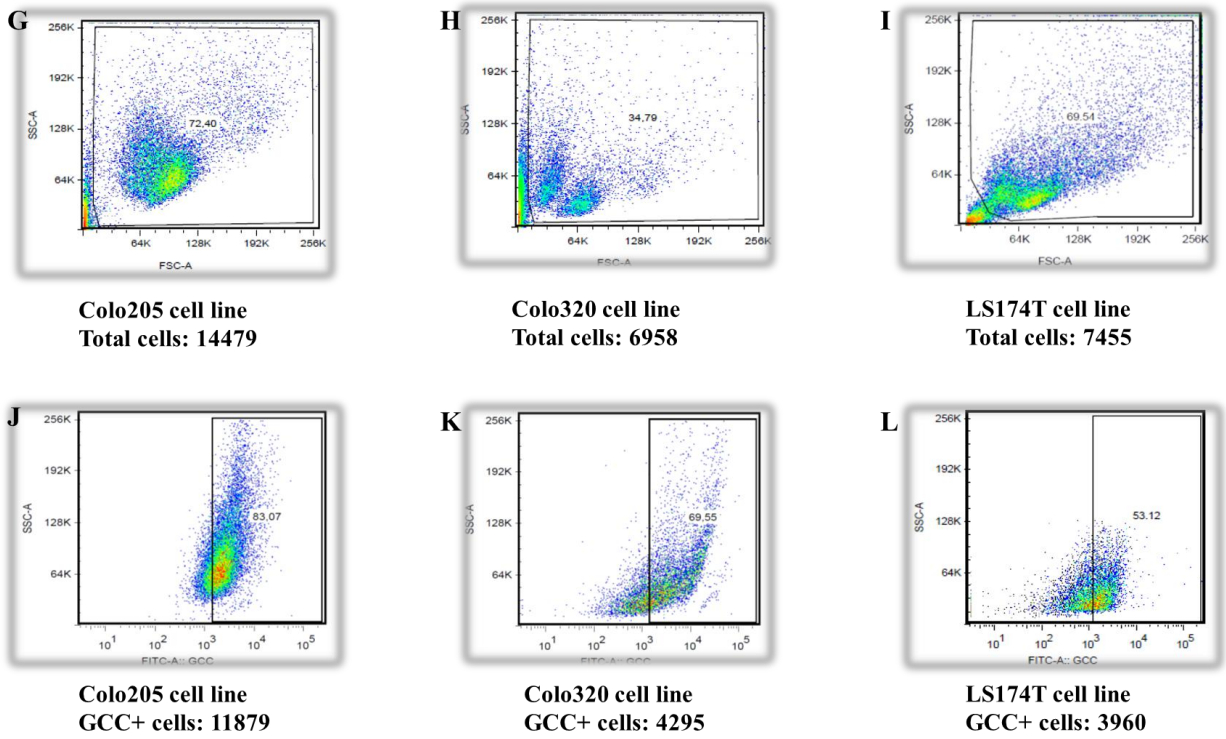

Figure 10 GCC antibody staining in six colon cancer cell lines during their first passage after thawing from frozen tubes. A, B, C, G, H and I show SW620, SW480, HCT116, Colo205, Colo320 and LS174T colon cancer cell lines for staining in scatter plot; D, E, F, J, K and L show GCC+ gate of six colon cancer cell lines.

Table 8 Summary of GCC staining in different colon cancer cell lines

	1 test GCC+ rate	2 test GCC+ rate	3 test GCC+ rate	Average GCC+ rate	Staining intensity of GCC	GCC+ rate at first passage after thawing from frozen
T84	74.77%	84.61%	76.94%	78.77%	high	97.01%
LS174T	28.47%	16.85%	43.41%	29.58%	moderate	53.12%
SW620	8.26%	9.37%	5.80%	7.81%	low	83.20%
SW480	8.88%	2.81%	9.08%	6.92%	low	70.35%
HCT116	9.09%	1.50%	1.03%	3.87%	low	95.52%
Colo205	2.49%	22.80%	6.84%	10.86%	low	83.07%
Colo320	5.48%	14.01%	6.71%	8.73%	low	69.55%

5. Staining of GCC antibody in T84 cell line by indirect method

5.1 Antibody titration: The primary GCC (537) antibody we used to bind T84 cells, and the secondary antibody was a mouse monoclonal antibody raised against N-terminus of GC-C with human origin. Each vial of primary GCC (537) antibody contains 100μg IgG2b in 1.0ml PBS

with <0.1% sodium azide and 0.1% gelatin. And the secondary antibody we used for labeling was goat anti-mouse IgG (H+L)-Alexa Fluor 488, which contains 1.5 mg goat anti-mouse Alexa Fluor 488 in 1.0 ml PBS (pH 7,6) with 0.05% NaN3, 15 mg/ml BSA. We tested different concentrations of primary GCC (537) antibody and different incubation times in order to establish a working condition for the GCC antibody. Our results showed that 1ml primary GCC (537) antibody and 4ml goat anti-mouse IgG (H+L)-Alexa Fluor 488 was the best working concentration for GCC labeling.

5.2 Antibody staining in T84 cell line: Antibodies such as GCC, CD7, CD25, CD44, CD45, CD4, CK and EpCAM were tested in T84 cell line. Unlike to high positive rates of GCC (84.24%), CK (93.39%), EpCAM (99.17%) and CD44 (81.10%), low positive rates were observed for CD45 (6.56%), CD4 (0.89%), CD25 (6.13%) and CD7 (6.16%) antibody staining (see Figure 11 and supplementary table 10).

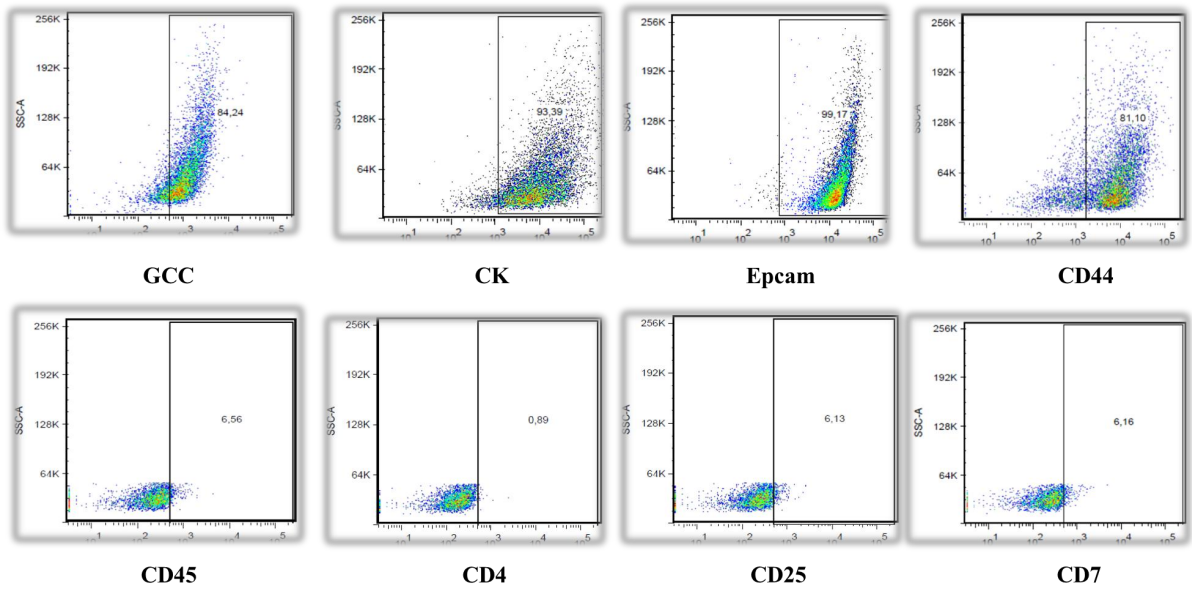

Figure 11 Summary of antibody staining in T84 colon cancer cell line. High positive rate for GCC (84.24%), CK (93.39%), EpCAM (99.17%), CD44 (81.10%) and low positive rate for CD45 (6.56%), CD4 (0.89%), CD25 (6.13%) and CD7 (6.16%) are found in Fig 11.

6. Staining of Alexa488-conjugated GCC antibody in T84 cell line

6.1 **Synthesis and titration of Alexa488-conjugated GCC antibodies:** It is well known that indirect staining methods always amplify binding signals based on primary antibody staining together with secondary antibody staining, while direct staining method by conjugated antibody should be a better choice for target cell detection (see Figure 12). The purified form of GCC

Antibody (537): sc-100302 used for fluorophore labeling was ordered from the same company (Santa Cruz). The Alexa Fluor®488 monoclonal antibody labeling kit includes five reaction vials; each vial was designed for labeling 100µg of a monoclonal primary antibody with fluorophore Alexa Fluor®488. The calculated final concentration of Alexa488 conjugated GCC antibody was 55µg/100µl.(see supplementary table 11, 12).

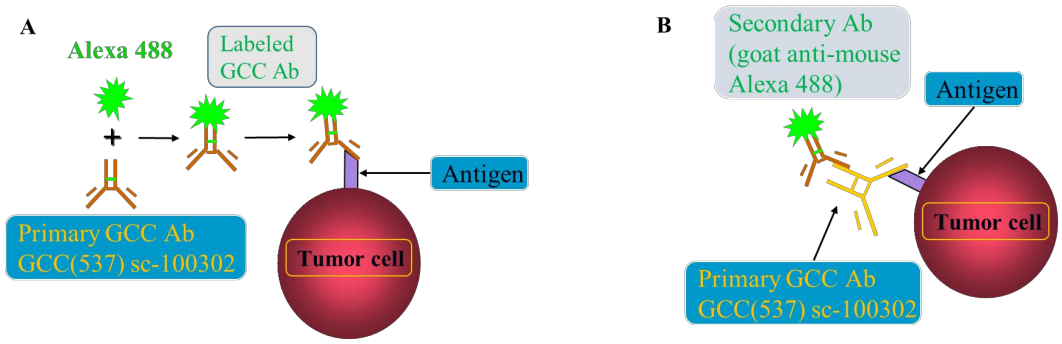

Figure 12 Illustration of antibody staining by direct and indirect staining methods. Fig A shows Alexa 488 conjugated GCC antibody staining by direct method, the intensity of signals relates to the real ratio of antibodies for labeling. Fig B shows double staining of primary GCC antibody with antigen and secondary antibody (Goat ant-mouse Alexa 488) with primary GCC antibody by indirect method, which amplifies the staining efficiency of GCC antibody.

6.2 Staining of Alexa488-conjugated GCC antibodies in T84 cell line: We performed seven tests to optimize the best working concentration and incubation time of Alexa488 conjugated GCC antibody. Because no Alexa 488 channel was available in flow cytometry, we selected the FITC channel with a similar excitation and emission peak for detecting Alexa488 conjugated GCC antibody. The percentage of GCC stained T84 cells increased from 22.33% to 69.50% with different volumes of Alexa488 conjugated GCC antibody (1µl-4µl per sample), while the incubation time of 60-minute subset (72.71%) showed the highest antibody combination (see Figure 13 and supplementary table 13). By fluoroscope we clearly saw membrane staining of GCC antibody with green fluorescence in T84 colon cells (see Figure 14).

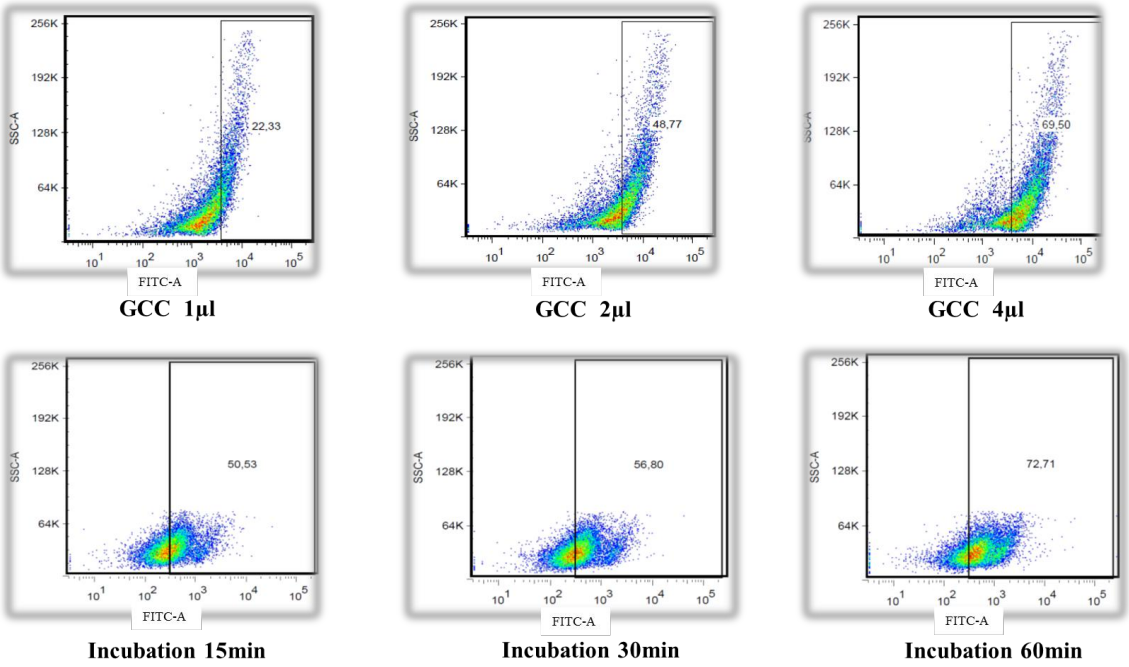

Figure 13 Optimization of Alexa488 conjugated GCC antibody with different volume and incubating time. The percentage of GCC positive tumor cells is 22.33% for 1µl, 48.77% for 2µl and 69.50% for 4µl. The percentage of GCC positive tumor cells is 50.53% for 15 minutes, 56.80% for 30 minutes and 72.71% for 60 minutes.

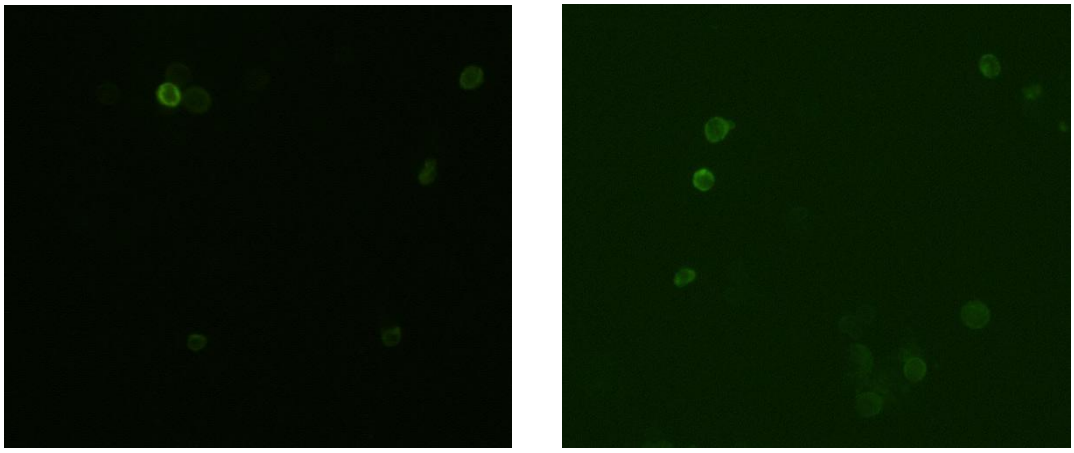

Figure 14 Fluoroscopic detection of GCC antibody staining in T84 cells . The cells surrounded with bright green fluorescence are T84 colon cancer calls. The left figure shows GCC stained cells by indirect method, while the right figure shows GCC stained cells by direct method.

7. Staining of FITC-conjugated GCC antibody in T84 cell line:

7.1 Antibody titration: FITC-conjugated mouse anti-human GCC antibody was the primary conjugated GCC antibody produced by United States Biological Company. The concentration of FITC-conjugated GCC antibody was 1mg/1ml and the total volume was 100µl per vial.

7.2 Optimization of GCC antibody staining in T84 cell line: We performed three experiments to optimize the working condition of FITC conjugated mouse anti-human GCC antibody. Based on the same concentration, we gradually increased the volume of FITC conjugated GCC antibody from 1µl to 15µl, and finally we selected 15µl as the working volume for GCC staining, which had an equal percentage of positive T84 cells (70.84%) stained by primary GCC antibody (72.31%) (See Figure 15 and supplementary table 14). The intracellular and surface staining of FITC-conjugated GCC antibody was performed in T84 cells to compare the efficiency of these two staining methods. However, intracellular staining of FITC-conjugated GCC antibody (90.23%) in T84 colon cells showed a higher GCC positive percentage than surface staining (78.64%) (See Figure 16), which suggested more GCC binding site existed outside the T84 cells.

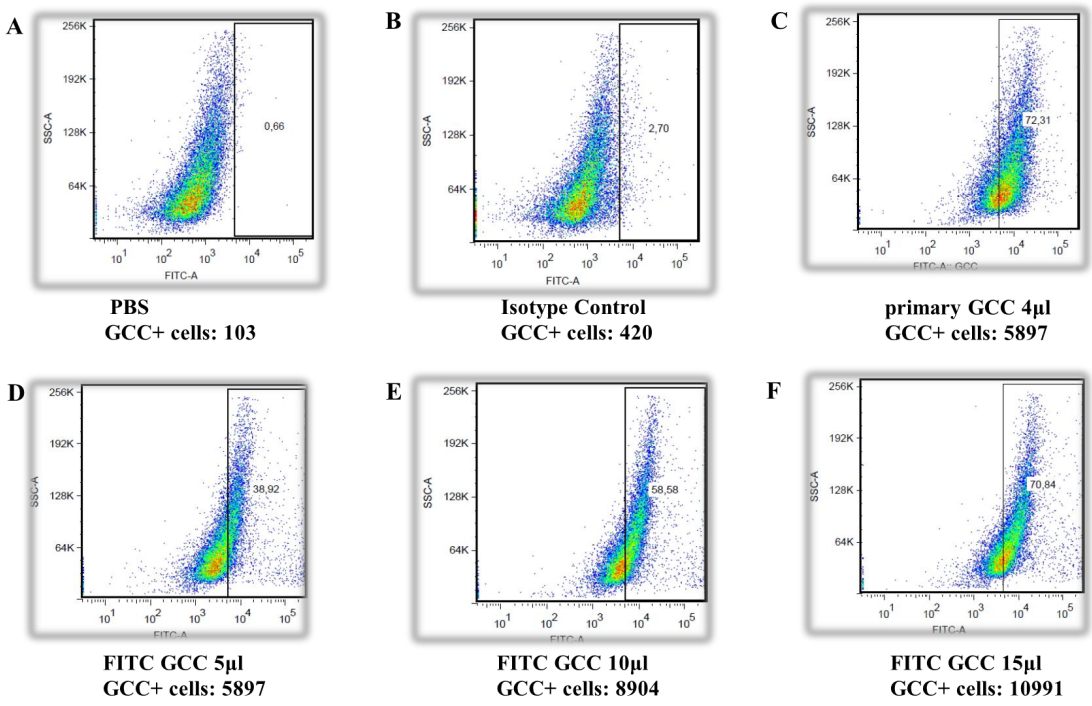

Figure 15 Optimization of FITC-conjugated GCC antibody staining in T84 cells. A, B, C show T84 cells stained by negative control (PBS), IC (IgG2bk) and positive control (primary unconjugated GCC antibody). D, E, F show the positive percentage of T84 cells stained by FITC-conjugated GCC antibody for 5µl (38.92%), 10µl (58.58%) and 15µl (70.84%) .

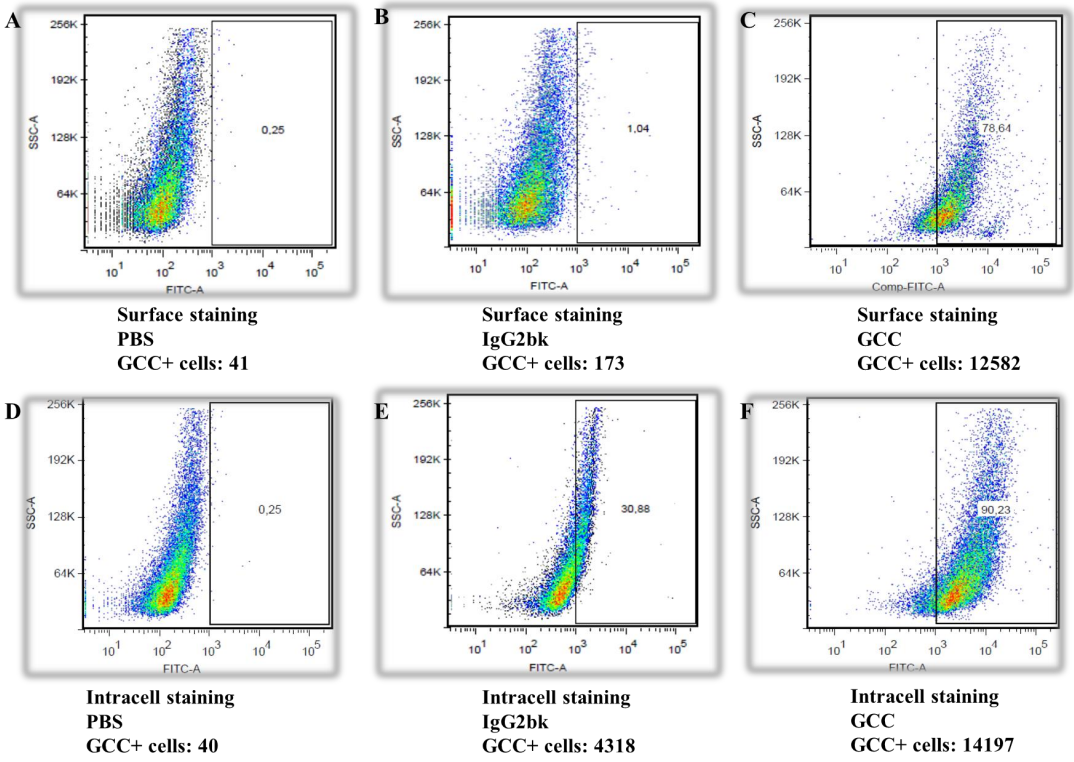

Figure 16 Surface and intracellular staining of FITC-conjugated GCC antibody in T84 cells. A, B, C show surface staining by negative control (PBS), IC (IgG2bk) and FITC-conjugated GCC antibody in T84 cells. D, E, F show intracellular staining by negative control (PBS), IC (IgG2bk) and FITC-conjugated GCC antibody in T84 cells.

8 Unspecific staining of GCC antibody in leukocytes:

8.1 Multi-stained of tumor cells by GCC, CK and EpCAM: We spiked T84 cells into blood from volunteers and enriched the T84 cells by CD45+ cell depletion, followed by CK, EpCAM and GCC antibody staining, in order to explore the efficiency of GCC antibody staining. Unfortunately, we observed high unspecific GCC staining of leukocytes besides T84 cells. Figure 17 and Figure 18 indicate unspecific GCC staining in leukocytes. Figure 17 clearly illustrates the composition of cells stained by GCC antibody, those cells multi-stained by CK, EpCAM and GCC antibody should be T84 cells (173 cells), while the total cell number stained by GCC antibody was 5281, thus the remaining 5108 cells (5281-173) should be leukocytes or tumor cells (CK- EpCAM- GCC+). In Figure 18 we show that many more GCC+ cells (124512-85215=39297 cells) enriched by GCC antibody staining, the remaining cells stained with GCC antibody should be leukocytes.

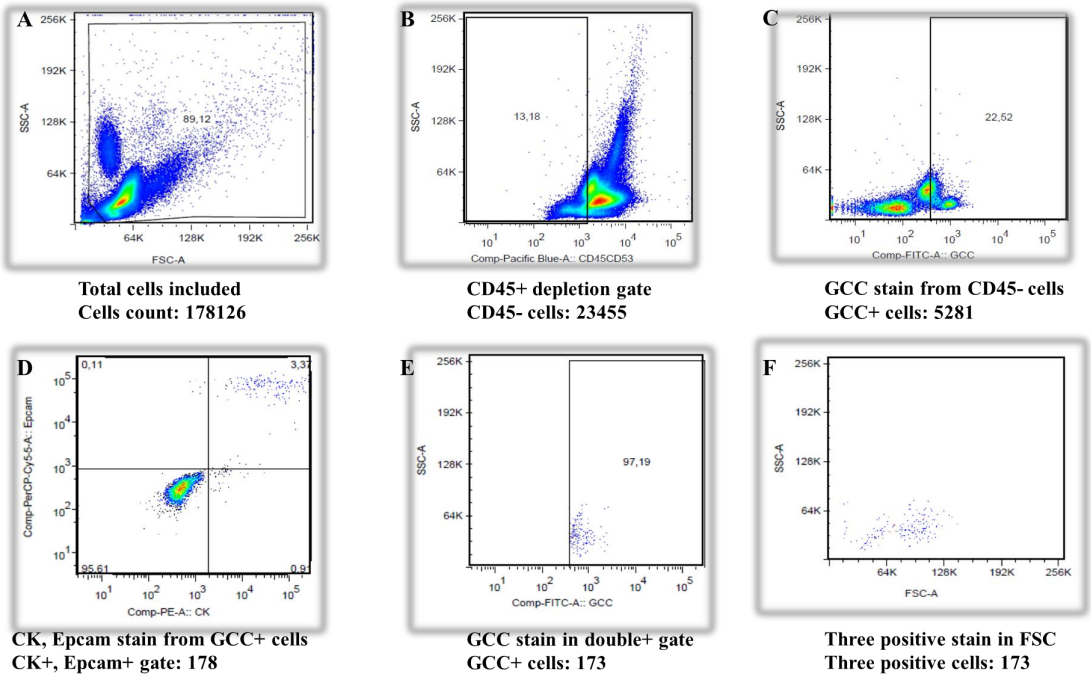

Figure 17 T84 cells and leukocytes multi-stained by GCC, CK and EpCAM. A: Total cells in scatter plot; B: CD45 negative gate after CD45+ depletion; C: GCC positive cells (5281 cells) enriched by GCC positive gated; D: CK and EpCAM double positive cells (178 cells) from GCC+ cell subgroup; E: GCC positive cells (173 cells) from CK and EpCAM double positive subgroup; F: Cells with CK, EpCA M and GCC multi-positive subgroup in scatter plot.

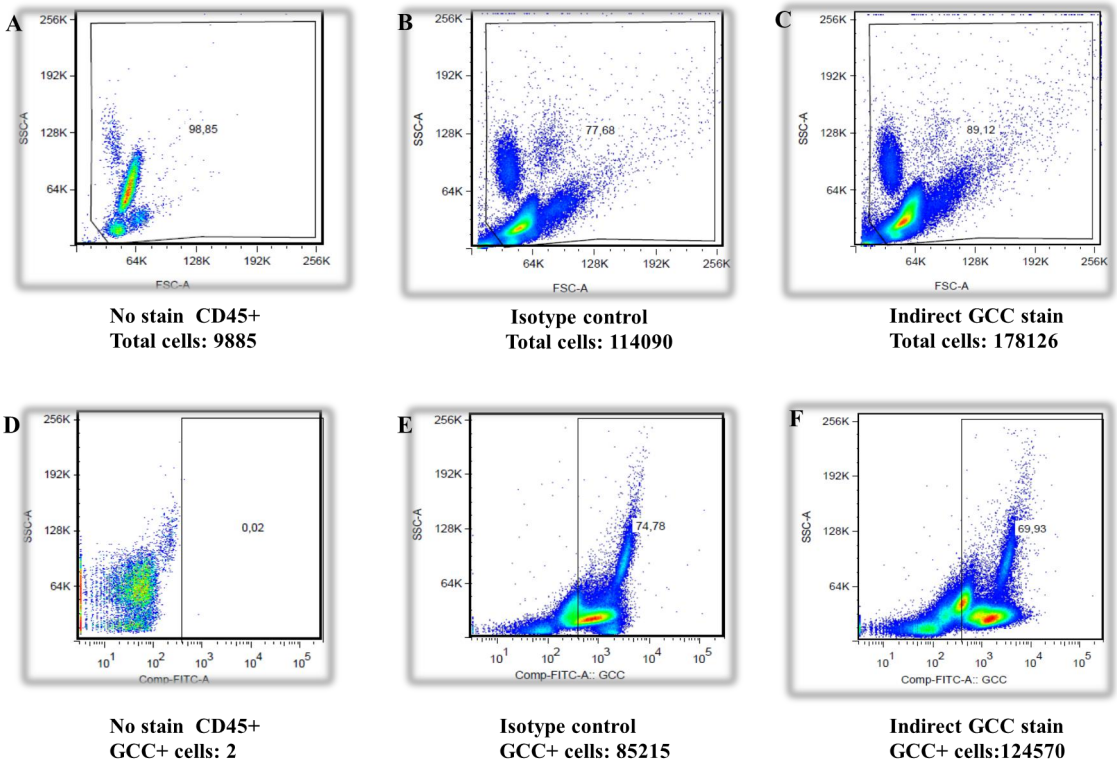

Figure 18 T84 cells and leukocytes stained by negative control, IC and GCC antibody. A, D: Negative control staining (CD45+ blood cells) in scatter plot and GCC+ gate, B, E: IC staining (cells staining by IgG2b antibody) in scatter plot and GCC+ gate, C, F show cells stained by GCC antibody and secondary antibody in scatter plot and GCC+ gate. E and F indicate much more leukocytes (39297 cells) stained by GCC antibody.

8.2 Multi-stained of tumor cells with Alexa488 conjugated GCC, CK and EpCAM: We spiked T84 cells into blood from volunteers and enriched the T84 cells by CK, EpCAM and Alexa488 conjugated GCC antibody staining in order to explore the efficiency of Alexa488 conjugated GCC antibody staining by direct labeling. We also observed high unspecific GCC staining on leukocytes besides T84 cells. Figure 19 and Figure 20 indicate unspecific GCC staining on a large population of leukocytes. Figure 19 clearly illustrated the composition of cells multi-stained by CK, EpCAM and Alexa488 conjugated GCC antibody should be T84 cells (109 cells), while the total cell number enriched by Alexa488 conjugated GCC antibody was 701, the remaining 592 cells (701-109) should be leukocytes or tumor cells (CK- EpCAM- GCC+). IN Figure 20 we detected more GCC+ cells (113020-84503=28517 cells) enriched by Alexa488 conjugated GCC antibody staining, the remaining cells stained with GCC antibody should be leukocytes.

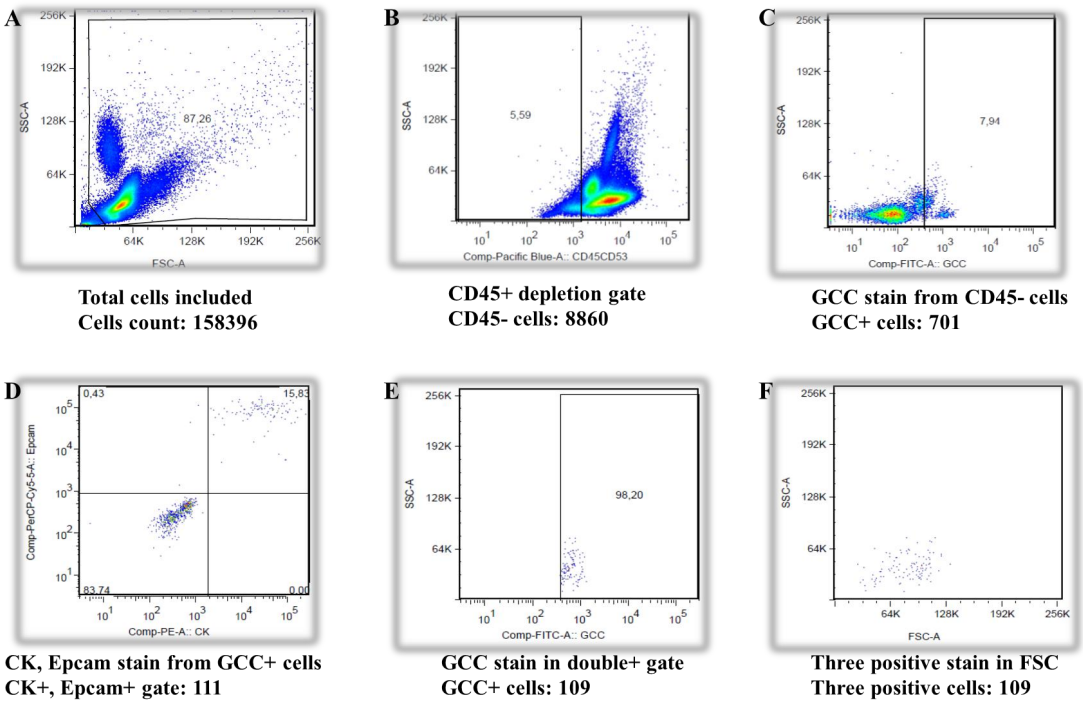

Figure 19 T84 cell recycled by Alexa488-conjugated GCC antibody by direct staining method. A: Total cells in scatter plot; B: CD45 negative cells separated after CD45+ depletion; C: GCC positive cells (701) enriched by GCC positive gated; D: CK and EpCAM double positive cells (111) from GCC+ cell subgroup; E: GCC positive cells (109) from CK and EpCAM double positive subgroup; F: CK, EpCAM and GCC positive subgroup cells (109) in scatter plot.

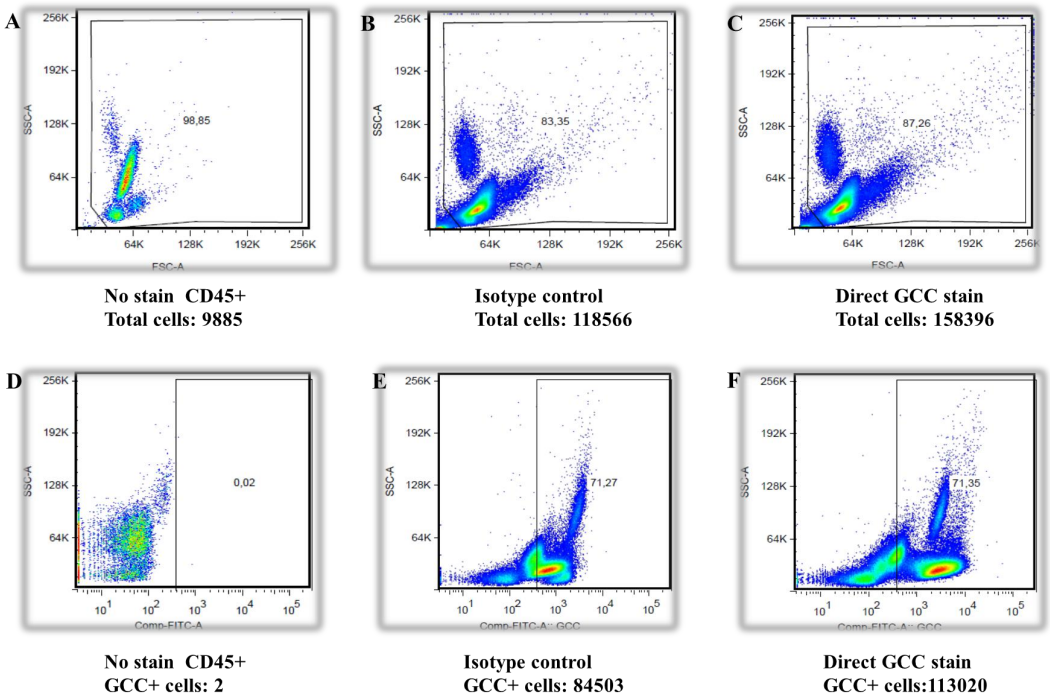

Figure 20 T84 cells and leukocytes stained with negative control, IC and Alexa 488-conjugated GCC antibody. A, D: Negative control staining (CD45+ blood cells) in scatter plot and GCC+ gate, B, E: IC staining (cells staining by IgG2b antibody) in scatter plot and GCC+ gate, C, F show cells stained by Alexa 488 conjugated GCC antibody in scatter plot and GCC+ gate. E and F indicate much more leukocytes (28517 cells) stained by GCC antibody.

8.3 Comparison of leukocytes single-stained with GCC, CK and EpCAM: Figure 21 clearly demonstrates a similar fraction of GCC, CK and EpCAM single positive population in leukocytes, which were supposedly caused by Fc fragments similar to their isotype control. However, besides granulocytes, the major subpopulation of GCC positive cells was derived from lymphocytes, which may be the reason for the nonspecific staining with the GCC antibody.

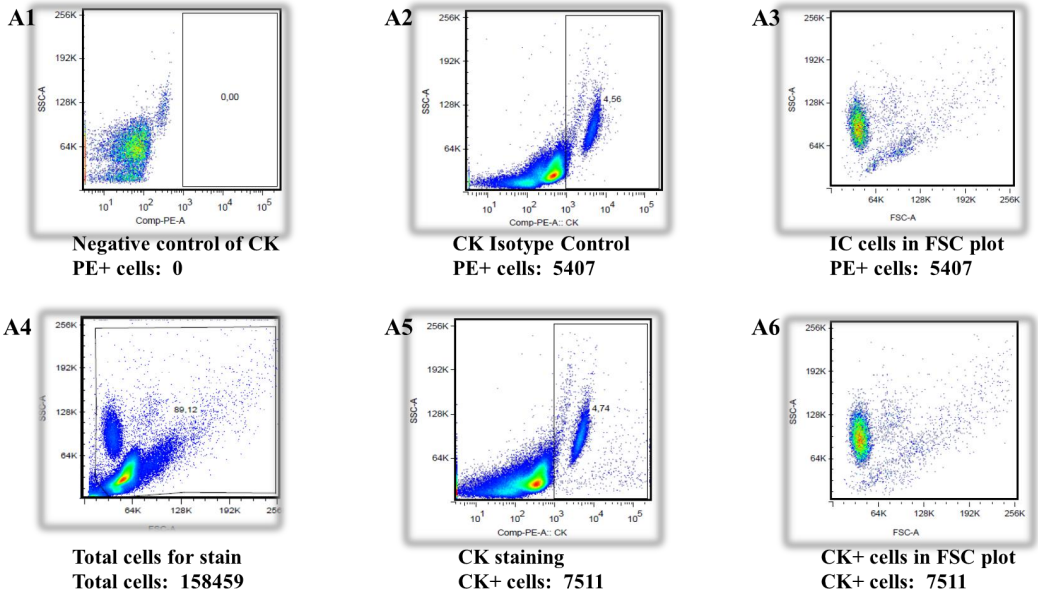

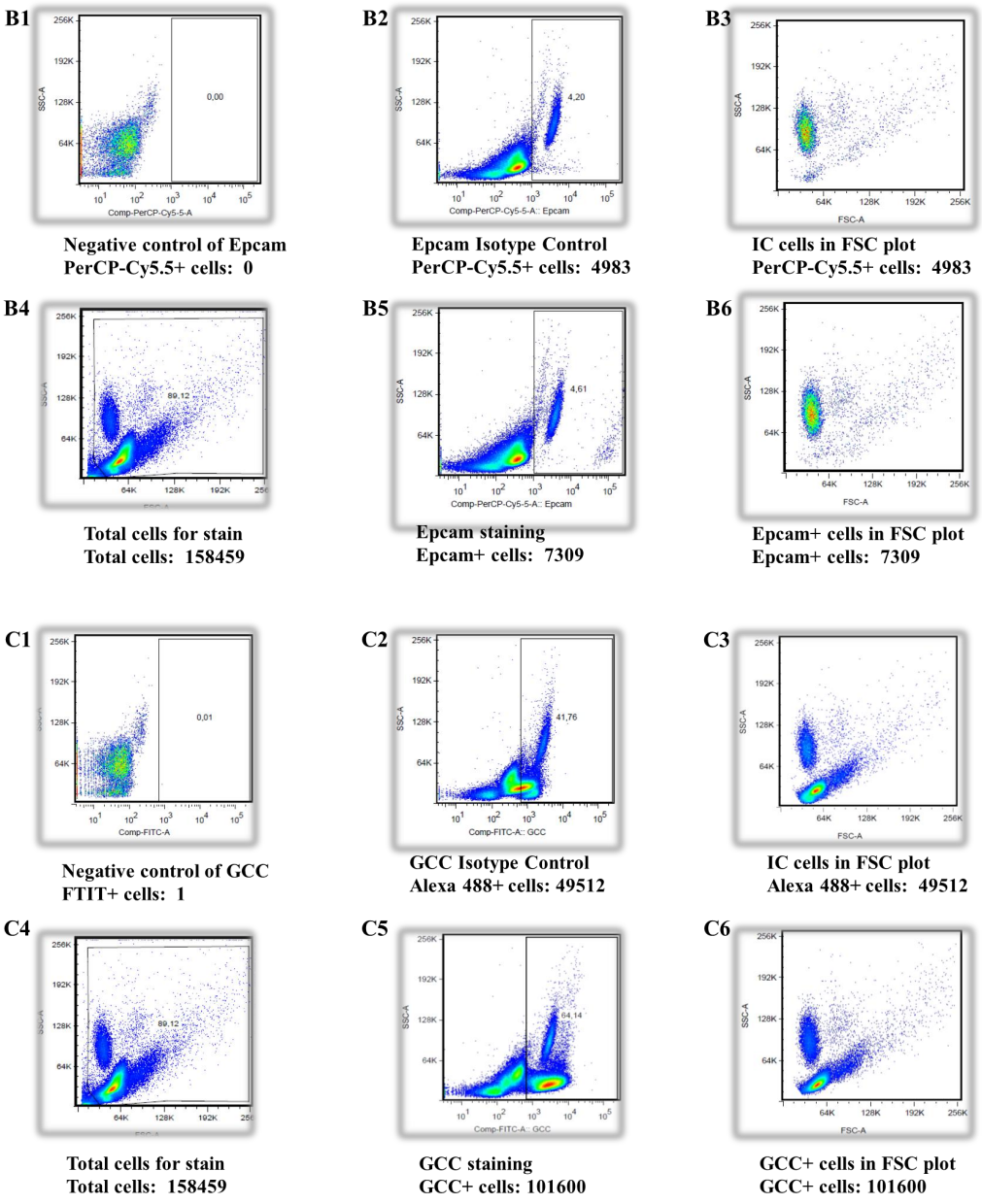

Figure 21 Comparison of leukocytes single-stained by GCC, CK and EpCAM. A1, B1, C1 show negative control in CK, EpCAM and GCC positive gate; A2, A3 show subgroups stained by IC in PE gate and FSC plot; A4 to A6 show total cells in FSC plot, CK+ cells in CK gate and CK+ cells in FSC plot; B2, B3 show subgroups stained by IC in PerCP-Cy5.5 gate plot and FSC plot; B4 to B6 show total cells in FSC plot, EpCAM+ cells in EpCAM gate and EpCAM+ cells in FSC plot; C2, C3 show subgroups stained by IC in Alexa488 gate plot and FSC plot; B4 to B6 show total cells in FSC plot, GCC+ cells in GCC gate and GCC+ cells in FSC plot.

8.4 Unspecific staining of GCC antibodies and secondary antibody in leukocytes: For the purpose of analyzing unspecific binding originating from the primary GCC antibodies, goat anti-mouse secondary antibodies and Alexa488 conjugated GCC antibody, we selected all these three antibodies for testing. Figure 22 indicated that 50.82% leukocytes stained by primary GCC antibody and secondary antibody, 53.11% leukocytes stained by goat anti-mouse secondary

antibody and nearly 47.92% leukocytes stained by Alexa488 conjugated GCC antibody. The results F, I, L in Figure 22 indicated that all three antibodies have unspecific binding with leukocytes. Figure 23 showed leukocytes stained by primary GCC antibody, secondary antibody and Alexa488 conjugated GCC antibody by fluoroscope detection.

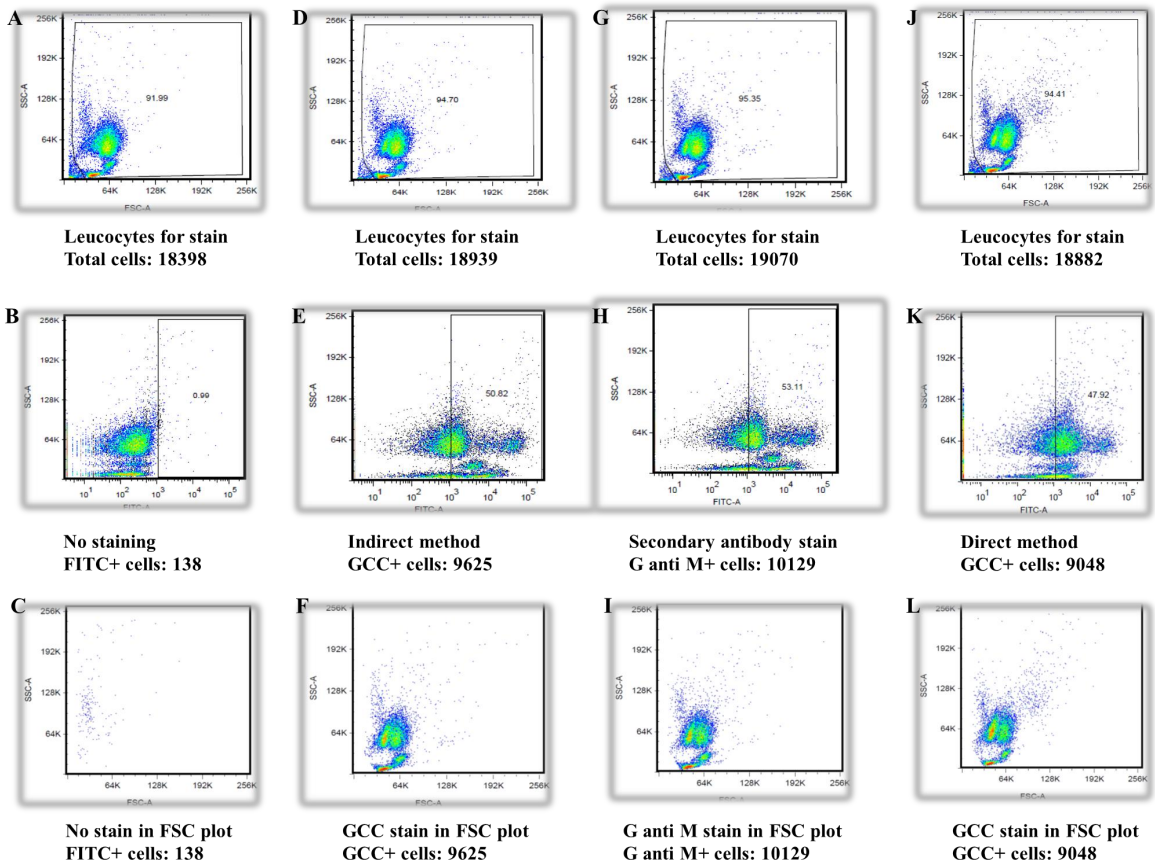

Figure 22 leukocytes stained by GCC antibodies and secondary antibody. A, B, C show leukocytes stained by negative control in FSC plot and FITC+ gate plot; D, E, F show 50.82% leukocytes stained by primary GCC antibody in FSC plot and GCC+ gate plot. G, H, I show 53.11% leukocytes stained by secondary antibody in FSC plot and FITC+ gate plot . J, K and L show that 47.92% leukocytes stained by Alexa488 conjugated GCC antibody in FSC plot and GCC+ gate plot .

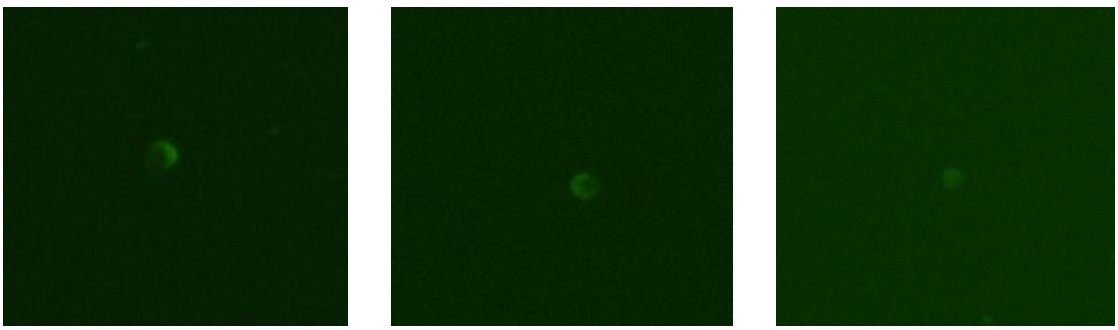

A B C

Figure 23 Illustration of leukocytes stained by antibodies in fluoroscopic detection. These cells with bright green fluorescence on membrane are leukocytes. Fig A show leukocyte stained by GCC antibody and secondary antibody,

Fig B show leukocyte stained by secondary antibody and Fig C show leukocyte stained by Alexa488 conjugated GCC antibody.

8.5 Summary of leukocytes stained with unconjugated and conjugated GCC antibodies: According to the results of previous studies, we performed six experiments of leukocytes staining by unconjugated and conjugated GCC antibodies, to compare the difference between these two GCC antibodies. Table 9 summarized the leukocyte staining by primary GCC antibody and Alexa488 conjugated GCC antibody based on indirect and direct staining methods. 82.71% of the total leukocytes were stained by unconjugated GCC+ antibody, while 48.76% of the total leukocytes were stained by Alexa488 conjugated GCC antibody. As compared with these two different staining methods, both of the antibodies showed high nonspecific staining in leukocytes (range from 29.24% to 87.39%).

Table 9 Summary of leukocytes stained by GCC based on indirect and direct staining methods

GCC antibody		Number of total leukocytes	Number of GCC+ cells	Percentage of GCC+ cells
Unconjugated antibody	GCC	18717	14597	77.99%
Unconjugated antibody	GCC	18900	16517	87.39%
Average		18808	15557	82.71%
Conjugated GCC antibody		18004	5265	29.24%
Conjugated GCC antibody		18618	8850	47.25%
Conjugated GCC antibody		6733	4306	63.95%
Conjugated GCC antibody		11309	8237	72.01%
Average		13666	6664	48.76%

9 Intracellular and surface staining of leukocytes by FITC conjugated GCC antibodies: Finally, we switched to another GCC antibody labeled with fluorophore FITC from US Bio-company. The intracellular and surface staining of the FITC-conjugated GCC antibody in T84 cells (see part 6.3 of results) and leukocytes was tested in order to assess the staining efficiency of GCC antibody in colon tumor cells and leukocytes. Figure 24 show the surface staining of

leukocytes by negative control (PBS), IC (IgG2bk) and FITC conjugated GCC antibody, the percentage of GCC+ leukocytes by surface staining was 53.67% of the total leukocytes, while the percentage of GCC+ leukocytes by intracellular staining was 93.47% in Figure 25. Furthermore, as isotype control, IgG2bk had higher positive intracellular staining than surface staining, which indicated more intracellular binding sites of IgG2bk than on the surface of leukocytes. Finally, nearly all kinds of leukocytes were involved in GCC staining as illustrated by the distribution of GCC positive staining in the FSC plot.

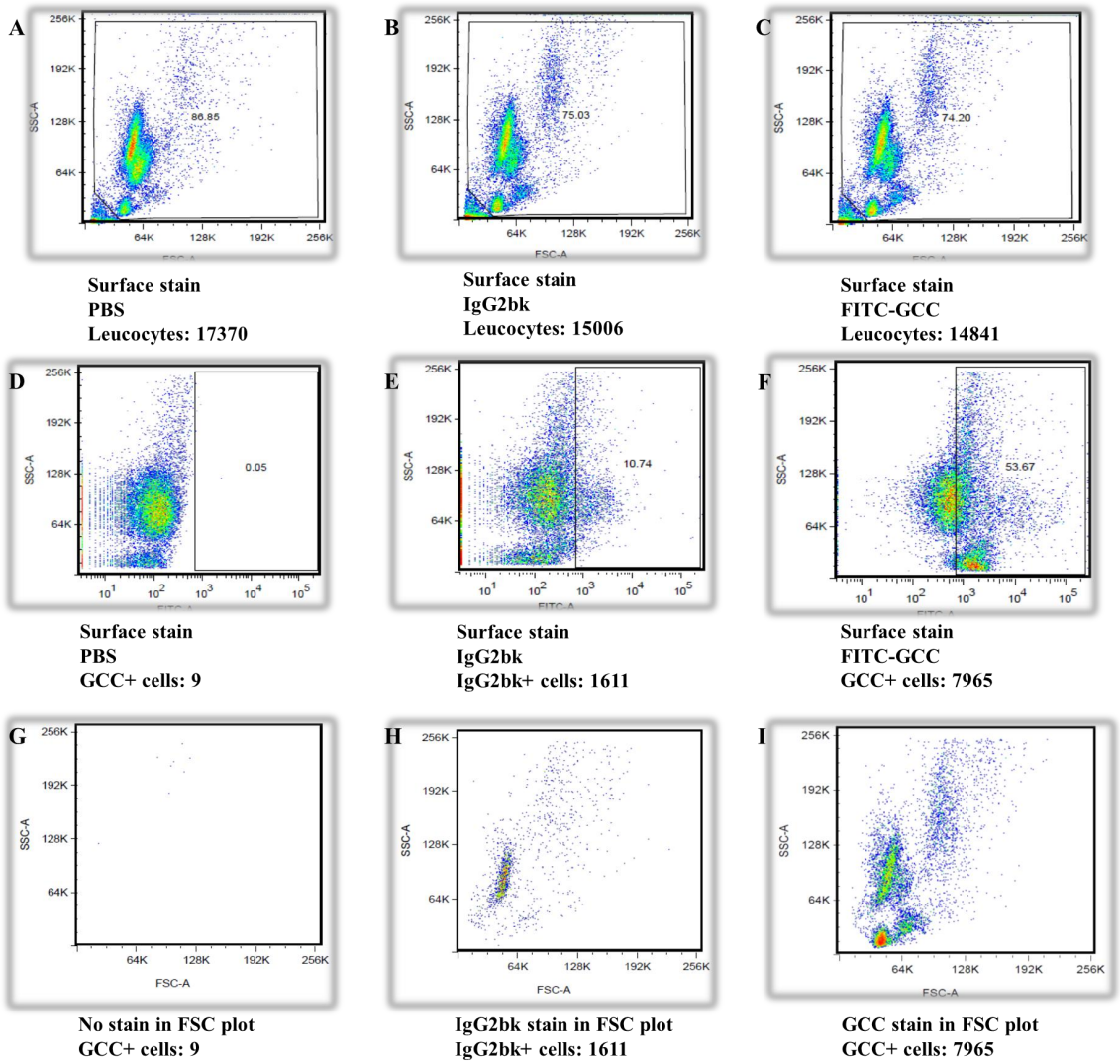

Figure 24 leukocytes surface stained by FITC-conjugated GCC antibody. A, B, C show total leukocytes used for negative control (PBS), IC (IgG2bk) and FITC-conjugated GCC antibody surface staining in FSC plot. D, E, F show positive surface staining of leukocytes by negative control (PBS), IC (IgG2bk) and FITC-conjugated GCC antibody in GCC+ gate, G, H, I show positive surface staining of leukocytes by negative control (PBS), IC (IgG2bk) and FITC-conjugated GCC antibody in scatter plot, the percentage of GCC+ leukocytes by surface staining is 53.67% (7965 cells) of the total leukocytes (14841 cells).

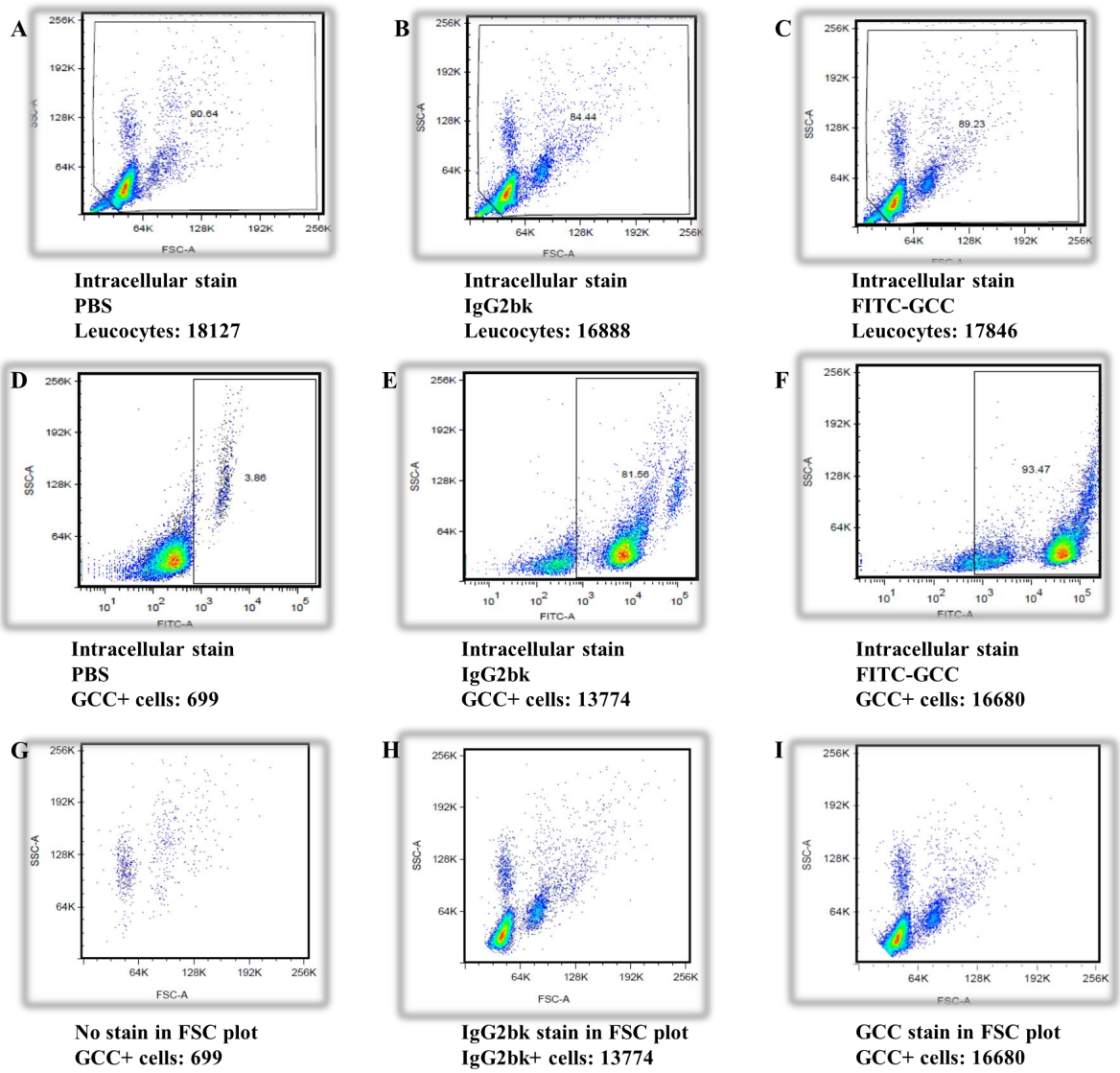

Figure 25 leukocytes intracellular stained by FITC-conjugated GCC antibody. A, B, C show total leukocytes used for negative control (PBS), IC (IgG2bk) and FITC-conjugated GCC antibody intracellular staining in FSC plot. D, E, F show positive intracellular staining of leukocytes by negative control (PBS), IC (IgG2bk) and FITC-conjugated GCC antibody in GCC+ gate, G, H, I show positive intracellular staining of leukocytes by negative control (PBS), IC (IgG2bk) and FITC-conjugated GCC antibody in scatter plot, the percentage of GCC+ leukocytes by intracellular staining is 93.47% (16680 cells) of the total leukocytes (17846 cells).

10 Summary of T84 cells and leukocytes stained by three GCC antibodies: All three GCC antibodies showing high positive staining in T84 colon cancer cells (average rate 74.74% to 80.61%) when compared to isotype control (average rate 1.87% to 3.81%) in Table 10. However, all GCC antibodies also showed high non-specific staining of leukocytes (average rate 50.29% to 73.96%) compared to isotype control (average rate 10.74% to 51.25%), which restricted the future application of all currently available GCC antibodies for CTC detection.

Table 10 Summary of T84 cells and leukocytes stained by three GCC antibodies

Types of GCC antibodies for labeling	T84 cells			Leukocytes		
	Test No	IC(IgG2bκ CD4) (percentage)	GCC+ cells (percentage)	Test No	IC(IgG2bκ CD4) (percentage)	GCC+ cells (percentage)
Unconjugated GCC antibody	1	1.01%	74.77%	1	74.78%	69.93%
	2	0.46%	84.61%			
	3	0.57%	76.94%			
	4	1.68%	91.26%			
	5	1.34%	78.60%	2	27.73% (IgG2bκ)	77.99%
	6	0.89%	84.24%			
	7	6.53%	83.67%			
	8	2.78%	70.84%			
Average percentage		1.90%	80.61%		51.25%	73.96%
Alexa 488 conjugated GCC	1	1.10%	73.42%	1	71.27%	71.35%
	2	6.53% (IgG2bκ)	83.51%	2	27.73% (IgG2bκ)	29.24%
Average percentage		3.81%	78.46%		49.50%	50.29%
FITC conjugated GCC	1	2.70% (IgG2bκ)	70.84%	1	10.74% (IgG2bκ)	53.67%
	2	1.04% (IgG2bκ)	78.64%			
Average percentage		1.87%	74.74%		10.74%	53.67%

Discussion

Colorectal cancer is a common gastrointestinal malignant tumor and its' metastasis contribute to high disease-related mortality worldwide. However, the tracking of circulating tumor cells is still under investigation and major difficulties include the lack of highly specific CTC biomarkers and multifarious process of CTC enrichment for analytical purposes [100, 101]. Searching for more specific biomarkers and optimizing the protocol of CTC enrichment are urgently required not only for metastatic tumor cell detection, but also for clinical diagnosis and potentially for treatment outcome [101]. Even though tumor markers such as EpCAM, CK and CEA are often applied tracking of malignant tumor cells of lung, breast, gastrointestinal, head and neck cancers, all of these markers lack sufficient sensitivity and specificity for carcinomas. As a member of the guanylyl cyclase family of trans-membrane receptors, GCC is selectively expressed in brush border membranes of intestinal epithelial cells from the duodenum to the rectum[102]. The special character of this highly selective expression on intestinal tissue makes GCC an excellent candidate for screening, imaging, diagnosis and targeted treatment of CRC [83, 103-105]. According to previous reports, GCC is not only a selective biomarker in intestinal and epithelial tumor cells, but also a cancer mucosa-associated antigen[106]. Beyond being a biomarker, GCC also emerged as a vital modulator in the GUCY2C hormone axis by regulating the cell proliferation of transit amplifying cells in crypts, DNA damage repair and differentiation along the secretory lineage of intestinal and epithelial cells [103, 104, 107, 108]. Owing to its distinctive biological behavior, we selected to evaluate GCC as a special biomarker for tracking CTCs of CRCs in patients with metastasis and investigate the possibility of CTCs multi-stained by GCC, CK and EpCAM. For the purpose of increasing the recovery rate of CTCs from CRC patients, we focused on the optimization of two key points in the CTC enrichment protocol, which were CD45+ cell depletion and a specific tumor antibody for CTC binding.

1. Optimization of CD45+ cell depletion in CTC enrichment protocol

Antibody based techniques are widely used for capturing CTCs which express epithelial tumor markers on their surface that are absent on normal leukocytes. For better identification of CTCs, removal of leukocytes by CD45+ depletion was required for reducing the background value, fluorophore-conjugated antibody staining was then followed to capture CTCs out of blood from patients with epithelial-derived cancers [55, 109, 110]. EpCAM and CK are also commonly used

for CTC enrichment because of their high expression in epithelial tumor cells, but absence in leukocytes [111]. Compared to the positive enrichment of CTCs, CD45+ cell depletion strategies can remove CD45+ leukocytes and enrich CTCs with both positive and negative tumor markers [92, 110]. Our CTC enrichment experiment and detection protocol was based on epithelial tumor markers and CD45+ cell depletion. We employed a negative enrichment protocol based on efficient removal of CD45+ leukocytes by CD45 cocktail and bead sorting, and the remaining small cell fraction was characterized by EpCAM and CK double positive staining. Our results from table 7 showed that single CK positive enrichment might harbor more epithelial cells by intracellular staining (average rate 188%) while single EpCAM positive cells may lose some of the tumor cells for surface staining (average rate 89%). However, lower recovery rate (average rate 54%) was illustrated by CK and EpCAM double staining, which indicated that more efficient optimization was required for increasing the recovery rate.

After separately assessing each step of the protocol, we tried to increase the recovery rate by optimizing the depletion step, because millions of CD45+ cells were eliminated in magnetic fields, which might include the trapping of some tumor cells. We postulated that part of those CD45- tumor cells were locked on the wall of FACS tube by massive CD45+ leukocytes, and were then removed together with CD45+ leukocytes after the depletion step (illustrated in Figure 6 of results). Based on this hypothesis, we added one more tube for gathering CD45- tumor cells from the supernatant with CD45+ cells by washing with PBS and adding recycling step (see Fig7 of results). Our results indicate that with this additional recycling step, an additional 16.23% of total tumor cells were recovered (see figure 8 and table 8). On the other hand, the dosage of the CD45 cocktail and beads was not critical for recovery. And other steps of the protocol were also less critical for recovery of CTCs.

Since CK and EpCAM are both epithelial biomarkers, the epithelium-based approach can't detect CTCs with non-epithelial phenotype or low EpCAM levels during the EMT process. Thus, as the EMT-independent biomarker, GCC may be an alternative for increasing the recovery rate of CTCs from CRC [111-113]. As CTC capture using anti-EpCAM antibody-based approaches depends on surface expression of EpCAM on tumor cells, such approaches fail to recognize the EpCAM negative subset of CTCs which may be associated with aggressive behavior [114, 115]. Additionally, the obvious drawback of the epithelial marker-based approach is that the EMT process results in metastatic cancer cells with a mesenchymal cell-like phenotype, down-regulation of epithelial markers such as EpCAM or CK and up-regulation of mesenchymal

markers [112, 116, 117]. Thus, GCC as a specific and EMT-unrelated marker was an alternative candidate to be evaluated.

2. GCC expression in tumor and normal adjacent mucosal tissues of the rectum

We initially investigated IHC staining for GCC in paired tumor and adjacent normal mucosal tissues from paraffin-embedded rectal samples, which indicated that GCC had significant over-expression in rectal tumor tissues at higher frequencies than adjacent normal mucosal tissues, in concordance with the data reported before. Buc et al analyzed 38 cases of malignant and adjacent normal mucosal tissues from the colon and rectum by IHC for expression of GCC, CK20 and CEA. They indicated that unlike CEA and CK20, the detection level of GCC was higher in tumors than in adjacent normal mucosal tissues, while CK20 or CEA were similar in both tissue samples [118]. Similar results were obtained by quantitative RT-PCR-based studies [119-121], in which researchers evaluated paired samples from normal adjacent mucosa and colorectal tumors, indicating that GCC-mRNA was significantly over-expressed in CRC tumors when compared with matched normal adjacent mucosa from the same patient, with the median GCCmRNA copy number being about 2-fold higher in tumors compared with normal mucosa [120, 121]. Furthermore, GCC was over-expressed at the mRNA and protein levels in more than 80% of colon and rectum tumors compared to normal adjacent intestinal mucosa [83, 108, 120, 121]. For investigating the functional role of different GCC expression in tumor and normal tissue samples, researchers measured the ligands of the GCC receptors and proved that guanylin and uroguanylin were essential endogenous ligands for the GCC receptor in vivo, and their loss and reduction at an early stage in colorectal tumors was always observed [100, 101, 122]. Guanylin was reported to be significantly decreased in nearly 90% of all colorectal tumors compared to adjacent normal mucosa [80]. It was assumed, that these hormones might be reduced by independent mechanisms at the levels of transcription (mRNA) and translation (protein), creating reinforcing mechanisms that ultimately silence the GUCY2C tumor suppressor [80]. Notably, unlike those decreased paracrine hormones or ligands, GCCmRNA and protein were universally increased in human colorectal tumors and their metastasis, compared to normal intestinal cells [83, 84, 120]. All these considerations support a hypothesis of reversing hormone expression loss to possibly prevent tumorigenesis, and underscore a considerable potential for GCC as a cell surface receptor for selective diagnostics and therapeutics of CRCs [80]. Importantly, although loss of guanylin and uroguanylin occurs early in tumor development, GCC receptor expression persists in CRC [82] with high specificity and might serve as a target for treatment of CRC patients [83, 120].

3. GCC expression in colon cancer cells and T84 cells

The central characteristic of GCC is its highly selective expression only in intestinal-derived normal and tumor cells as well as their metastases, without detectable expression in extra-intestinal tissues or tumors. Despite GCC expression being detected and described in numerous studies by PCR and IHC in colon cancer cell lines and paraffin-embedded tissue samples, only few studies investigated the diversity of GCC antibody binding to colon cancer cell lines or CTCs from CRC patients by flow cytometry. For the purpose of applying GCC antibodies in CTC enrichment, we first evaluated the binding characteristics of GCC antibodies to colon cancer cell lines by flow cytometry. Our findings are consistent with previous PCR analyses indicating a high GCC expression in T84 cells, moderate in LS174T cells and low in other colon cancer cells. T84 has been reported as a transplantable human carcinoma cell line derived from a lung metastasis of a colon carcinoma of a 72-year-old male. Additionally, T84 cell line has also been used as an excellent model system for studying electrolyte transport processes and the functions of voltage-dependent channels by electrical circuit analysis and membrane-associated cell transport systems [123, 124]. Our results demonstrate high expression of GCC, CK, EpCAM, CD44, and low expression of CD45, CD4, CD25 and CD7 in the T84 cell line. We therefore selected the T84 cell line as the positive control for GCC antibody staining and included spiked T84 cells as CTC analogues for evaluation of CTC enrichment protocols.

As a problem we have observed that all the colon cancer cell lines displayed a high percentage of GCC receptor (ranged from 53.12% to 97.01%) at their first passage after thawing, which progressively decreased after several passages of culture. It is likely that the expression of GCC receptors on colon cancer cells was influenced by the culture conditions. In the context of the GCC paracrine hormone axis, the guanylin and uroguanylin content may be an important regulator of GCC receptor distribution on colon cancer cell lines. Immediately after cell recovery from frozen tubes, the scarcity of these hormones may have increased the expression of GCC receptors, while after several passages of cell culture, stable content of hormones might have down-regulated the GCC receptor into a low steady state level, which, however, may only be relevant for the cell line culture conditions and not necessarily in vivo.

4. GCCmRNA detection in peripheral blood of metastatic CRC patients

Previous reports have described absence of GCCmRNA in blood from normal volunteers, patients with non-malignant pathologies of the intestine or patients with extra-intestinal malignancies, and presence only in blood from patients with intestinal malignancies. This highly selective expression of GCCmRNA related to intestinal cell malignancies provides an opportunity to study GCCmRNA expression as a marker for hematogenous spread of intestinal malignancies. The combination of high sensitivity of the PCR and high specificity of GCC expression in CRC cells make GCCmRNA a suitable biomarker for detecting metastatic cancer cells in the peripheral blood of CRC patients. It was demonstrated that high tumor-related mRNA levels in peripheral blood could predict short term survival and poor prognosis, because high mRNA levels suggest high metastatic tumor burden. We also observed that high GCCmRNA levels in peripheral blood was significantly associated with tumor emboli in vessels, lymph node metastases, mesenteric root lymph node metastases, poor DFS and OS. Tumor emboli in vessels is the essential pathological factor indicating tumor cluster in the drawing vessels from the primary site, and it is also the pathological correlation of circulating micro-metastasis[125]. The relationship of tumor emboli in vessels with poor survival, tumor recurrence and tumor diversion have been frequently reported [126-129]. Recent studies further revealed that tumors with blood vessel invasion, lymph node metastasis, and advanced clinical stage were significantly associated with poor prognosis of CRC patients in multivariate analysis [129, 130], which was also confirmed by our study. Our results not only revealed that tumor emboli in vessels had a significant correlation with both DFS and OS, but also demonstrated an association with high GCCmRNA levels. Furthermore, GCCmRNA levels showed a similarly significant correlation with DFS and OS when compared with tumor emboli in vessels (all $P<0.001$). All these findings taken together underline the prognostic value of GCCmRNA in CRC patients.

Similarly, presence of mesenteric root lymph node metastases was always related to poor overall survival despite standard chemotherapy and radiotherapy after radical surgery [131-133]. High ligation of the inferior mesenteric artery has been recommended in recent surgical guidelines, which make it possible to detect mesenteric root lymph node metastasis and guide post-surgical therapy [134, 135]. The incidence of metastasis to the mesenteric root lymph node was reported to be relatively low in CRC patients, ranging from 0.3% to 11.1%[131, 132], but the 5-year survival was significantly inferior to those without metastasis[132]. It was reported that the 5-year survival rate was 68.2% for patients with marginal lymph node involvement and only 30% for patients with central lymph node metastases, which was approximately half of those with marginal lymph node

metastases[133]. In our study, mesenteric root lymph node metastases showed high correlation with a high GCCmRNA level as well as poor DFS and OS.

We subsequently included GCCmRNA into univariate survival and multivariate COX regression analysis, both showed GCCmRNA as a hazard factor for predicting patients' survival. Univariate analysis in our study revealed that high GCCmRNA was significantly associated with poor DFS and OS status. Within TNM stage groups, GCCmRNA maintained its correlation with survival in each stage, especially in stage II and stage III subgroups. Together with core survival factors such as tumor emboli in vessels, mesenteric root lymph node metastases, tumor location, CA199 levels and differentiation types, GCCmRNA was selected in the multivariate Cox regression model with a high score. When we excluded GCCmRNA from the multivariate Cox regression model of DFS and OS, obvious alteration of other hazard factors were observed. Additionally, the likelihood ratio of multivariate Cox regression model was tested to compare the efficiency of GCCmRNA when included in or excluded from equations, both results indicated a significant difference ($P<0.001$). In summary, our study of GCCmRNA in peripheral blood of CRC patients with DFS and OS has revealed GCCmRNA as circulating tumor marker for survival prediction in clinical practice, which strongly supports further investigation of GCC antibodies for direct CTC staining. Additionally, one PCR-based study of Inge Kehler in our lab indicated that GCC was highly expressed in colon cancer cells, but negative in PBMC from healthy donors.

5. Nonspecific staining of conjugated GCC antibodies in leukocytes

CTC detection methods can be subdivided into two principles: nucleic acid-based approaches and cell-based approaches [136]. Here we attempted to improve assay sensitivity, specificity and reproducibility by multi-staining of CTC with GCC, CK and EpCAM antibodies for optimizing cytometry-based CTC detection. We have discussed GCC antibody staining in colon cancer cell lines by indirect staining in part 3 of the discussion, here we further explore the staining of unconjugated and conjugated GCC antibodies in leukocytes. We performed a series of experiments, including: unconjugated GCC antibody and secondary antibody staining, Alexa 488 conjugated GCC antibody staining, and FITC conjugated GCC antibody staining in both colon cancer cell lines and leukocytes. Unfortunately, no conjugated anti-GCC antibody was commercially provided at the time we initiated our experiments, therefore we conjugated the GCC antibody ourselves with Alexa488 by labeling kits. We ultimately produced sufficient amounts of the Alexa488 conjugated GCC antibody and tested it for both T84 cell line and leukocyte staining characteristics. The T84 cell staining showed similar staining ability of the Alexa488 conjugated

GCC antibody compared with the unconjugated GCC antibody. The surface staining of T84 cells by Alexa488 conjugated GCC antibody under fluoroscope also showed equally bright green fluorescence compared to the unconjugated GCC antibody. Thus, it can be considered that Alexa488 conjugated GCC antibody has similar antigen-binding and staining characteristics as the unconjugated GCC antibody.

However, subsequent analysis of GCC antibody staining on leukocytes presented a big hurdle for its application in CTC enrichment and detection. All experiments showed high unexpected staining of leukocytes by the unconjugated and Alexa 488 conjugated GCC antibodies. It was a common problem for unconjugated antibodies, since indirect staining might increase nonspecific binding to leukocytes [137, 138]. We simultaneously tested unconjugated GCC antibody, goat anti-mouse secondary antibody and Alexa488 conjugated GCC antibody in search of the source of nonspecific staining. As a result, all of these three antibodies had high staining and all of them had similar composition of stained leukocytes. Although theoretically, direct staining by conjugated antibodies has the advantages of reducing nonspecific staining [137, 139], this had no advantage for the GCC antibodies we investigated.

We further compared multi-staining of GCC, CK and EpCAM by direct staining and observed that those GCC+/ CK-/ EpCAM- subgroup cells were mostly leukocytes. Furthermore, we compared the subpopulation of single staining by GCC, CK and EpCAM in order to further characterize the non-specifically GCC stained subpopulation. As shown in Figure 21, we clearly found that CK and EpCAM single positive populations had similar non-specific portions with isotype control, mainly derived from granulocytes, but could be eliminated by CD45+ cell depletion. Additionally, isotype control had similar nonspecific staining with all corresponding antibodies, which suggested that the Fc region might be the essential part of antibodies for nonspecific staining. Current studies have proved Fc-fragment of the antibody as nonspecific binding site to Fc receptors expressed on leukocytes. The effect of Fc receptor binding can be minimized by pretreatment with Fc receptor block reagent [140, 141]. Fc-receptors are widely expressed on specific subsets of leukocytes, and each subtype might be a potential source of nonspecific binding [142, 143]. Unlike Fc fragments, the F-(ab) domains with variable regions of antibodies can provide specific binding sites to the epitope [142]. Given that there is similar nonspecific staining in both isotype control and conjugated antibody, Fc regions of CK, EpCAM and GCC antibodies should be responsible for those undesirable bindings. The isotype of IgG1 for EpCAM and IgG2a for CK in our protocol was recently reported to display nonspecific binding of leukocytes, particularly monocytes, whereas the IgG2b isotype(for GCC) does not [141, 143]. Similar

experiments were repeated for confirming the existence of nonspecific binding of GCC antibodies to leukocytes. Unfortunately, the high nonspecific binding rates to leukocytes revealed that both antibodies are unsuitable for CTC enrichment and detection.

Additional experiments with the FITC conjugated GCC antibody (the only commercially conjugated GCC antibody we could find till now) attempted to test the performance of a different sub-clone (2G7 in contrast to the previously tested 1B11) in T84 cells and leukocytes. Unfortunately, these results still showed a high nonspecific surface (53.67%) and intracellular (93.47%) staining of leukocytes. In summary, all GCC antibodies failed to reliably distinguish colon cancer cells from leukocytes. Unspecific binding might occur due to electrostatic interactions (FITC charge), glycolipid interaction on the cell membrane (binding of antibodies to membrane), protein-protein interactions (binding of antibodies or fluorochromes to Fc receptor) and DNA binding (released from dead cells). Among all these principles of unspecific staining, despite Fc receptor blocking, undesirable binding of antibodies or fluorochromes to Fc receptors on leukocytes was likely responsible for the unspecific staining in our study. Fc receptors are classified on the basis of the type of antibodies they recognize. Those commonly binding IgG antibodies are called Fc-gamma receptors (abbreviated FcγR), which include several family members such as FcγRI, FcγRIIA, FcγRIIB, FcγRIIIA and FcγRIIIB, and are present in almost all leukocytes. Our data suggest that the majority cells with nonspecific binding were lymphocytes and granulocytes, which theoretically could be eliminated by removing the Fc region of a directly labeled GCC antibody. Secondly, sufficient Fc receptor blocking is also a crucial step to avoid nonspecific binding of antibody. Depletion is the most important procedure for CTC enrichment and staining, thorough depletion could remove unwanted leukocytes, reduce nonspecific background and increase recovery rate of targeted cells [144]. Our study demonstrated that by sufficient CD45+ cell depletion, undesirable staining by Fc region of antibody to CD45+ granulocytes was diminished in the CK and EpCAM positive gate. Fc receptor blocking is also the best way to decrease the interaction of Fc region with Fc receptors on leukocytes. Our experiments used goat serum as Fc receptor blocking for colon tumor cell staining and Fc receptor blocking kits for tumor cell detection from blood samples, which should avoid most of nonspecific binding caused by Fc receptors. Therefore, the nonspecific staining of our two conjugated GCC antibodies is mainly due to their Fc region and undesirable binding sites. Further gene recombination approaches to remove Fc regions and undesirable binding sites may solve this problem in the future.

6. Conclusions and future direction

In conclusion, (1) CTC enrichment was optimized by additional recycling of depleted CD45+ leukocytes; (2) GCC was found significantly over-expressed in tumors compared to adjacent normal mucosa by IHC staining; 3) GCC was expressed in almost all colon cancer cell lines; 4) high GCCmRNA level in peripheral blood of CRC patients was a valuable biomarker predicting poor DFS and OS; 5) based on currently available reagents, the unconjugated as well as the conjugated GCC antibodies showed undesirable nonspecific binding of leukocytes, which precluded further application in peripheral blood samples. Due to its high specific expression in primary and metastatic CRC cells, GCC remains a desirable target for more specific antibodies, that could be developed without an Fc region and a highly specific binding site to eliminate nonspecific binding to leukocytes and facilitate detection of CTCs in CRC patients.

Recently, the feasibility of hormone replacement for treatment of CRC is underscored by the development of the FDA-approved GUCY2C ligand linaclotide (Linzess™), which can be orally administered to patients to restore GCC activation [145]. Other GCC-specific peptide compounds are currently being developed for gastrointestinal diseases [145, 146]. We hope that future improvement of GCC antibodies will enable us to reliably detect CTCs in patients with colorectal cancer, allowing early detection of metastatic cells and provide meaningful impact on the way CRC is detected and treated in the future.

Bibliography

1. Ferlay J, Soerjomataram I, Dikshit R, Eser S, Mathers C, Rebelo M, Parkin DM, Forman D and Bray F. Cancer incidence and mortality worldwide: Sources, methods and major patterns in GLOBOCAN 2012. International Journal of Cancer. 2015; 136(5):E359-E386.
2. Siegel RL, Miller KD and Jemal A. Cancer Statistics, 2015. Ca-Cancer J Clin. 2015; 65(1):5-29.
3. Jasperson KW, Tuohy TM, Neklason DW and Burt RW. Hereditary and Familial Colon Cancer. Gastroenterology. 2010; 138(6):2044-2058.
4. Whiffin N, Hosking FJ, Farrington SM, Palles C, Dobbins SE, Zgaga L, Lloyd A, Kinnersley B, Gorman M, Tenesa A, Broderick P, Wang Y, Barclay E, Hayward C, Martin L, Buchanan DD, et al. Identification of susceptibility loci for colorectal cancer in a genome-wide meta-analysis. Hum Mol Genet. 2014; 23(17):4729-4737.
5. Dunlop MG, Dobbins SE, Farrington SM, Jones AM, Palles C, Whiffin N, Tenesa A, Spain S, Broderick P, Ooi LY, Domingo E, Smillie C, Henrion M, Frampton M, Martin L, Grimes G, et al. Common variation near CDKN1A, POLD3 and SHROOM2 influences colorectal cancer risk. Nat Genet. 2012; 44(7):770-776.
6. Vogelstein B, Papadopoulos N, Velculescu VE, Zhou SB, Diaz LA and Kinzler KW. Cancer Genome Landscapes. Science. 2013; 339(6127):1546-1558.
7. Yoruker EE, Holdenrieder S and Gezer U. Blood-based biomarkers for diagnosis, prognosis and treatment of colorectal cancer. Clin Chim Acta. 2016; 455:26-32.
8. Pino MS and Chung DC. The Chromosomal Instability Pathway in Colon Cancer. Gastroenterology. 2010; 138(6):2059-2072.
9. Carethers JM and Jung BH. Genetics and Genetic Biomarkers in Sporadic Colorectal Cancer. Gastroenterology. 2015; 149(5):1177-+.
10. Obrocea FL, Sajin M, Marinescu EC and Stoica D. Colorectal cancer and the 7th revision of the TNM staging system: review of changes and suggestions for uniform pathologic reporting. Rom J Morphol Embryol. 2011; 52(2):537-544.
11. von Winterfeld M, Hoffmeister M, Ingold-Heppner B, Jansen L, Tao S, Herpel E, Schirmacher P, Dietel M, Chang-Claude J, Autschbach F, Brenner H and Blaker H. Frequency of therapy-relevant staging shifts in colorectal cancer through the introduction of pN1c in the 7th TNM edition. Eur J Cancer. 2014; 50(17):2958-2965.
12. Merkel S, Weber K, Croner RS, Golcher H, Gohl J, Agaimy A, Semrau S, Siebler J, Wein A, Hohenberger W and Wittekind C. Distant metastases in colorectal carcinoma: A proposal for a new M1 subclassification. Eur J Surg Oncol. 2016.
13. Brenner H, Kloor M and Pox CP. Colorectal cancer. Lancet. 2014; 383(9927):1490-1502.
14. Cree IA. Improved blood tests for cancer screening: general or specific? Bmc Cancer. 2011; 11:499.
15. Joosse SA and Pantel K. Tumor-Educated Platelets as Liquid Biopsy in Cancer Patients. Cancer Cell. 2015; 28(5):552-554.
16. Normanno N and Cree IA. Genomics driven-oncology: challenges and perspectives. Bmc Cancer. 2015; 15.
17. Mead R, Duku M, Bhandari P and Cree IA. Circulating tumour markers can define patients with normal colons, benign polyps, and cancers. Brit J Cancer. 2011; 105(2):239-245.
18. Crowley E, Di Nicolantonio F, Loupakis F and Bardelli A. Liquid biopsy: monitoring cancer-genetics in the blood. Nat Rev Clin Oncol. 2013; 10(8):472-484.
19. Spindler KL, Pallisgaard N, Vogelius I and Jakobsen A. Quantitative cell-free DNA, KRAS, and BRAF mutations in plasma from patients with metastatic colorectal cancer during treatment with cetuximab and irinotecan. Clin Cancer Res. 2012; 18(4):1177-1185.
20. Snook AE, Magee MS and Waldman SA. GUCY2C-targeted cancer immunotherapy: past, present and future. Immunol Res. 2011; 51(2-3):161-169.
21. Welinder C, Jansson B, Lindell G and Wenner J. Cytokeratin 20 improves the detection of circulating tumor cells in patients with colorectal cancer. Cancer Lett. 2015; 358(1):43-46.

22. Ganepola GA, Nizin J, Rutledge JR and Chang DH. Use of blood-based biomarkers for early diagnosis and surveillance of colorectal cancer. World J Gastrointest Oncol. 2014; 6(4):83-97.
23. Krol J, Loedige I and Filipowicz W. The widespread regulation of microRNA biogenesis, function and decay. Nat Rev Genet. 2010; 11(9):597-610.
24. Garzon R, Marcucci G and Croce CM. Targeting microRNAs in cancer: rationale, strategies and challenges. Nat Rev Drug Discov. 2010; 9(10):775-789.
25. Zandberga E, Kozirovskis V, Abols A, Andrejeva D, Purkalne G and Line A. Cell-free microRNAs as diagnostic, prognostic, and predictive biomarkers for lung cancer. Gene Chromosome Canc. 2013; 52(4):356-369.
26. Shaw JA, Brown J, Coombes RC, Jacob J, Payne R, Lee B, Page K, Hava N and Stebbing J. Circulating tumor cells and plasma DNA analysis in patients with indeterminate early or metastatic breast cancer. Biomark Med. 2011; 5(1):87-91.
27. Spitzer MH and Nolan GP. Mass Cytometry: Single Cells, Many Features. Cell. 2016; 165(4):780-791.
28. Schwarzenbach H, Eichelser C, Kropidlowski J, Janni W, Rack B and Pantel K. Loss of Heterozygosity at Tumor Suppressor Genes Detectable on Fractionated Circulating Cell-Free Tumor DNA as Indicator of Breast Cancer Progression. Clin Cancer Res. 2012; 18(20):5719-5730.
29. Kuhlmann JD, Schwarzenbach H, Wimberger P, Poetsch M, Kimmig R and Kasimir-Bauer S. LOH at 6q and 10q in fractionated circulating DNA of ovarian cancer patients is predictive for tumor cell spread and overall survival. Bmc Cancer. 2012; 12.
30. Diehl F, Schmidt K, Choti MA, Romans K, Goodman S, Li M, Thornton K, Agrawal N, Sokoll L, Szabo SA, Kinzler KW, Vogelstein B and Diaz LA. Circulating mutant DNA to assess tumor dynamics. Nat Med. 2008; 14(9):985-990.
31. Chan KC, Jiang P, Zheng YW, Liao GJ, Sun H, Wong J, Siu SS, Chan WC, Chan SL, Chan AT, Lai PB, Chiu RW and Lo YM. Cancer genome scanning in plasma: detection of tumor-associated copy number aberrations, single-nucleotide variants, and tumoral heterogeneity by massively parallel sequencing. Clin Chem. 2013; 59(1):211-224.
32. Leary RJ, Sausen M, Kinde I, Papadopoulos N, Carpten JD, Craig D, O'Shaughnessy J, Kinzler KW, Parmigiani G, Vogelstein B, Diaz LA, Jr. and Velculescu VE. Detection of chromosomal alterations in the circulation of cancer patients with whole-genome sequencing. Sci Transl Med. 2012; 4(162):162ra154.
33. Dawson SJ, Tsui DW, Murtaza M, Biggs H, Rueda OM, Chin SF, Dunning MJ, Gale D, Forshew T, Mahler-Araujo B, Rajan S, Humphray S, Becq J, Halsall D, Wallis M, Bentley D, et al. Analysis of circulating tumor DNA to monitor metastatic breast cancer. N Engl J Med. 2013; 368(13):1199-1209.
34. Yung TK, Chan KC, Mok TS, Tong J, To KF and Lo YM. Single-molecule detection of epidermal growth factor receptor mutations in plasma by microfluidics digital PCR in non-small cell lung cancer patients. Clin Cancer Res. 2009; 15(6):2076-2084.
35. Liu PJ, Liang HY, Xue L, Yang C, Liu Y, Zhou K and Jiang XF. Potential clinical significance of plasma-based KRAS mutation analysis using the COLD-PCR/TaqMan (R)-MGB probe genotyping method. Exp Ther Med. 2012; 4(1):109-112.
36. Chen Z, Feng J, Buzin CH, Liu Q, Weiss L, Kernstine K, Somlo G and Sommer SS. Analysis of cancer mutation signatures in blood by a novel ultra-sensitive assay: monitoring of therapy or recurrence in non-metastatic breast cancer. PLoS One. 2009; 4(9):e7220.
37. Brevet M, Johnson ML, Azzoli CG and Ladanyi M. Detection of EGFR mutations in plasma DNA from lung cancer patients by mass spectrometry genotyping is predictive of tumor EGFR status and response to EGFR inhibitors. Lung Cancer. 2011; 73(1):96-102.
38. Murtaza M, Dawson SJ, Tsui DWY, Gale D, Forshew T, Piskorz AM, Parkinson C, Chin SF, Kingsbury Z, Wong ASC, Marass F, Humphray S, Hadfield J, Bentley D, Chin TM, Brenton JD, et al. Non-invasive analysis of acquired resistance to cancer therapy by sequencing of plasma DNA. Nature. 2013; 497(7447):108-+.
39. Haas J, Katus HA and Meder B. Next-generation sequencing entering the clinical arena. Mol Cell Probes. 2011; 25(5-6):206-211.
40. Forshew T, Murtaza M, Parkinson C, Gale D, Tsui DW, Kaper F, Dawson SJ, Piskorz AM, Jimenez-Linan M, Bentley D, Hadfield J, May AP, Caldas C, Brenton JD and Rosenfeld N. Noninvasive

identification and monitoring of cancer mutations by targeted deep sequencing of plasma DNA. Sci Transl Med. 2012; 4(136):136ra168.
41. Li CN, Hsu HL, Wu TL, Tsao KC, Sun CF and Wu JT. Cell-free DNA is released from tumor cells upon cell death: A study of tissue cultures of tumor cell lines. J Clin Lab Anal. 2003; 17(4):103-107.
42. Alix-Panabieres C and Pantel K. Circulating Tumor Cells: Liquid Biopsy of Cancer. Clinical Chemistry. 2013; 59(1):110-118.
43. Winer-Jones JP, Vahidi B, Arquilevich N, Fang C, Ferguson S, Harkins D, Hill C, Klem E, Pagano PC, Peasley C, Romero J, Shartle R, Vasko RC, Strauss WM and Dempsey PW. Circulating tumor cells: clinically relevant molecular access based on a novel CTC flow cell. PLoS One. 2014; 9(1):e86717.
44. Harouaka R, Kang Z, Zheng SY and Cao L. Circulating tumor cells: advances in isolation and analysis, and challenges for clinical applications. Pharmacol Ther. 2014; 141(2):209-221.
45. Hou HW, Warkiani ME, Khoo BL, Li ZR, Soo RA, Tan DSW, Lim WT, Han J, Bhagat AAS and Lim CT. Isolation and retrieval of circulating tumor cells using centrifugal forces. Sci Rep-Uk. 2013; 3.
46. Gertler R, Rosenberg R, Fuehrer K, Dahm M, Nekarda H and Siewert JR. Detection of circulating tumor cells in blood using an optimized density gradient centrifugation. Recent Results Cancer Res. 2003; 162:149-155.
47. Hvichia GE, Parveen Z, Wagner C, Janning M, Quidde J, Stein A, Muller V, Loges S, Neves RP, Stoecklein NH, Wikman H, Riethdorf S, Pantel K and Gorges TM. A novel microfluidic platform for size and deformability based separation and the subsequent molecular characterization of viable circulating tumor cells. Int J Cancer. 2016; 138(12):2894-2904.
48. Kim MS, Sim TS, Kim YJ, Kim SS, Jeong H, Park JM, Moon HS, Kim SI, Gurel O, Lee SS, Lee JG and Park JC. SSA-MOA: a novel CTC isolation platform using selective size amplification (SSA) and a multi-obstacle architecture (MOA) filter. Lab on a Chip. 2012; 12(16):2874-2880.
49. Yusa A, Toneri M, Masuda T, Ito S, Yamamoto S, Okochi M, Kondo N, Iwata H, Yatabe Y, Ichinosawa Y, Kinuta S, Kondo E, Honda H, Arai F and Nakanishi H. Development of a New Rapid Isolation Device for Circulating Tumor Cells (CTCs) Using 3D Palladium Filter and Its Application for Genetic Analysis. Plos One. 2014; 9(2).
50. Kaifi JT, Kunkel M, Das A, Harouaka RA, Dicker DT, Li GF, Zhu JJ, Clawson GA, Yang ZH, Reed MF, Gusani NJ, Kimchi ET, Staveley-O'Carroll KF, Zheng SY and El-Deiry WS. Circulating tumor cell isolation during resection of colorectal cancer lung and liver metastases: a prospective trial with different detection techniques. Cancer Biology & Therapy. 2015; 16(5):699-708.
51. Zheng S, Lin H, Liu JQ, Balic M, Datar R, Cote RJ and Tai YC. Membrane microfilter device for selective capture, electrolysis and genomic analysis of human circulating tumor cells. J Chromatogr A. 2007; 1162(2):154-161.
52. Lu YT, Zhao L, Shen Q, Garcia MA, Wu D, Hou S, Song M, Xu X, Ouyang WH, Ouyang WW, Lichterman J, Luo Z, Xuan X, Huang J, Chung LW, Rettig M, et al. NanoVelcro Chip for CTC enumeration in prostate cancer patients. Methods. 2013; 64(2):144-152.
53. Xu T, Lu B, Tai YC and Goldkorn A. A Cancer Detection Platform Which Measures Telomerase Activity from Live Circulating Tumor Cells Captured on a Microfilter. Cancer Research. 2010; 70(16):6420-6426.
54. Parkinson DR, Dracopoli N, Petty BG, Compton C, Cristofanilli M, Deisseroth A, Hayes DF, Kapke G, Kumar P, Lee JSH, Liu MC, McCormack R, Mikulski S, Nagahara L, Pantel K, Pearson-White S, et al. Considerations in the development of circulating tumor cell technology for clinical use. J Transl Med. 2012; 10.
55. Talasaz AH, Powell AA, Huber DE, Berbee JG, Roh KH, Yu W, Xiao WZ, Davis MM, Pease RF, Mindrinos MN, Jeffrey SS and Davis RW. Isolating highly enriched populations of circulating epithelial cells and other rare cells from blood using a magnetic sweeper device. P Natl Acad Sci USA. 2009; 106(10):3970-3975.
56. Miller MC, Doyle GV and Terstappen LW. Significance of Circulating Tumor Cells Detected by the CellSearch System in Patients with Metastatic Breast Colorectal and Prostate Cancer. J Oncol. 2010; 2010:617421.
57. Nagrath S, Sequist LV, Maheswaran S, Bell DW, Irimia D, Ulkus L, Smith MR, Kwak EL, Digumarthy S, Muzikansky A, Ryan P, Balis UJ, Tompkins RG, Haber DA and Toner M. Isolation of rare circulating tumour cells in cancer patients by microchip technology. Nature. 2007; 450(7173):1235-1239.

58. Stott SL, Hsu CH, Tsukrov DI, Yu M, Miyamoto DT, Waltman BA, Rothenberg SM, Shah AM, Smas ME, Korir GK, Floyd FP, Gilman AJ, Lord JB, Winokur D, Springer S, Irimia D, et al. Isolation of circulating tumor cells using a microvortex-generating herringbone-chip. P Natl Acad Sci USA. 2010; 107(43):18392-18397.
59. Sheng WA, Ogunwobi OO, Chen T, Zhang JL, George TJ, Liu C and Fan ZH. Capture, release and culture of circulating tumor cells from pancreatic cancer patients using an enhanced mixing chip. Lab on a Chip. 2014; 14(1):89-98.
60. Fehm T, Hoffmann O, Aktas B, Becker S, Solomayer EF, Wallwiener D, Kimmig R and Kasimir-Bauer S. Detection and characterization of circulating tumor cells in blood of primary breast cancer patients by RT-PCR and comparison to status of bone marrow disseminated cells. Breast Cancer Research. 2009; 11(4).
61. Schwarzenbach H, Alix-Panabieres C, Muller I, Letang N, Vendrell JP, Rebillard X and Pantel K. Cell-free Tumor DNA in Blood Plasma As a Marker for Circulating Tumor Cells in Prostate Cancer. Clin Cancer Res. 2009; 15(3):1032-1038.
62. Balasubramanian P, Yang LY, Lang JC, Jatana KR, Schuller D, Agrawal A, Zborowski M and Chalmers JJ. Confocal Images of Circulating Tumor Cells Obtained Using a Methodology and Technology That Removes Normal Cells. Mol Pharmaceut. 2009; 6(5):1402-1408.
63. Lustberg M, Jatana KR, Zborowski M and Chalmers JJ. Emerging technologies for CTC detection based on depletion of normal cells. Recent Results Cancer Res. 2012; 195:97-110.
64. Harb W, Fan A, Tran T, Danila DC, Keys D, Schwartz M and Ionescu-Zanetti C. Mutational Analysis of Circulating Tumor Cells Using a Novel Microfluidic Collection Device and qPCR Assay. Translational Oncology. 2013; 6(5):528-+.
65. Basiji DA, Ortyn WE, Liang L, Venkatachalam V and Morrissey P. Cellular image analysis and imaging by flow cytometry. Clin Lab Med. 2007; 27(3):653-+.
66. Krivacic RT, Ladanyi A, Curry DN, Hsieh HB, Kuhn P, Bergsrud DE, Kepros JF, Barbera T, Ho MY, Chen LB, Lerner RA and Bruce RH. A rare-cell detector for cancer. P Natl Acad Sci USA. 2004; 101(29):10501-10504.
67. Allen JE, Saroya BS, Kunkel M, Dicker DT, Das A, Peters KL, Joudeh J, Zhu JJ and El-Deiry WS. Apoptotic circulating tumor cells (CTCs) in the peripheral blood of metastatic colorectal cancer patients are associated with liver metastasis but not CTCs. Oncotarget. 2014; 5(7):1753-1760.
68. Alix-Panabieres C, Schwarzenbach H and Pantel K. Circulating tumor cells and circulating tumor DNA. Annu Rev Med. 2012; 63:199-215.
69. Forte VA, Barrak DK, Elhodaky M, Tung L, Snow A and Lang JE. The potential for liquid biopsies in the precision medical treatment of breast cancer. Cancer Biol Med. 2016; 13(1):19-40.
70. Savagner P. The epithelial-mesenchymal transition (EMT) phenomenon. Ann Oncol. 2010; 21 Suppl 7:vii89-92.
71. Kokkinos MI, Wafai R, Wong MK, Newgreen DF, Thompson EW and Waltham M. Vimentin and epithelial-mesenchymal transition in human breast cancer - Observations in vitro and in vivo. Cells Tissues Organs. 2007; 185(1-3):191-203.
72. Shook D and Keller R. Mechanisms, mechanics and function of epithelial-mesenchymal transitions in early development. Mech Develop. 2003; 120(11):1351-1383.
73. Friedlander TW, Premasekharan G and Paris PL. Looking back, to the future of circulating tumor cells. Pharmacol Ther. 2014; 142(3):271-280.
74. Berman JM, Cheung RJ and Weinberg DS. Surveillance after colorectal cancer resection. Lancet. 2000; 355(9201):395-399.
75. Sinicrope FA and Sugarman SM. Role of adjuvant therapy in surgically resected colorectal carcinoma. Gastroenterology. 1995; 109(3):984-993.
76. Weinberg DS, Desnoyers R, Gelmann A, Boman BM and Waldman SA. Postoperative management of local colorectal cancer: therapy and surveillance. Semin Gastrointest Dis. 2000; 11(3):152-156.
77. Carrithers SL. Diarrhea or colorectal cancer: Can bacterial toxins serve as a treatment for colon cancer? P Natl Acad Sci USA. 2003; 100(6):3018-3020.
78. Lucas KA, Pitari GM, Kazerounian S, Ruiz-Stewart I, Park J, Schulz S, Chepenik KP and Waldman SA. Guanylyl cyclases and signaling by cyclic GMP. Pharmacol Rev. 2000; 52(3):375-414.

79. Qian X, Prabhakar S, Nandi A, Visweswariah SS and Goy MF. Expression of GC-C, a receptor-guanylate cyclase, and its endogenous ligands uroguanylin and guanylin along the rostrocaudal axis of the intestine. Endocrinology. 2000; 141(9):3210-3224.
80. Wilson C, Lin JE, Li P, Snook AE, Gong JP, Sato T, Liu CB, Girondo MA, Rui H, Hyslop T and Waldman SA. The Paracrine Hormone for the GUCY2C Tumor Suppressor, Guanylin, Is Universally Lost in Colorectal Cancer. Cancer Epidem Biomar. 2014; 23(11):2328-2337.
81. Fajardo AM, Piazza GA and Tinsley HN. The role of cyclic nucleotide signaling pathways in cancer: targets for prevention and treatment. Cancers (Basel). 2014; 6(1):436-458.
82. Pattison AM, Merlino DJ, Blomain ES and Waldman SA. Guanylyl cyclase C signaling axis and colon cancer prevention. World J Gastroentero. 2016; 22(36):8070-8077.
83. Birbe R, Palazzo JP, Walters R, Weinberg D, Schutz S and Waldman SA. Guanylyl cyclase C is a marker of intestinal metaplasia, dysplasia, and adenocarcinoma of the gastrointestinal tract. Hum Pathol. 2005; 36(2):170-179.
84. Carrithers SL, Barber MT, Biswas S, Parkinson SJ, Park PK, Goldstein SD and Waldman SA. Guanylyl cyclase C is a selective marker for metastatic colorectal tumors in human extraintestinal tissues. P Natl Acad Sci USA. 1996; 93(25):14827-14832.
85. Frick GS, Pitari GM, Weinberg DS, Hyslop T, Schulz S and Waldman SA. Guanylyl cyclase C: a molecular marker for staging and postoperative surveillance of patients with colorectal cancer. Expert Rev Mol Diagn. 2005; 5(5):701-713.
86. Snook AE, Eisenlohr LC, Rothstein JL and Waldman SA. Cancer mucosa antigens as a novel immunotherapeutic class of tumor-associated antigen. Clin Pharmacol Ther. 2007; 82(6):734-739.
87. Liu Y, Qian J, Feng JG, Ju HX, Zhu YP, Feng HY and Li DC. Detection of circulating tumor cells in peripheral blood of colorectal cancer patients without distant organ metastases. Cell Oncol. 2013; 36(1):43-53.
88. Fava TA, Desnoyers R, Schulz S, Park J, Weinberg D, Mitchell E and Waldman SA. Ectopic expression of guanylyl cyclase C in CD34+ progenitor cells in peripheral blood. J Clin Oncol. 2001; 19(19):3951-3959.
89. Bustin SA, Gyselman VG, Williams NS and Dorudi S. Detection of cytokeratins 19/20 and guanylyl cyclase C in peripheral blood of colorectal cancer patients. Br J Cancer. 1999; 79(11-12):1813-1820.
90. Vlems FA, Diepstra JH, Cornelissen IM, Ligtenberg MJ, Wobbes T, Punt CJ, van Krieken JH, Ruers TJ and van Muijen GN. Investigations for a multi-marker RT-PCR to improve sensitivity of disseminated tumor cell detection. Anticancer Res. 2003; 23(1A):179-186.
91. Tien YW, Chang KJ, Jeng YM, Lee PH, Wu MS, Lin JT and Hsu SM. Tumor angiogenesis and its possible role in intravasation of colorectal epithelial cells. Clin Cancer Res. 2001; 7(6):1627-1632.
92. Liu ZA, Fusi A, Klopocki E, Schmittel A, Tinhofer I, Nonnenmacher A and Keilholz U. Negative enrichment by immunomagnetic nanobeads for unbiased characterization of circulating tumor cells from peripheral blood of cancer patients. J Transl Med. 2011; 9.
93. Khoja L, Lorigan P, Dive C, Keilholz U and Fusi A. Circulating tumour cells as tumour biomarkers in melanoma: detection methods and clinical relevance. Annals of Oncology. 2015; 26(1):33-39.
94. Ornatsky O, Bandura D, Baranov V, Nitz M, Winnik MA and Tanner S. Highly multiparametric analysis by mass cytometry. J Immunol Methods. 2010; 361(1-2):1-20.
95. Brown M and Wittwer C. Flow cytometry: principles and clinical applications in hematology. Clin Chem. 2000; 46(8 Pt 2):1221-1229.
96. Valet G. Past and present concepts in flow cytometry: a European perspective. J Biol Regul Homeost Agents. 2003; 17(3):213-222.
97. Tagde A, Singh H, Kang MH and Reynolds CP. The glutathione synthesis inhibitor buthionine sulfoximine synergistically enhanced melphalan activity against preclinical models of multiple myeloma. Blood Cancer J. 2014; 4:e229.
98. Gross A, Schoendube J, Zimmermann S, Steeb M, Zengerle R and Koltay P. Technologies for Single-Cell Isolation. Int J Mol Sci. 2015; 16(8):16897-16919.
99. Schulz S, Hyslop T, Haaf J, Bonaccorso C, Nielsen K, Witek ME, Birbe R, Palazzo J, Weinberg D and Waldman SA. A validated quantitative assay to detect occult micrometastases by reverse transcriptase-polymerase chain reaction of guanylyl cyclase C in patients with colorectal cancer. Clin Cancer Res. 2006; 12(15):4545-4552.

100. Notterman DA, Alon U, Sierk AJ and Levine AJ. Transcriptional gene expression profiles of colorectal adenoma, adenocarcinoma, and normal tissue examined by oligonucleotide arrays. Cancer Research. 2001; 61(7):3124-3130.
101. Birkenkamp-Demtroder K, Christensen LL, Olesen SH, Frederiksen CM, Laiho P, Aaltonen LA, Laurberg S, Sorensen FB, Hagemann R and Orntoft TF. Gene expression in colorectal cancer. Cancer Research. 2002; 62(15):4352-4363.
102. Lucas KA, Pitari GM, Kazerounian S, Ruiz-Stewart I, Park J, Schulz S, Chepenik KP and Waldman SA. Guanylyl cyclases and signaling by cyclic GMP. Pharmacological Reviews. 2000; 52(3):375-413.
103. Pitari GM, Di Guglielmo MD, Park J, Schulz S and Waldman SA. Guanylyl cyclase C agonists regulate progression through the cell cycle of human colon carcinoma cells. P Natl Acad Sci USA. 2001; 98(14):7846-7851.
104. Li P, Schulz S, Bombonati A, Palazzo JP, Hyslop TM, Xu Y, Baran AA, Siracusa LD, Pitari GM and Waldman SA. Guanylyl cyclase C suppresses intestinal tumorigenesis by restricting proliferation and maintaining genomic integrity. Gastroenterology. 2007; 133(2):599-607.
105. Lin JE, Li P, Snook AE, Schulz S, Dasgupta A, Hyslop TM, Gibbons AV, Marszlowicz G, Pitari GM and Waldman SA. The Hormone Receptor GUCY2C Suppresses Intestinal Tumor Formation by Inhibiting AKT Signaling. Gastroenterology. 2010; 138(1):241-254.
106. Pitari GM, Li P, Lin JE, Zuzga D, Gibbons AV, Snook AE, Schulz S and Waldman SA. The paracrine hormone hypothesis of colorectal cancer. Clin Pharmacol Ther. 2007; 82(4):441-447.
107. Li P, Lin JE, Chervoneva I, Schulz S, Waldman SA and Pitari GM. Homeostatic control of the crypt-villus axis by the bacterial enterotoxin receptor guanylyl cyclase C restricts the proliferating compartment in intestine. Am J Pathol. 2007; 171(6):1847-1858.
108. Hyslop T and Waldman SA. Guanylyl cyclase C as a biomarker in colorectal cancer. Biomarkers in Medicine. 2013; 7(1):159-167.
109. Yu M, Stott S, Toner M, Maheswaran S and Haber DA. Circulating tumor cells: approaches to isolation and characterization. J Cell Biol. 2011; 192(3):373-382.
110. Lu YS, Liang HY, Yu T, Xie JJ, Chen SM, Dong HY, Sinko PJ, Lian S, Xu JG, Wang JC, Yu SH, Shao JW, Yuan B, Wang L and Jia L. Isolation and characterization of living circulating tumor cells in patients by immunomagnetic negative enrichment coupled with flow cytometry. Cancer. 2015; 121(17):3036-3045.
111. Punnoose EA, Atwal SK, Spoerke JM, Savage H, Pandita A, Yeh RF, Pirzkall A, Fine BM, Amler LC, Chen DS and Lackner MR. Molecular Biomarker Analyses Using Circulating Tumor Cells. Plos One. 2010; 5(9).
112. Gorges TM, Tinhofer I, Drosch M, Rose L, Zollner TM, Krahn T and von Ahsen O. Circulating tumour cells escape from EpCAM-based detection due to epithelial-to-mesenchymal transition. Bmc Cancer. 2012; 12.
113. Floor S, van Staveren WCG, Larsimont D, Dumont JE and Maenhaut C. Cancer cells in epithelial-to-mesenchymal transition and tumor-propagating-cancer stem cells: distinct, overlapping or same populations. Oncogene. 2011; 30(46):4609-4621.
114. Grover PK, Cummins AG, Price TJ, Roberts-Thomson IC and Hardingham JE. Circulating tumour cells: the evolving concept and the inadequacy of their enrichment by EpCAM-based methodology for basic and clinical cancer research. Annals of Oncology. 2014; 25(8):1506-1516.
115. Antolovic D, Galindo L, Carstens A, Rahbari N, Buchler MW, Weitz J and Koch M. Heterogeneous detection of circulating tumor cells in patients with colorectal cancer by immunomagnetic enrichment using different EpCAM-specific antibodies. Bmc Biotechnol. 2010; 10.
116. Ksiazkiewicz M, Markiewicz A and Zaczek AJ. Epithelial-Mesenchymal Transition: A Hallmark in Metastasis Formation Linking Circulating Tumor Cells and Cancer Stem Cells. Pathobiology. 2012; 79(4):195-208.
117. Biddle A and Mackenzie IC. Cancer stem cells and EMT in carcinoma. Cancer Metast Rev. 2012; 31(1-2):285-293.
118. Buc E, Der Vartanian M, Darcha C, Dechelotte P and Pezet D. Guanylyl cyclase C as a reliable immunohistochemical marker and its ligand Escherichia coli heat-stable enterotoxin as a potential protein-delivering vehicle for colorectal cancer cells. Eur J Cancer. 2005; 41(11):1618-1627.

119. Debruyne PR, Waldman SA and Schulz S. Pathological staging and therapy of oesophageal and gastric cancer. Expert Opin Pharmaco. 2003; 4(7):1083-1096.
120. Schulz S, Hyslop T, Haaf J, Bonaccorso C, Nielsen K, Witek ME, Birbe R, Palazzo J, Weinberg D and Waldman SA. A validated quantitative assay to detect occult micrometastases by reverse transcriptase-polymerase chain reaction of guanylyl cyclase C in patients with colorectal cancer. Clin Cancer Res. 2006; 12(15):4545-4552.
121. Witek ME, Nielsen K, Walters R, Hyslop T, Palazzo J, Schulz S and Waldman SA. The putative tumor suppressor Cdx2 is overexpressed by human colorectal adenocarcinomas. Clin Cancer Res. 2005; 11(24):8549-8556.
122. Steinbrecher KA, Tuohy TMF, Goss KH, Scott MC, Witte DP, Groden J and Cohen MB. Expression of guanylin is downregulated in mouse and human intestinal adenomas. Biochem Bioph Res Co. 2000; 273(1):225-230.
123. Moal VLL and Servin AL. Pathogenesis of Human Enterovirulent Bacteria: Lessons from Cultured, Fully Differentiated Human Colon Cancer Cell Lines. Microbiol Mol Biol R. 2013; 77(3):380-439.
124. Musa-Aziz R, Oliveira-Souza M and Mello-Aires M. Signaling pathways in the biphasic effect of ANG II on Na+/H+ exchanger in T84 cells. J Membrane Biol. 2005; 205(2):49-60.
125. Heriot and Kumar. Rectal cancer recurrence: factors and mechanisms. Colorectal Dis. 2000; 2(3):126-136.
126. Ueno H, Mochizuki H, Shinto E, Hashiguchi Y, Hase K and Talbot IC. Histologic indices in biopsy specimens for estimating the probability of extended local spread in patients with rectal carcinoma. Cancer. 2002; 94(11):2882-2891.
127. Chapuis PH, Lin BPC, Chan C, Dent OF and Bokey EL. Risk factors for tumour present in a circumferential line of resection after excision of rectal cancer. Brit J Surg. 2006; 93(7):860-865.
128. Hiranyakas A, da Silva G, Wexner SD, Ho YH, Allende D and Berho M. Factors influencing circumferential resection margin in rectal cancer. Colorectal Disease. 2013; 15(3):298-303.
129. Liang P, Nakada I, Hong JW, Tabuchi T, Motohashi G, Takemura A, Nakachi T, Kasuga T and Tabuchi T. Prognostic significance of immunohistochemically detected blood and lymphatic vessel invasion in colorectal carcinoma: Its impact on prognosis. Ann Surg Oncol. 2007; 14(2):470-477.
130. Sternberg A, Amar M, Alfici R and Groisman G. Conclusions from a study of venous invasion in stage IV colorectal adenocarcinoma. J Clin Pathol. 2002; 55(1):17-21.
131. Kanemitsu Y, Hirai T, Komori K and Kato T. Survival benefit of high ligation of the inferior mesenteric artery in sigmoid colon or rectal cancer surgery. Br J Surg. 2006; 93(5):609-615.
132. Uehara K, Yamamoto S, Fujita S, Akasu T and Moriya Y. Impact of upward lymph node dissection on survival rates in advanced lower rectal carcinoma. Digest Surg. 2007; 24(5):375-381.
133. Hida J and Okuno K. High ligation of the inferior mesenteric artery in rectal cancer surgery. Surg Today. 2013; 43(1):8-19.
134. Tjandra JJ, Kilkenny JW, Buie WD, Hyman N, Simmang C, Anthony T, Orsay C, Church J, Otchy D, Cohen J, Place R, Denstman F, Rakinic J, Moore R, Whiteford M and Force SPT. Practice parameters for the management of rectal cancer (revised). Dis Colon Rectum. 2005; 48(3):411-423.
135. Nelson H, Petrelli N, Carlin A, Couture J, Fleshman J, Guillem J, Miedema B, Ota D and Sargent D. Guidelines 2000 for colon and rectal cancer surgery. J Natl Cancer I. 2001; 93(8):583-596.
136. Sun YF, Yang XR, Zhou J, Qiu SJ, Fan J and Xu Y. Circulating tumor cells: advances in detection methods, biological issues, and clinical relevance. J Cancer Res Clin. 2011; 137(8):1151-1173.
137. Friis T, Pedersen KB, Hougaard D and Houen G. Immunocytochemical and Immunohistochemical Staining with Peptide Antibodies. Methods Mol Biol. 2015; 1348:311-325.
138. Ivell R, Teerds K and Hoffman GE. Proper Application of Antibodies for Immunohistochemical Detection: Antibody Crimes and How to Prevent Them. Endocrinology. 2014; 155(3):676-687.
139. Pastor MV. Direct immunofluorescent labeling of cells. Methods Mol Biol. 2010; 588:135-142.
140. Kuonen F, Touvrey C, Laurent J and Ruegg C. Fc Block Treatment, Dead Cells Exclusion, and Cell Aggregates Discrimination Concur to Prevent Phenotypical Artifacts in the Analysis of Subpopulations of Tumor-Infiltrating CD11b(+) Myelomonocytic Cells. Cytom Part A. 2010; 77a(11):1082-1090.
141. Andersen MN, Al-Karradi SN, Kragstrup TW and Hokland M. Elimination of erroneous results in flow cytometry caused by antibody binding to Fc receptors on human monocytes and macrophages. Cytometry A. 2016.

142. Hulspas R, O'Gorman MRG, Wood BL, Gratama JW and Sutherland DR. Considerations for the Control of Background Fluorescence in Clinical Flow Cytometry. Cytom Part B-Clin Cy. 2009; 76b(6):355-364.
143. Biancotto A and McCoy JP. Studying the Human Immunome: The Complexity of Comprehensive Leukocyte Immunophenotyping. Curr Top Microbiol. 2014; 377:23-60.
144. Lapin M, Tjensvoll K, Oltedal S, Buhl T, Gilje B, Smaaland R and Nordgard O. MINDEC-An Enhanced Negative Depletion Strategy for Circulating Tumour Cell Enrichment. Sci Rep-Uk. 2016; 6.
145. Busby RW, Bryant AP, Bartolini WP, Cordero EA, Hannig G, Kessler MM, Mahajan-Miklos S, Pierce CM, Solinga RM, Sun LJ, Tobin JV, Kurtz CB and Currie MG. Linaclotide, through activation of guanylate cyclase C, acts locally in the gastrointestinal tract to elicit enhanced intestinal secretion and transit. Eur J Pharmacol. 2010; 649(1-3):328-335.
146. Tchernychev B, Ge P, Kessler MM, Solinga RM, Wachtel D, Tobin JV, Thomas SR, Lunte CE, Fretzen A, Hannig G, Bryant AP, Kurtz CB, Currie MG and Silos-Santiago I. MRP4 Modulation of the Guanylate Cyclase-C/cGMP Pathway: Effects on Linaclotide-Induced Electrolyte Secretion and cGMP Efflux. J Pharmacol Exp Ther. 2015; 355(1):48-56.

Affidavit

I, Liu Yong certify under penalty of perjury by my own signature that I have submitted the thesis on the topic "Targeted guanylyl cyclase C for optimization of circulating colorectal cancer cells enrichment and isolation", I wrote this thesis independently and without assistance from third parties, I used no other aids than the listed sources and resources.

All points based literally or in spirit on publications or presentations of other authors are, as such, in proper citations (see "uniform requirements for manuscripts (URM)" the ICMJE www.icmje.org) indicated. The sections on methodology (in particular practical work, laboratory requirements, statistical processing) and results (in particular images, graphics and tables) correspond to the URM (s.o) and are answered by me. My interest in any publications to this dissertation corresponds to those that are specified in the following joint declaration with the responsible person and supervisor. All publications resulting from this thesis and which I am author correspond to the URM (see above) and I am solely responsible.

The importance of this affidavit and the criminal consequences of a false affidavit (section 156,161 of the Criminal Code) are known to me and I understand the rights and responsibilities stated therein.

Date Signature

Declaration of any eventual publications

Liu Yong has included into the thesis data and results of his previous work in China, which has already been published:

Publication: Liu Y, Qian J, Feng JG, Ju HX, Zhu YP, Feng HY and Li DC. Detection of circulating tumor cells in peripheral blood of colorectal cancer patients without distant organ metastases. Cell Oncol. 2013; 36(1):43-53.

Contribution in detail: The contribution of Liu Yong in the publication including the majority of study design, data acquisition, data analysis, manuscript writing, editing and review.

Signature, date and stamp of the supervising University teacher

_____

Signature of the doctoral candidate

_____

Curriculum Vitae

For reasons of data protection, the Curriculum vitae is not published in the online version.

Curriculum Vitae

For reasons of data protection, the Curriculum vitae is not published in the online version.

Acknowledgement

I would like to thank Prof. Ulrich Keilholz for giving me the great opportunity to do my doctoral research in his laboratory, providing equipment, cell lines and reagents for deep insight into CTC enrichment and detection approaches and supervising me for my Doctoral Thesis. I would also like to thank all those patients treated in Surgical Department of Colorectal Cancer of Zhejiang Cancer Hospital agree to provide tissues and blood samples for our scientific research, all of my co-workers in Surgical Department of Colorectal Cancer of Zhejiang Cancer Hospital helped for collecting specimens and data from patients, Jianguo Feng in Laboratory of Molecular Biology of Zhejiang Cancer Research Institute assistant for detecting GCCmRNA from peripheral blood of colorectal cancer patients, Guoping Cheng and Gu Zhang in Department of pathology of Zhejiang Cancer Hospital for cooperation and performed IHC staining and scoring of rectal cancer tissue samples, Inge Kehler in Lab of Keilholz for providing valuable data of her study into my thesis. On top of that I would like to thank my co-workers in the Lab of Keilholz and in Surgical Department of Colorectal Cancer of Zhejiang Cancer Hospital with special thanks to Esmeralda Heiden, Stefano Meucci, Anika Nonnenmacher, Sandra Liebs, Inge Kehler, Soo-Ann Yap, Carolin Denk and Christoph Hapke for their technical support and theoretical guidance for molecular biology research. Additional thanks to Department of Medical Clinic of Gastroenterology, Infectiology and Rheumatology and Department of Radiation Oncology and Radiotherapy provide BD FACS CANTO II for flow cytometry detection and data analysis. At last, many thanks to Pamela Glowacki, Zhonghua Helmke and Franziska Grimm in Charité International Cooperation provide essential support of language translation, study registration and accommodation arrangement.